https://ntrs.nasa.gov/search.jsp?R=19810014456 2020-03-21T14:17:52+00:00Z

N O T I C E

THIS DOCUMENT HAS BEEN REPRODUCED FROM MICROFICHE. ALTHOUGH IT IS RECOGNIZED THAT CERTAIN PORTIONS ARE ILLEGIBLE, IT IS BEING RELEASED IN THE INTEREST OF MAKING AVAILABLE AS MUCH INFORMATION AS POSSIBLE

X-RAY BURSTERS AND THE X-RAY SOURCES OF THE GALACTIC BULGE

Walter H.G. Lewin
and
Paul C. Joss

(NASA-CR-164240) X-RAY BURSTERS AND THE X-RAY SOURCES OF THE GALACTIC BULGE (Massachusetts Inst. of Tech.) 150 p
HC A07/MF A01 CSCL 03A
N81-22989
Unclas
G3/89 22046

X-RAY BURSTERS AND THE X-RAY SOURCES OF THE GALACTIC BULGE[+]

by

Walter H.G. Lewin and Paul C. Joss

Center for Space Research, Center for Theoretical Physics
and Department of Physics
Massachusetts Institute of Technology
Cambridge, Mass. 02139

for

SPACE SCIENCE REVIEWS

CSR-HEA-80-8

September 1, 1980*

[+]This work was supported by the National Aeronautics and Space Administration under contract NAS5-24441 and grant NSG-7643, and by the National Science Foundation under grant AST78-21993.

*Most information that reached the authors after this date is not covered in this review.

TABLE OF CONTENTS

		Page
1.	INTRODUCTION AND BRIEF SUMMARY	1
2.	LACK OF PULSATIONS AND ECLIPSES	3
	2.1 Pulsations	3
	2.2 Eclipses	4
3.	GLOBULAR CLUSTER X-RAY SOURCES	5
	3.1 Centrally Condensed Clusters	5
	3.2 Formation of the X-Ray Sources	6
	3.3 Massive Black Holes?	7
	3.4 Mass Determinations	8
	3.5 NGC6712	9
4.	X-RAY BURST SOURCES	9
	4.1 Brief History and Highlights	10
	4.2 Type I Burst Sources	14
	4.2.1 Angular Distribution	14
	4.2.2 Persistent X-Ray Emission, Transients and Binaries	15
	4.2.3 Burst Profiles	16
	4.2.4 Burst Intervals	17
	4.2.5 Energy Ratio (α) between Persistent Emission and Bursts	19
	4.2.6 Burst Spectra, "Standard Candles," Black-body Radii and Neutron Stars	20
	4.2.7 Identifications, Optical Properties and Optical/X-Ray Bursts	22
	a. Optical Identifications	22
	b. Optical Spectra of Burst Sources	22
	c. Orbital Periods, Spectral Types and Masses of Companion Stars	23
	d. Simultaneous Optical/X-Ray Observations and Optical Bursts	25
	e. The Need for a Companion Star	27
	4.2.8 Infrared Bursts?	28
	4.2.9 Radio Properties	29
	4.3 The Rapid Burster (MXB 1730-335)	30
	4.3.1 Type I and Type II Bursts	30
	4.3.2 Type II Burst Profiles and Saturation	30
	4.3.3 E-At Relation for Type II Bursts	31
	4.3.4 Type II Bursting Patterns (Modes)	31
	4.3.5 Anomalous Bursts	32
	4.3.6 Recurrent Transient Behavior	32
	4.3.7 X-Ray Emission Between Type II Bursts	33
	4.3.8 Persistent Emission in Burst-Off State?	34
	4.3.9 Black-body Radii	34
	4.3.10 Infrared Bursts?	34
	4.3.11 Radio Bursts?	37
	4.4 Type II Bursts from Other Sources?	38
5.	FAST TRANSIENTS (BURSTS?)	39

6. THEORY 40

6.1 Thermonuclear Flash Models for Type I Bursts 41
6.1.1 Historical Development 41
6.1.2 The Overall Physical Picture 43
6.1.3 Numerical Models 45
6.1.4 General Relavistic Effects 50
6.1.5 Future Work 52
6.2 Accretion-Instability Models for Type II Bursts 53
6.3 Theory versus Observation 55
6.3.1 Type I Bursts 55
6.3.2 Type II Bursts and the Rapid Burster 57
6.3.3 The Fast X-Ray Transients 57
6.3.4 Relation to Binary X-Ray Pulsars and the Ages of Burst Sources 58
6.4 The Highly-Compact-Binary Model for Galactic Bulge Sources 59

7. CONCLUDING REMARKS 62

ACKNOWLEDGEMENTS 64

REFERENCES 65

Figure Captions 81

Tables 98

Figures 105

1. Introduction and Brief Summary

There is a class of bright ($\gtrsim 10^{34}$ ergs s^{-1}) X-ray sources which distinguish themselves from the massive X-ray binaries by the following characteristics:

- Their star-like optical counterparts are faint ($M_V \approx +3$) in contrast to the luminous massive binary systems (for which $M_V \approx -6$).
- Their spectra are generally devoid of normal stellar absorption features (see Fig. 1).
- The ratio of their X-ray to optical luminosities, L_X/L_{opt}, ranges from $\sim 10^2$ to $\sim 10^4$. For the massive systems this ratio ranges from $\sim 10^{-3}$ to $\sim 10^1$ (see Fig. 1).
- With one exception (4U1626-67), their X-ray spectra are softer than the spectra of the massive X-ray binary systems.
- With one exception (4U1626-67), they show no periodic pulsations such as are often observed from highly magnetized, rotating neutron stars in the massive X-ray binary systems.
- They show no X-ray eclipses as are commonly observed in the massive binary systems.
- Many of them produce X-ray bursts. In contrast, no X-ray bursts have definitely been observed from any of the massive binary systems (see Fig. 1).

In our galaxy, about ten bright X-ray sources are located in globular clusters. Their X-ray properties are similar to those listed above. About seven of them produce X-ray bursts (see Table 1). None of the globular cluster X-ray sources have been optically identified with stellar objects. Such identifications would be very difficult, since most of these globular clusters are centrally condensed (see Fig. 2) and several are highly reddened

due to interstellar extinction. The similarities between the globular cluster X-ray sources and the above class of X-ray sources lead one to consider them as a single class of objects. They are often referred to as the "galactic bulge sources" since they are concentrated toward the galactic center. Their apparent location outside regions of active star formation identity them as being probable members of an older stellar population.

Figure 1 shows the ratios of the X-ray luminosities, L_x, to the optical luminosities, L_{opt}, of all optically identified compact galactic X-ray sources with $L_x > 10^{34}$ ergs s^{-1}. The figure also shows which of them (i) are associated with an O or a B star (i.e., contained in massive X-ray binary systems), (ii) show no normal stellar absorption features at maximum light, and (iii) are X-ray burst sources. The sources under (ii) and (iii) have values for $L_x/L_{opt} > 10$, whereas the sources under (i), with one exception, all have values for $L_x/L_{opt} < 10$. This, combined with the bimodal distribution clearly visible in Figure 1, strongly suggests that we are dealing here with two different classes: the massive binaries, on the left in Figure 1, and the galactic bulge sources, on the right in Figure 1. (Her X-1 is special, as it does not fit neatly into either class.)

In this article we shall discuss the observed X-ray, optical, infrared and radio properties of the galactic bulge sources, with an emphasis on those that produce type I X-ray bursts. (The "type I/type II" classification will be discussed in Chap. 4.) There is persuasive evidence that these burst sources and many other galactic bulge sources are neutron stars in low-mass, close-binary stellar systems. As noted above, several burst sources are found in globular clusters with high central densities (see Fig. 2); they were probably formed by capture during close encounters between neutron stars and nuclear burning stars.

The commonly observed X-ray bursts (of type I) are probably due to thermonuclear flashes of freshly accreted material on the surfaces of neutron stars. Optical bursts, associated with the type I X-ray bursts, have been observed from three sources. The optical flux, which arrives a few seconds after the X-ray flux, is probably due to X-ray heating of an accretion disk surrounding the neutron star and the delay in emission is predominantly caused by travel time differences.

The X-ray bursts of type II, as observed from the Rapid Burster (MXB1730-335), are almost certainly due to an accretion instability which converts gravitational potential energy into heat and radiation, and are thus of a fundamentally different nature than the type I bursts.

2. LACK OF PULSATIONS AND ECLIPSES

2.1 Pulsations

More than twenty galactic bulge sources have been observed intensively in search of periodic pulsations. Except for 4U1626-67, no pulsations were found. Cominsky et al.[52] analyzed the persistent flux of seven burst sources and found upper limits on the pulsed fractions of 1-10% for periods from $\sim$1.6 to 10^3 s (Table 2). Spada, Rappaport and Li (private communication) searched for periodicities in seven of the brightest (non-bursting) sources near the galactic center. They also found none, with typical upper limits of 3 percent in the range $\sim$2 ms - 2 s. Upper limits to pulsed fractions of 10 percent (periods in the range 3-100 s) and 30 percent (periods in the range 2 minutes - 2 days) were obtained by Parsignault and Grindlay[248]. Upper limits to pulsations from the general region of the galactic center have been reported by Cordova, Garmire and Lewin[57].

Pulsations are expected from accreting neutron stars if they have magnetic fields misaligned with their rotation axes and sufficiently strong to channel the accretion flow, as is presumably the case among the binary X-ray pulsars of stellar Population I. The critical surface magnetic field strength is uncertain but is most likely of the order of 10^{12} gauss (ref. 8). The surface magnetic fields of older neutron stars may have largely decayed away, or their rotation and magnetic dipole axes may have become coaligned (see refs. 77 and 256 and references therein). It is, perhaps, also possible that differences in the formation may have prevented the development of strong surface magnetic fields in neutron stars that now comprise the galactic bulge sources[144]. The strong magnetic fields of young neutron stars funnels the material towards the magnetic poles and may suppress thermonuclear flashes in the accreted material. This could explain why type I X-ray burst sources do not pulse and why X-ray pulsars do not burst[142,148,275] (see Sect. 6.3.4.).

Thus, the absence of detected pulsations does not constitute a strong argument against the neutron-star nature of the collapsed objects in these systems.

2.2 Eclipses

No X-ray eclipses have been found among the galactic bulge sources. Joss and Rappaport[149] have shown that an X-ray source powered by accretion through Roche-lobe overflow from a low-mass companion (of $\sim$0.3 solar masses) has a low probability ($\sim$25 percent) of being eclipsed by its companion. The eclipse probability varies as the cube root of the mass of the companion and would therefore still be about 10 percent for a companion of only 0.02 solar masses. The available estimates of the masses of companion stars of galactic bulge sources (see Sect. 4.2.7.c) indicates that the very low-mass model of Joss and

Rappaport is probably insufficient by itself to account for the absence of X-ray eclipses in all ~20 sources for which a careful search for eclipses was made (see Sect. 6.4). Milgrom[232] proposed a model in which an accretion disc casts an X-ray shadow in the orbital plane of a low-mass binary, thereby excluding from our detection those systems which would otherwise show eclipses.

Thus, the absence of eclipses does not argue compellingly against the binary nature of these systems. In Section 4.2.7 we shall discuss the observational evidence that these systems are highly compact binary systems containing low-mass (<1 solar mass) or degenerate companion stars. Theoretical models and the evolution of systems of this type will be discussed in Chapter 6.

3. GLOBULAR CLUSTER X-RAY SOURCES

It was first pointed out by Katz[156] that X-ray sources occur with unusually high frequency in globular clusters. In terms of their typical intrinsic properties, these sources seem to be indistinguishable from other galactic bulge sources[33]. An examination of the circumstances surrounding the frequent occurrence of such sources in globular clusters may throw light on the nature of the entire class of galactic bulge X-ray sources[175,176,177].

3.1 Centrally Condensed Globular Clusters

The structure of a globular cluster can be broadly characterized by three observables: the core radius r_c, the tidal radius, and the central brightness B (ref. 159). Peterson and King[252] summarized the data as of 1975, and several studies updating and extending their work have been carried out since then, with special attention to the clusters containing X-ray sources (see, e.g., refs. 13,14,35,160,251). The data show a striking correlation between

the presence of an X-ray source and the quantity B/r_c, which is a measure of the central density of luminous stars (Fig. 2).

In recognition of the correlation with high central density, it was widely expected that the cluster sources (listed in Table 1) would be found to lie close to the cluster centers. This expectation was confirmed by position measurements, carried out with the rotating modulation collimator detectors on the SAS-3 X-ray observatory, which showed that in five cases the positional error circles with radii of 20 to 30 arc seconds (90% confidence) included the optical centers of the clusters[134]. Recent work with the Einstein X-ray observatory has further refined the positional measurements of X-ray sources in globular clusters[93] (see Sect. 3.4).

3.2 Formation of the X-Ray Sources in Globular Clusters

The evidence clearly points away from any explanation of the cluster sources based on the evolution of primordial binary stellar systems that might be found in all clusters, and toward an explanation based on the formation of the X-ray sources under the circumstances peculiar to the dense cores of the most centrally condensed clusters. (It is conceivable, however, that the central density of a cluster is somehow related to the number of primordial binaries that were able to form within it.) One plausible circumstance is a high concentration of collapsed remnants of the short-lived massive stars that were presumably present at the birth of the cluster (i.e., degenerate dwarfs, neutron stars and/or black holes that were not ejected from the clusters by the processes of their formation and that subsequently settled toward the cluster centers). The frequency of close encounters between such remnants and other stars certainly increases with increasing central density of the cluster.

Clark[42] suggested that the cluster sources are neutron stars that have acquired close stellar companions by capture. Fabian, Pringle and Rees[75] estimated that captures could occur with sufficient frequency in dense cluster cores through tidal dissipation of orbital energy in two-body encounters, and Press and Teukolsky[254] confirmed the viability of this mechanism by detailed calculations. Hills[114] examined the formation of binary systems through star-exchange interactions between neutron stars and primordial low-mass binaries, but the unknown frequency of binaries in clusters makes the importance of this process uncertain. Capture of collapsed remnants by other stars through three-body encounters in a dense subcluster near the cluster center may also be significant[76].

3.3 Massive Black Holes?

It has been proposed that the deep potential well of a centrally condensed cluster might retain gas lost by stars and that a black hole of sufficient mass, formed perhaps in a collapse of the dense core, could accrete this gas at the rate required to produce the observed X-ray luminosities[11,266]. Evidence has been reported[101] for the existence of gas in the cores of four X-ray globular clusters in amounts sufficient to supply a black hole if its mass exceeds 10^2 solar masses. Shortly after the discovery of X-ray bursts (Sect. 4.1), Grindlay and Gursky[95] argued that the X-ray burst source located in the globular cluster NGC6624 is a very massive (larger than a few hundred solar masses) black hole. Their argument was largely based on the spectral hardening that was observed in two bursts[98]. However, Canizares[34] showed that their calculations were erroneous and that the observed effect does not constitute a strong constraint on the properties of the X-ray star. In addition, the discovery of more burst sources (Sect. 4.1) showed that as a rule the spectra soften during burst decay, and this further

weakened the argument for massive black holes. It was also pointed out by Lewin[172] and Lewin et al.[186] that the galactic distribution of the observed burst sources argues against an association with massive black holes.

3.4 Mass Determinations of X-Ray Sources in Globular Clusters

A new approach to determine the mass of X-ray sources in globular clusters has recently become available by use of precise position measurements. Bahcall and Wolff[12] showed that the expectation value of the distance of an object of mass M from the center of a dynamically relaxed cluster of stars, each of mass m, is $0.9\ R_c(m/M)^{1/2}$ arc seconds. In typical X-ray clusters R_c is about 7 arc seconds (see Table 1). Thus an X-ray source with four times the average mass of cluster stars[246] (≈0.5 solar mass) would have an expectation distance of about 3 arc seconds from the center, while a black hole with more than a hundred times the average mass would rarely be found outside of 1 arc second. The position measurements with SAS-3 permitted the conclusion that the cluster X-ray sources are, on average, more massive than the visible stars in the clusters[134].

Grindlay and co-workers[93], using the Einstein Observatory, determined the locations of eight X-ray sources located in globular clusters to an accuracy of several arc seconds. They found that at a 90 percent confidence level the mass of each X-ray source lies between 1 and 5 solar masses under the assumption that the masses of all eight sources are about equal, that the cluster cores are isothermal and that the masses of the cluster stars are approximately constant. This important result is an independent confirmation of the low-mass character of these systems (see Sect. 4.2.7).

Another point to keep in mind regarding the low-mass binary picture for these objects is that it implies a fair chance of finding two X-ray sources within the same cluster. No such pairs have been found so far by the Einstein

Observatory[93]. Of the ~25 known centrally condensed clusters, seven contain an X-ray source (see Fig. 2 and Table 1). Thus, it is easily found that the a priori probability of finding more than one X-ray source in any one of the ~25 centrally condensed clusters is ~0.7 if the low-mass binary model is correct.

3.5 NGC6712

Among globular clusters that contain X-ray sources, NGC6712 has an exceptionally low central density (see Fig. 2). This anomaly is intriguing in the light of calculations by Shapiro[264], which suggest that core collapse may be followed by distension and dissolution of the remaining cluster through the injection of kinetic energy by interactions of stars with a massive central body. Perhaps X-ray binaries as well as a massive black hole are produced in the processes of core collapse, and in NGC6712 we are witnessing the aftermath as the cluster proceeds to self-destruct. Some consequences of this scenario of the evolution and death of globular clusters have been explored by Lightman, Press and Odenwald[202].

An alternative, and more mundane, possibility is that NGC6712, despite its low central density, has nonetheless managed to produce a binary X-ray source.

4. X-RAY BURST SOURCES

In this chapter we shall review the observational data on X-ray burst sources. A large amount of observational material has been obtained in the past five years. The Rapid Burster, with all its idiosyncrasies, will be treated in Section 4.3 separately from the other burst sources. We begin with a short historical review of the important issues and contributions as we perceived them at MIT, where much of the observational work was carried out.

4.1 Brief History and Highlights

X-ray bursts were discovered in December 1975 independently by Grindlay and Heise[98,99] and by Belian, Conner and Evans[21,22] (Figs. 3 and 4). Grindlay et al.[98,99] were able to associate the two bursts they observed with a known X-ray source in the globular cluster NGC6624, while the Los Alamos group[21-23] could not make an association with a known X-ray source, since their positional accuracy for the many burst events they observed was insufficient (Fig. 4). Subsequently, using existing SAS-3 data from May 1975, Clark et al.[46] found a series of ten bursts from the source in NGC6624.

Within two months, in February 1976, two additional burst sources (possibly transients) were discovered by Lewin and co-workers[166,167,187] within a few degrees of the galactic center. The presence of a third burst source was suspected and searched for in early March 1976. It was found[168] (MXB1728-34; MXB stands for MIT X-Ray Burst Source), and in the process another source with extraordinary bursting behavior was discovered[168,180]. Bursts from this object were observed in rapid succession on time scales of seconds to minutes. This behavior gave the source its name: the Rapid Burster (the official designation is MXB1730-335). The bursts from the Rapid Burster varied by about a factor of $\sim$100 in duration, but bursts with durations in excess of $\sim$15 s had nearly equal peak fluxes (Fig. 21). The energy in a burst was approximately proportional to the waiting time to the next burst; the system clearly behaved like a relaxation oscillator[180].

The activity of this source stopped by mid-April 1976. About a year later, White and Burnell[304], using the Ariel 5 satellite, observed a recurrence of bursts from the Rapid Burster. This established that the burst activity was a recurrent phenomenon. We now know that the periods of burst activity occur at intervals of approximately six months, and persist for $\sim$2-6 weeks (see Sect. 4.3.6).

A previously unknown, highly reddened globular cluster[160] was found in March 1976 by Liller[204] in the error circle (radius = 4 arc min) for the Rapid Burster[111] (Fig. 20). The globular cluster was called Liller I in the expectation that more such globular clusters would be found. Some workers indeed believed that perhaps all burst sources would be associated with globular clusters (see ref. 78 and the discussion following Lewin's talk at the Texas Symposium[172] in December 1976). Within a year, over twenty burst sources were found, largely due to observations made with SAS-3 (by W. Lewin and his co-workers) and OSO-8 (by J. Swank and her co-workers). A first catalog of burst sources was compiled in September 1976 and contained 15 sources[171]. By December 1976 the number of burst sources was about 22 (ref. 172), and it became clear from the distribution of these sources that, as a class, they were not associated with globular clusters[172,186].

Whether or not burst sources, as a class, are associated with globular clusters was at the time an important issue, since it had immediate implications for the nature of the burst sources, the globular cluster X-ray sources and the whole class of galactic bulge sources. As described in Section 3.3, it was proposed by Grindlay and Gursky[95] that burst sources are associated with massive (greater than a few hundred solar masses) black holes in the cores of globular clusters, and it was thought by some that most or all burst sources would be found in globular clusters[78]. However, by December 1976 it became clear that this was not the case[172], and the massive black hole idea evaporated (see Sect. 3.3 for other problems with the massive black hole picture).

In 1977, Swank et al.[268], using OSO-8, were the first to show that the spectral evolution of a particular long burst (of ~600 s duration) was consistent with the cooling of a collapsed object whose surface behaved like a

black body (Fig. 14). Hoffman, Lewin and Doty[120,121] confirmed the consistency with black-body cooling for a series of bursts from two burst sources (Fig. 6), and they showed that throughout the cooling the effective black-body radii of these two objects did not change. They found values of ~10 km for both sources if source distances of ~10 kpc were assumed. In 1978, Van Paradijs[291] showed evidence that bursts of average intensity are "standard candles" at burst maximum and that their radii are all near 7 km if the average values of their peak burst luminosities are near the Eddington limit of a ~1.4 solar mass object with a hydrogen-rich surface. (When examined in detail, bursts are not precise standard candles; in a series of bursts from one source, peak fluxes can differ substantially[194].) The measured black-body radii strongly indicated that the collapsed objects are neutron stars.

Several models were proposed in 1976 and 1977 to explain the bursts. Svestka[267], Henriksen[113], Joss and Rappaport[319], Baan[10], and Lamb et al.[163] considered various possible instabilities in the accretion flow at or near the magnetopause of a neutron star or white dwarf, while Wheeler[302] and Liang[201] investigated potential instabilities in an accretion disk surrounding a collapsed object, and Grindlay[91] suggested a thermal instability in accretion onto a massive black hole.

A very different mechanism was proposed by Woosley and Taam[308] and Maraschi and Cavaliere[208], who suggested thermonuclear flashes in the surface layers of an accreting neutron star. However, after the discovery of the Rapid Burster[168], it became apparent that the rapidly repetitive bursts could not be due to thermonuclear flashes; if they were, a very high flux of persistent X-ray emission due to the release of gravitational potential energy by the accretion of the matter onto the neutron-star surface should be present, and this was not observed. Thus, the nuclear flash theory could not explain all burst phenomena, and that was not in its favor.

A break came in September 1977 when Hoffman, Marshall and Lewin discovered that the Rapid Burster emits two very different kinds of bursts[126,127] (Figs. 22 and 23). They introduced the classification of type I and type II bursts (Table 3) and suggested that the rapidly repetitive type II bursts are due to accretion instabilities, thus deriving their energy from (and accounting for the release of) gravitational potential energy, but that the type I bursts are due to thermonuclear flashes. This is to date still the most plausible explanation. Other burst sources, which emit only type I bursts, evidently release the gravitational potential energy (due to accretion) as a persistent X-ray flux (see Sect. 4.2.2). Detailed calculations performed since 1977 have strengthened the idea that thermonuclear flashes on the surfaces of neutron stars produce the type I bursts (ref. 142 and other references given in Chap. 6).

In the summer of 1977, the burst source MXB1735-44 was the first to be firmly optically identified by J. McClintock; its spectrum was very similar to that of Sco X-1 (refs. 223,225). This identification was made possible by the precise ($\sim$20 arc sec) X-ray source position obtained by the SAS-3 rotating modulation collimator (RMC) observations. (The RMC observations were directed by H. Bradt, G. Jernigan and R. Doxsey.) MXB1735-44 was also the first burst source from which, in the summer of 1978, a simultaneous optical and X-ray burst was observed. This observation was the result of a combined Harvard-MIT effort[104,105,228], and it came after an extensive world-wide coordinated burst watch in 1977 failed to detect any radio, infrared or optical burst coincident with an observed X-ray burst (refs. 1,24,137,277,281,286).

Infrared bursts from the Rapid Burster were first reported by Kulkarni et al.[162] in 1979, and radio bursts from this source were reported by Calla et al.[30,31]. The connection between these bursts (if they are real) and the X-ray bursts is still unclear to date.

It was long suspected that, as a class, burst sources are low-mass close-binary systems (see Sects. 4.2.2, 4.2.7 and 6.4). However, in early 1980, Kaluzienski et al.[155] obtained the first direct indication that the transient[19,55,153] burst source[155] Cen X-4 is a close-binary system with an orbital period of ≈8 hours.

We shall now discuss in detail the observational characteristics of X-ray burst sources.

4.2 Type I Burst Sources

4.2.1 Angular Distribution

Type I bursts show distinct spectral softening during burst decay and, in general, recur on time scales of hours to days[127] (Table 3). A sky map of type I burst sources is shown in Figure 5. The sources are listed in Table 4. It is immediately clear from this map that the burst sources are associated with the Galaxy, and their apparent locations outside regions of current or recent active star formation identify them as probable members of an old stellar population. Eight of the 32 sources shown in Figure 5 are located in globular clusters (see Table 1), but the majority of them do not lie in globular clusters. Six (perhaps seven) have been optically identified with faint stellar objects (see Sect. 4.2.7). The positions of many more burst sources (see Fig. 4) have been reported in the literature[20-23,73], but we omit them because it is presently uncertain that all of these are type I burst sources. However, it is very likely that many of the events observed by the Los Alamos group[20-23,73] were of type I and, in retrospect, there seems to be little doubt that they discovered type I X-ray bursts from the Norma region (refs. 21-23).

The type I burst sources are a subset of the known galactic bulge X-ray sources[172-186], which have the general characteristics listed in Chapter 1. It

is believed that many, and perhaps all of the galactic bulge sources are accreting neutron stars that produce type I bursts under some circumstances (e.g., if the accretion rate is neither too large nor too small) (see Sects. 4.2.2, 4.2.4, 6.1.3 and 6.3.1).

4.2.2 Persistent X-Ray Emission, Transients and Binaries

Almost all burst sources emit a detectable persistent (though variable) flux of X-rays. In Table 4 we list the names of burst sources, the names of the associated sources of persistent X-ray emission, and their persistent fluxes in Uhuru flux units even for those burst sources which are not listed in the 4U-catalogue[79]. We also indicate the variability of the persistent flux by showing the ratio of the maximum to minimum observed flux.

The suggestion of a connection between burst sources and transient X-ray sources (refs. 3,53,151) was first made by Lewin et al.[187] for the sources MXB1742-29 and MXB1743-29 near the galactic center. MXB1659-29 is a burst source[183] (Fig. 9) and a transient[69,173,174,189,265]. When bursts from this source were first detected in October 1976, the persistent flux was below the SAS-3 detectability threshold. In March 1978 the source flared up, but X-ray bursts were not detected[173,189]. The Rapid Burster is a recurrent transient with a recurrence period of about 6 months (see Sect. 4.3.6). Cen X-4, 4U1608-52 and Aql X-1 are transient sources of the spectrally "soft" type, and they all produce type I X-ray bursts. The bursts are probably only produced when the persistent X-ray flux is within certain limits (for references see Table 4). The association of burst sources with soft transients has provided circumstantial evidence supporting the binary nature of these systems[74,174].

Kaluzienski et al.[155] reported an indication of a 8.2 ± 0.2 hour period in the persistent flux from Cen X-4. This period, if real, most likely results from binary orbital motion, and such a short period strongly supports

earlier suggestions that these systems are low-mass, close-binary stellar systems[149] (see also Sects. 3.2, 4.2.7 and 6.4).

4.2.3 Burst Profiles

Bursts come in large varieties, with rise times in the range of ∿1 s to ∿10 s and decay times in the range of seconds to minutes. The decay times, in general, are much shorter at high energies than at low energies. This can be seen clearly in Figure 6, which shows a superposition of five bursts from MXB1728-34. In the range 1.2-3 keV, the burst decay takes several minutes; in contrast, in the range 19-27 keV, the decay time is only a few seconds. This spectral softening in the burst "tails" can also be seen in most of the individual bursts shown in Figures 7-11. It has been suggested that the observed lengths and X-ray energy dependences of the burst "tails" might be explained by scattering of X-rays due to large (∿3μm) interstellar grains[2]. However, this idea is strongly contradicted by the observational data[297].

Figure 7 shows bursts from five different burst sources. Figures 8-11 show series of bursts from several sources. These figures illustrate that bursts from a given source often look similar but that this tendency is by no means a universal phenomenon.

Figure 12 shows a burst from MXB1728-34 observed with the HEAO-1 X-ray observatory[125]. The rise of the burst is only several tenths of a second. The burst shows a clear "flattening" as burst maximum is approached, as is often observed in other bursts (see Figs. 6-11). Statistically significant intensity changes on time scales of tens of milliseconds were detected in this burst (Fig. 12), and the presence of ∿12.5 ms quasi periodic fluctuations was also reported (ref. 81).

Figure 13 shows double-peaked burst profiles from three different burst sources; they look very similar. The depth of the dips and the separation between the peaks increase with energy. Hoffman, Cominsky and Lewin[118] suggest that perhaps many type I burst sources, on occasion, exhibit this type of structure.

A relation between burst profiles and persistent emission was first found in 1976 by Clark et al.[49] for 3U/MXB1820-30. They observed a gradual shortening in decay time (i.e., in the range 1-6 keV the decay time changed from ~4.7 s to <3 s) while the level of persistent emission increased by a factor of ~5.

Another change in burst profile correlated with the level of persistent emission was observed by the Hakucho team. Murakami et al.[234] observed 4U1608-52 during an active phase in April 1979. The majority of the bursts had a fast rise ($\lesssim$2 s) and a fast decay ($\lesssim$15 s). Two months later, when the persistent flux had decreased substantially (by a factor of ~5) the bursts had a slower rise and a slower decay. In addition, the maximum observed burst flux was lower at that time (by a factor of ~3) than it was during the early part of the active phase (see Sect. 6.1.3). The possible relation of such effects to the thermonuclear flash model for type I X-ray bursts has been discussed by various authors[82,234] (see Sect. 6.1.3).

4.2.4 Burst Intervals

Burst intervals can be regular or irregular on time scales of hours to days. The burst occurence rate is sometimes (but not always) related to the level of persistent X-ray emission.

In May 1976, the persistent flux of 3U/MXB1820-30 increased by a factor of ~5 while the burst intervals gradually decreased by 50 percent. The persistent flux continued to increase, and the bursts stopped completely[49].

Bursts have only been detected from this source when its persistent flux was relatively low (for references see Table 4).

In October 1976, MXB1659-29 produced bursts at fairly regular intervals of ~2.5 hours; no persistent flux could be detected (i.e., its flux was less than 2 percent of that of the Crab Nebula). Bursts were also detected in June 1977. In March 1978, the persistent flux was much higher (~8% of that of the Crab Nebula), and no bursts were observed (see Table 4 for references). Bursts from the other transient sources Cen X-4, 4U1608-52 and Aql X-1 were only observed after the persistent X-ray flux had flared up substantially (see Sect. 4.2.2).

In several other cases (MXB1837+05, MXB1735-44, and MXB1636-53), large fluctuations in the observed burst intervals were not noticeably correlated with variations in the persistent X-ray flux[120,194,200].

According to the thermonuclear flash model in its present, still rather simple, form (see Chap. 6 and references therein), one would expect no type I bursts at very low[165] or very high[142,144] values of the accretion rate onto the neutron star. Moreover, the burst intervals are expected to decrease if the accretion rate and the resulting persistent X-ray flux increase. This is sometimes observed[49] (see above); however, more theoretical work is required to explain why, in several cases, the burst intervals can change by an order of magnitude or more without an appreciable change in the associated persistent X-ray fluxes.

A possibly interesting connection between the irregular burst behavior of 4U/MXB1735-44 and MXB1837+05 (= Ser X-1 = 4U1837+04) and the thermonuclear flash model is suggested by the following considerations[194,296]. One prediction of these calculations is that thermonuclear flashes will not occur above a certain accretion rate, which corresponds to an accretion-driven

luminosity that is a substantial fraction of the Eddington limit for a solar-mass object[142]. If the maximum burst luminosity is of the order of the Eddington limit, as indicated by theoretical considerations[141,142] and by the phenomenological work of Van Paradijs et al.[296], the ratio γ of the persistent X-ray flux to the maximum burst flux is an approximate measure of the X-ray luminosity in units of the Eddington limit. For 4U/MXB1735-44 and MXB1837+05 this ratio equals 0.2 and 0.3, respectively. These values are the two highest among 12 burst sources for which γ was reasonably well determined[296]. This result suggests that the irregular burst behavior of 4U/MXB1735-44 and MXB1837+05 is related to their large persistent luminosities, which may be near the critical values above which X-ray bursts do not occur.

4.2.5 Energy Ratio (α) between Persistent Emission and Bursts

Let α be the ratio of time-averaged energy in the persistent flux to that emitted in bursts. In most cases $\alpha \gtrsim 10^2$ (refs. 171,296). This is consistent with the idea that type I bursts are produced by thermonuclear flashes of helium and/or heavier elements; the gravitational potential energy liberated at the surface of a neutron star and released as persistent X-ray emission should be $\sim$100 MeV per accreted nucleon, while the energy released by nuclear reactions and released as burst emission should be $\sim$1 MeV per accreted nucleon.

For MXB1659-29, in October 1976, α was less than 25 (ref. 190). This value is perhaps uncomfortably low for the nuclear flash model in its present form. Moreover, there are two reported cases where type I burst intervals were very short. In 1976, three type I bursts in quick succession were observed with SAS-3 from MXB1743-28, with intervals of only 17 min and 4 min (ref. 187). In 1979, the Hakucho observatory detected two type I bursts from 4U1608-52 with an interval of only $\sim$10 min (ref. 235); this leads to a value

for α of at most 2.5. How these results fit into the thermonuclear flash model is unclear (see Sect. 6.3.1).

4.2.6 Burst Spectra, "Standard Candles", Black-body Radii and Neutron Stars

Why do we believe that burst sources are neutron stars? Of course, the ability of the thermonuclear flash model to explain many of the burst properties is very persuasive. However, substantial evidence in favor of neutron stars preceded the development of the thermonuclear flash model. It was first pointed out by Swank et al.[268] that the burst spectra fit that of a black body reasonably well (Fig. 14). For one particular burst of $\sim$600 s duration, they derived radii of the burst emission region (under the assumption that it was a spherical surface at a distance of 10 kpc) and found values of $\sim$100 km during the first 20 s and $\sim$15 km later on in the burst. Hoffman, Lewin and Doty[120,121] found for MXB1728-34 and MXB1636-53 that near burst maximum, before the decay begins, the black-body temperature is $\sim 3 \times 10^7$ K. The object cools rapidly during the decay portion of the burst (note the spectral softening in Figs. 6-11), but the black-body radii remained constant (at $\sim$10 km) throughout the burst decay. However, no satisfactory fits to black-body spectra could be found during the early part of the bursts[120,121] (see also ref. 125). The above dimensions suggest that the burst emission regions are on or near the surfaces of neutron stars.

Van Paradijs[291] carried this analysis a step further in a study of the average characteristics of bursts from each of ten sources. He showed that all ten sources, interpreted as black bodies emitting isotropically, have nearly the same ratio of radiating surface area to average peak burst luminosity. If the peak luminosity is a "standard candle", the effective black-body radius is approximately the same for all burst sources. If, moreover, the peak

luminosities are assumed to be equal to the Eddington limit for a 1.4 solar mass object with a hydrogen envelope (1.8×10^{38} ergs s^{-1}), the radii are found to have an average value of ~7 km with a scatter of only ~20 percent[291]. In a later paper, Van Paradijs[292] made corrections for general relativistic effects (see also refs. 86 and 273) and adjusted the maximum burst luminosity so that the ten sources would be distributed evenly about the galactic center (at an assumed distance of 9 kpc). He again concluded that burst sources are neutron stars and have, on average, nearly equal peak luminosities.

Lewin et al.[194] have shown that, when examined in detail, individual burst maxima are not standard candles. They showed that the standard deviation in the maximum flux of 53 bursts from MXB1735-44 was 37 percent of the mean value. The highest observed flux at burst maximum was about seven times higher than the lowest. Similar results were subsequently found by Murakami et al.[234] for bursts from 4U1608-52. The spread in maximum burst fluxes in a series of 57 bursts from Ser X-1 is much less[314]. The observed spreads, even in the cases of MXB1735-44 and 4U1608-52, may still be small enough to justify the use of the average values in the analysis of global properties of X-ray burst sources[291].

There are indications that in some cases the Eddington limit is exceeded near the peak of some bursts (refs. 86,103,121; see Sect. 6.1.5). Hoffman, Lewin and Doty[121] found that in July 1976 the peak luminosities (in the energy range 1-30 keV) in bursts from MXB1728-34 were $(2.0 \pm 0.2) \times 10^{39}$ $(D/10)^2$ ergs s^{-1}, if the emission is isotropic. Here, D is the distance to the source in kpc. If D = 5 kpc (ref. 291), the peak luminosity exceeds the Eddington limit for a 1.4 solar mass object with a hydrogen-rich envelope by a factor of ~3. Grindlay et al.[103] reported that the peak luminosity of a burst from 4U1722-30 (located in Terzan 2) may have exceeded the Eddington limit by a factor of ~10.

If the double-peaked bursts, shown in Figure 13, are fitted to black-body spectra[118] at various stages in the burst, the temperature at first increases and then decreases; the corresponding black-body radii at first decrease and then increase. The fitted radii remain constant (typically ~10 km) during the smooth portion of burst decay as the temperature decreases. Similar fluctuations in the fitted radius and temperature during a type I burst from Terzan 2 have been reported by Grindlay et al.[103]. It is possible to interpret this variation as a physical change in the size of the emission region[103,118].

On the basis of (i) the derived black-body radii (~10 km) of the emitted bursts and (ii) the success of the thermonuclear flash model, it seems safe to conclude that type I X-ray burst sources are neutron stars.

4.2.7 Identifications, Optical Properties and Optical/X-Ray Bursts

4.2.7a Optical Identifications

Of the 31 burst sources listed in Table 4, six (and perhaps a seventh) have been optically identified (for references see Table 4, ref. 28 and references therein). The optical counterparts are intrinsically faint blue objects. With the exception of the nearby transient burst source Cen X-4, (see Sect. 4.2.2 and Fig. 15), their apparent visual magnitudes are all greater than 17 mag. Studies of these optical counterparts and of the X-ray properties of burst sources (and other galactic bulge sources) have provided persuasive evidence that they are low-mass, close-binary stellar systems. We shall review here some of these studies.

4.2.7b Optical Spectra of Burst Sources

Canizares, McClintock and Grindlay[37] made spectroscopic studies of the optical counterparts of the X-ray burst sources 4U/MXB1735-44, 4U/MXB1636-53 and MXB1659-29 (refs. 90,223,224,226). The spectra are remarkably similar in overall shape and in the locations and strengths of spectral features. They

lack normal stellar absorption lines and are dominated by emission features (see Fig. 16). They lack strong Balmer emission lines but occasionally show weak Balmer absorption and/or emission at Hα and Hβ. The spectra show evidence for Doppler shifts due to velocity differences of $\gtrsim 10^3$ km s^{-1} and possibly $\sim 10^4$ km s^{-1}. The high velocity features, several of which have symmetrical redshifted and blueshifted components, suggest that the objects contain gas streams and accretion disks[37]. The ratio of X-ray to optical luminosity is $\gtrsim$ 500-1000 (see Fig. 1), and the optical emission is probably largely the result of X-ray heating of the accretion disk. The spectra of 4U/MXB1735-44 and MXB1659-29 are variable on a time scale of hours, and it seems likely that this is also the case for 4U/MXB1636-53 (ref. 37). The absence of normal stellar features in the spectra and the faintness of the objects require that if the suspected binary companions are main-sequence stars, their spectral types are later than F0 (ref. 37).

4.2.7c Orbital Periods, Spectral Types and Masses of Companion Stars

There is direct evidence for the existence of low-mass companion stars in four X-ray sources: the burst/transient X-ray sources Cen X-4 and Aql X-1 (see Sect. 4.2.2), the transient source A0620-00, and the X-ray pulsar 4U1626-67. During transient flareups, the optical counterparts of A0620-00, Cen X-4 and Aql X-1 brighten by several magnitudes and then fade (refs. 28,36,38,153,209,242,243,262,283,303,310 and references therein). The optical counterparts were very blue at maximum light, and their spectra showed emission lines but none of the absorption lines normally observed from stellar atmospheres (refs. 38,209,233,283,310). As the X-ray flux decreased, the optical counterpart faded and became redder and stellar absorption lines appeared (refs. 243,283,293,299). The spectra then indicated the presence of

main-sequence stars with spectral types between K5 and K7 for A0620-00 (ref. 243), between K3 and K7 for Cen X-4 (refs. 293,299) and between G3 and K3 for Aql X-1 (ref. 283). This suggests masses of the companion stars in the range of ~0.5 to ~1 solar mass.

In these three cases, the companion stars were only found after the X-ray flux, and thus the optical flux due to X-ray heating, had greatly decreased. Unless the X-ray flux is very low, the intrinsic optical flux of a low-mass companion star is negligible compared to that due to X-ray heating.

The burst/transient X-ray sources 4U1608-52 and MXB1659-29 were optically identified[90,92] during X-ray flareups. However, during X-ray quiescence, these objects are extremely faint. A year after the flareup of MXB1659-29 (see Sect. 4.2.2), its optical counterpart was so faint ($V > 23$) that it could no longer be detected (H. Pedersen, private communication). Such optical faintness during X-ray quiescence greatly inhibits the measurement of the spectral type of the companion star.

4U1626-67 is a 7.7 s X-ray pulsar; it is not a burst source. Its orbital period is ~42 min (ref. 231), and the mass of the companion star is less than ~0.1 solar mass (ref. 198). It required an extremely arduous observational effort to measure the optical pulsations from the companion star in this system[231]. These pulsations apparently result from the reprocessing of a relatively small amount of pulsed X-rays which reach the companion star despite the shadowing by an accretion disk that surrounds the pulsar, and the existence of these pulsations revealed the binary character of this system[231]. The great difficulty of demonstrating the binary nature of 4U1626-67, even in the presence of X-ray pulsations, suggests that it may be very difficult to obtain direct evidence for the binary character of many other galactic bulge sources. In Figure 17 we show the dimensions of the 4U1626-67 system.

Of all sources listed in Figure 1 with $L_x/L_{opt} > 10$, the following have well established orbital periods: 4U1626-67 (≈42 min); 4U2129+47 (≈5.3 h), 4U1822-37 (≈6.57 h), Sco X-1 (≈0.78 d) and Cyg X-2 (≈9.8 d) (refs. 28,230,231,263,284,320,321,326 and references therein). There are two other sources for which the orbital periods are less certain: Cen X-4 (≈8.2 h) and Aql X-1 (≈1.3 d) (refs. 155,301). In the case of A0620-00, there is a suggestion[221,243] of an orbital period of ≈7.8 d. We note that the long orbital period reported for Cyg X-2 is consistent with a low-mass system; the mass-losing star appears to be an evolved but low-mass (≈0.7 $M_\odot$) subgiant in a relatively wide binary system[320,321].

4.2.7a Simultaneous Optical/X-Ray Observations and Optical Bursts

Simultaneous optical and X-ray bursts have been observed from three burst sources: 4U/MXB1735-44, Ser X-1 (= MXB1837+05 = 4U1837+04) and 4U/MXB1636-53 (refs. 105,109,228,250). The observations were made during the 1978, 1979 and 1980 worldwide coordinated burst watches[327,328,329]. In these observations, the X-ray emission can be used as a probe that illuminates the surroundings of the X-ray star; some of the X-radiation is reprocessed into visible and ultraviolet light. A careful comparison of the X-ray flux (i.e., the probing signal) and the responding optical flux allows one to deduce important information on the character and geometry of the optically emitting regions. In all cases the optical burst was delayed by a few seconds: ≈2.8 s for one burst from 4U/MXB1735-44 (ref. 228), ≈1.4 s for one burst from Ser X-1 and ≈3.5 s for each of three events (see Fig. 18) from 4U/MXB1636-53 observed in 1979 (ref. 249). This delay is apparently due to travel time differences (the reprocessing times have been shown to be negligible here[249]) between the X-rays and the optical photons, which are most likely produced in an accretion disk that is a few light seconds across[249]. A total of 40 optical bursts have

been observed to date by H. Pedersen from MXB1636-53; many of them were simultaneously observed with the Hakucho X-ray observatory. In the summer of 1980 several of these optical bursts were simultaneously observed in the U,B and V bands and in the R and I bands. These data are being analyzed at the time of this writing (H. Pedersen, M. Oda and L. Cominsky, private communication).

Table 5 lists the ratios of optical (B band) to X-ray (≈2 to ≈20 keV) energy fluxes observed for both the persistent emission and the bursts from three sources. Corrections for extinction could only be made for two of the three sources; the corrected values are listed in parentheses. A comparison of the results for 4U/MXB1735-44 and 4U/MXB1636-53, both of which are corrected for extinction, indicates that the flux ratios for the two sources differ by at least a factor ≈5 for both the persistent and burst emission. As pointed out by Hackwell et al.[109], the ratio of persistent fluxes from Ser X-1 is 6±1 times lower than those for 4U/MXB1735-44, while for the bursts, the ratio for Ser X-1 is 7±3 times lower. This is consistent with the idea that these two objects are intrinsically similar but that the optical extinction for Ser X-1 is a factor of ≈6 times higher than for 4U/MXB1735-44 (ref. 109). However, the extinction to Ser X-1 has not been measured and is very uncertain[179], so that this suggestion cannot be verified at present.

Mason et al.[220] observed an optical burst from the counterpart of 2S1254-690 (ref. 87). The burst had the gross temporal characteristics of a type I X-ray burst, and it is likely that it was associated with such a burst (though there were no simultaneous X-ray observations). The source lies in the very large error region of the burst source which we designate 14??-6? in Table 4 (ref. 7). There was an indication that the optical burst was modulated with a frequency of 36.4 Hz (ref. 220). We note that if the optical

burst was modulated at such a high frequency, it is unlikely that it was associated with a type I X-ray burst; if the burst comes from a region with dimensions of a few light seconds[249], such a high-frequency modulation should be washed out by light-travel-time effects.

Simultaneous X-ray and optical observations[227] of 4U1626-67, using SAS-3 and the CTIO 1.5 m telescope, revealed optical flares which were correlated with intense, quasi-periodic ($\sim 10^3$ s) X-ray flares that had been discovered previously[147,198] (Fig. 19). The simultaneous observations also showed that the 7.7 s optical pulsations were in phase with the 1-3 keV X-ray pulsations to within 0.5 s. McClintock et al.[227] concluded that a significant portion ($\gtrsim 8\%$) and possibly the bulk of the optical emission is produced within $\sim$0.5 lt-s of the neutron star. This indicates that relatively little optical emission comes from the X-ray heated surface of the dwarf companion; most of it probably comes from an accretion disk[227] (see also Sect. 4.2.7c and ref. 231). Although 4U1626-67 is not a burst source, these results lend support to the emerging model of galactic bulge sources as highly compact binary systems with low-mass companion stars, wherein most of the optical light results from the reprocessing of X-radiation in an accretion disk[149,198,232,256] (see also Sects. 4.2.7c and 6.4).

4.2.7e The Need for a Companion Star

From the above considerations, it seems very likely that galactic bulge sources, as a class, are low-mass, close-binary stellar systems. There is an additional argument in favor of binary systems, which comes from the X-ray observations alone and which historically predates those based on the optical and the combined optical/X-ray observations. In principle, a collapsed object of roughly solar mass could be adequately powered by accretion from the interstellar medium to produce the observed persistent high X-ray luminosity

if it were in a dense ($> 10^6$ cm^{-3}) interstellar cloud[245]. This seems very unlikely, however, since no intrinsic low-energy absorption is observed in the spectra of the persistent emission. Moreover, the galactic latitude of some of these sources argues strongly against the presence of such dense clouds. Hence, another supply of accreting matter must be present. In some cases, the sources might be isolated neutron stars with massive fossil accretion disks[247]; however, if this were so in all cases, it is difficult to understand why they occur preferentially in the cores of centrally condensed globular clusters.

4.2.8 Infrared Bursts from Type I Burst Sources?

Apparao and Chitre[5] have suggested that the very bright ($\sim 10^{37}$ ergs s^{-1}) infrared bursts reported from the Rapid Burster (Sect. 4.3.10) are due to a cyclotron maser instability and that they are associated with type I bursts (see also ref. 162). If this is so, infrared bursts may also be associated with type I bursts from the sources listed in Table 4. Since the ratio of the integrated infrared flux[139,162] to the typical type I X-ray burst flux from the Rapid Burster[127] is of order 10^{-1}, one could perhaps expect similar values for type I bursts from other sources.

Lewin et al.[179] have reported evidence that this was not the case for a type I burst from Ser X-1 (= MXB1837+05 = 4U1837+04). During the worldwide coordinated burst watch in 1977, a type I X-ray burst from this source was observed with SAS-3 on 1977 June 17. Simultaneous infrared observations at 2.2 μm were made, but no infrared bursts were observed[179]. The flux values for the type I bursts from the Rapid Burster and Ser X-1 are comparable[179], but the 3σ upper limit to the integrated infrared burst flux from Ser X-1 was about an order of magnitude below values reported for the Rapid Burster[139,162]. This result, while suggestive, is clearly insufficient to

determine that there is no association between type I X-ray bursts and the bright infrared bursts reported from the direction of the Rapid Burster (see Sect. 4.3.10).

4.2.9 Radio Properties of Type I Burst Sources

During the 1977 coordinated burst observations, five different type I X-ray burst sources were observed at radio frequencies. No radio bursts were detected.

Johnson et al.[137] carried out radio observations of the Rapid Burster and 4U/MXB1820-30 for ~10 h each, and MXB1837+05 and MXB1906+00 for ~30 h each. The observations were made in April and June 1977 at 2695 MHz and 8085 MHz with the NRAO Green Bank interferometer. X-ray bursts were detected with SAS-3, but no radio bursts were observed. Table 6 summarizes these results.

Thomas et al.[281] observed 4U/MXB1636-53 with the Parkes 64 m dish at 14.7 GHz for a total of ~4 h in June 1977. During this time an X-ray burst was detected but no radio bursts were seen. The 2σ upper limit to the radio flux for a ~6 s integration during the X-ray burst is ~200 mJy. A 2σ upper limit of 22 mJy was determined for any persistent radio source coincident with the X-ray position.

Ulmer et al.[286] observed MXB1837+05 with the VLA at 4884 MHz. Upper limits of 1 mJy were obtained for the time-averaged radio emission during three periods of observation in April and June 1977. An X-ray burst of ~17 s duration was observed with SAS-3 during simultaneous radio observations on June 12. No radio bursts were observed. The average X-ray burst flux was ~0.2-0.4 mJy, while upper limits on the radio flux were 15 mJy for a 30 s integration coincident with the X-ray burst and 4 mJy for a 10 min integration.

4.3 The Rapid Burster (MXB1730-335)

The Rapid Burster (MXB1730-335) was discovered by Lewin et al. in March 1976 (refs. 168,180). Its behavior is unlike any other known source. When the source is burst active, it can produce bursts in quick succession with intervals as short as ∿10s (see Fig. 21). As discovered by Hoffman, Marshall and Lewin[127], two distinctly different types of bursts are produced by this source, which led to the classification of type I and type II X-ray bursts[127].

4.3.1 Type I and Type II Bursts

In contrast to the type I bursts, the type II bursts do not show a significant amount of spectral softening during burst decay, and, in general, they recur on time scales about one to two orders of magnitude shorter than those of type I bursts[127] (see Table 3). The Rapid Burster is the only object known to produce both type I and type II bursts[127] (see Table 3, Figs. 22 and 23). Type I bursts were detected at intervals of several (∿3-4) hours[127] and are only (but not always) observed when there is also type II activity[127,218]. The type I bursts sometimes have a noticeable effect on the type II bursts[127].

The average power in type II bursts is about 130 times that in type I bursts (when the latter are present)[127]. This is consistent with the idea that the type I bursts result from the release of nuclear energy (∿1 MeV per nucleon for helium burning) and the type II bursts result from the release of gravitational potential energy (∿100 MeV per nucleon) (refs.141, 142, 144, 165, 208, 319; see also Sect. 6.3.2).

4.3.2 Type II Burst Profiles and Saturation

The type II bursts from the Rapid Burster have rise times of ∿1 s, and they last from a few seconds up to about ten minutes (refs. 16,131,172,180, 215,218,287,305). Structure on time scales down to 50 ms has been observed[287]. When the burst duration is in excess of about 15 s, they

saturate in intensity and have "flat" maxima, as shown in Figures 21 and 24. Inoue et al.[131] reported that in observations with Hakucho in August 1979, the "saturated" peak flux actually varied by a factor of four. Basinska et al.[16] subsequently found that in March 1976 the saturated peak flux (among a total of ~220 type II bursts observed with SAS-3) varied by a factor of ~3; during 1979 March ~3-5, they varied by a factor of 1.7. Both sets of data suggest that the variability of the peak flux (in saturated bursts) is highest when the time-averaged X-ray luminosity is high, which seems to occur early in each burst-active period[218].

4.3.3 E-Δt Relation For Type II Bursts

For moderately energetic type II bursts from the Rapid Burster (total emitted energies in excess of ~4 x 10^{38} ergs for isotropic emission and an assumed distance of 10 kpc), the integrated burst energy, E, is approximately proportional to the "waiting time", Δt, to the next burst (refs. 131, 172, 180, 218, 305). For weak bursts, this approximately linear relation breaks down[172,180,305] (see Fig. 25).

4.3.4 Type II Bursting Patterns (Modes)

There seem to be prefered type II burst recurrence patterns in the Rapid Burster. H. Marshall et al.[218] distinguished two patterns (modes), as illustrated in Figures 26 and 27 (see also ref. 172). They suggested that mode I occurs near turn-ons of the burst-active periods and mode II later on. In mode I, there is a large spread in burst energies (by a factor of ~100), and histograms of the distribution of the burst energies show a distinct double peak (Fig. 27). In mode II, the bursts do not vary as much in energy as in mode I, and the energy distribution is not double peaked.

At times, the type II bursts from the Rapid Burster can be of almost equal energy and spaced at nearly equal time intervals. On UT 1976 March 10.7 the bursts were nearly constant in energy and spaced almost regularly at ∿16 s intervals. On UT 1976 April 4.2 the burst energies were again nearly constant, and the bursts were then spaced at intervals of ∿30 s (see Fig. 16 in ref. 172). On the latter occasion one could select trains of bursts of ∿10 min duration whose recurrence intervals would fit nearly constant periods[219].

There seems to be at least one other stable bursting mode[131] whereby the bursts are very energetic (they last ∿1-10 minutes). These very long bursts were first observed with SAS-3 by F. Marshall in March 1979, probably during the early part of the turn-on of a burst-active phase[16,215] (Fig. 24). The very long bursts observed ∿5 months later by Inoue et al.[131] with Hakucho[161] were detected for more than a week, and they too were observed early on in a burst-active period.

4.3.5 Anomalous Bursts

"Anomalous" bursts from the Rapid Burster were reported by Ulmer et al[287]. These bursts have rise times of about 3 s and low peak intensities (no more than 20% the intensity of saturated type II bursts), and they violate the E-Δt relation for type II bursts. They appeared only after the detection of very energetic type II bursts. They probably do not have a distinct spectral softening during burst decay (as is also the case for the type II bursts), but this is somewhat uncertain[127]. It is unclear whether these "anomalous" bursts are more closely related to type I or type II bursts.

4.3.6 Recurrent Transient Behavior

The Rapid Burster is a recurrent transient X-ray source with a recurrence period of about six months[97,170,218,304]. The duration of the periods of burst activity are not well known since X-ray observations of the Rapid

Burster are scant (see Fig. 28). One period of burst activity (in 1976) lasted at least five weeks, another (in 1978) could not have lasted longer than three weeks. The time-averaged type II burst flux can vary by a factor of $\sim$2 in a few days[218] and tends to be higher during the early part of a burst-active phase than later on[16,218]. The "light curve" of the time-averaged type II burst flux[218] is not as smooth as that of some of the classical "soft" transients. The intervals between transient outbursts ($\sim$6 months) are short and among the most regular of all X-ray transients[3,53,151]. The recurrent outbursts are most likely due to periodic enhanced accretion onto the X-ray star, which varies for reasons that are currently unknown.

4.3.7 X-Ray Emission Between Type II Bursts

An upper limit to the X-ray emission between type II bursts from the Rapid Burster was set at less than 4×10^{37} ergs s^{-1} (for an assumed source distance of 10 kpc) in early March 1976, when the time-averaged burst luminosity was about 2×10^{37} ergs s^{-1} (ref. 180). White et al.[305] set an upper limit for interburst emission during April 1977 of 3×10^{36} ergs s^{-1}, or 20% of the time-averaged burst luminosity that was then observed.

Further detailed analysis of the March 1976 SAS-3 data established the presence of X-ray emission between type II bursts. The enhanced emission which can be seen by careful inspection of Figure 21 was observed after the occurrence of very energetic type II bursts[218,295] ($\sim 3 \times 10^{39}$ ergs for an assumed source distance of 10 kpc). This emission can last for $\sim$1-5 min; it rises in $\lesssim$20 s and decays in $\lesssim$30 s shortly before the next type II burst occurs (see Fig. 29). In March 1976 this emission (at maximum intensity) was about half the time-averaged type II burst flux, and the mean flux contained in this emission equaled about 5 percent of the time-averaged type II burst flux.

Emission between type II bursts was also observed with HEAO-1 in March 1978 (ref. 128) and with Hakucho in August 1979 (ref. 280). During the latter observations, between August 8 and 10, the observed luminosity between bursts was $\sim 2 \times 10^{37}$ ergs s^{-1} (for an assumed source distance[160] of 10 kpc). This value was comparable to or somewhat smaller than the time-averaged type II burst luminosity.

4.3.8 Persistent Emission in Burst-Off State?

Several attempts have been made to find out whether the Rapid Burster emits X-rays when there are no bursts. The best upper limit was recently reported by Grindlay[93], based on observations with the Einstein Observatory. On 1979 April 10 the mean X-ray luminosity was less than 10^{34} ergs s^{-1} (for an assumed source distance[160] of 10 kpc).

4.3.9 Black-body Radii of the Rapid Burster

The spectral data for both type I and type II bursts from the Rapid Burster can be fit reasonably well by black-body spectra[218]. For the type I bursts, a radius of about 9 ± 2 km is found for the emitting region (under the assumptions of a spherical emitting surface and a source distance of 10 kpc), and the radius remains approximately constant throughout each burst. During the type I burst decay the temperature decreases rapidly from a maximum temperature of $\sim 3 \times 10^7$ K. For type II bursts a constant temperature of $\sim 1.8 \times 10^7$ K is found and the radius of the emitting region decreases from ~ 16 km to $\lesssim 10$ km. For short type II bursts this can happen in only a few seconds[218]. These scale sizes indicate that the Rapid Burster is probably a neutron star (see also ref. 318, Sects. 4.2.6 and 6.1.4).

4.3.10 Infrared Bursts from the Rapid Burster?

Infrared bursts have been detected from the direction of the Rapid Burster by two groups, first during 1979 April 4-5 by Apparao *et al.*[6] and

Kulkarni et al.[162] and then during 1979 September 5-12 by Jones et al.[139]. No simultaneous X-ray observations were made during these observations. It is not clear whether the Rapid Burster was in a burst-active phase during either of these observation periods (see Fig. 28). It was probably not in a burst-active phase during 1979 September 5-12, since by August 23 the preceding burst-active phase had already almost ceased (M. Oda, private communication).

The observations by Apparao et al.[6] and Kulkarni et al.[162] were made at ∿1.6 μm, while Jones et al.[139] made their observations at ∿2.2 μm. During April 1979, six bursts were detected in 2.6 h of observation (Fig. 30), and during September 1979 two bursts were detected in a total of ∿5.3 hours of observation (Fig. 30). The interval between bursts 3 and 4 (see Fig. 30) was ∿144 s, and that between bursts 5 and 6a was ∿114 sec. The interval between feature 1a and 2a (see Fig. 30) was ∿54 s. The peak fluxes are comparable for all eight observed infrared bursts. Two of the seven brief infrared "flashes" (1d and 2c), observed in September 1979 (Fig. 30). were unresolved (half width <0.3 s). Similar brief flashes were not found in the April 1979 data; however, it is not clear whether such features would have been detected if they were present, as the time resolution for the April 1979 observations was 0.6 s and the signals were ∿2-3 times noisier than during the September 1979 observations.

During 1979 August 9-12, Sato et al.[259] made infrared observations (at 0.8 μm, 1.6 μm, 2.2 μm and 3.6 μm) of the Rapid Burster. The Rapid Burster was definitely in a burst-active phase[131,259] (see Fig. 28). No infrared bursts were detected in a total of ∿6 h of observing. For one particular type II X-ray burst (of > 126 s duration) the upper limits to the integrated burst fluxes at 1.6 μm and at 2.2 μm are more than one order of magnitude lower than

those reported by Kulkarni et al.[162] and Jones et al.[139]. A few days later, during 1979 August 16-23, Glass[85] made infrared observations (at 2.2 μm) of the Rapid Burster for a total of ∿3.5 h while type II X-ray bursts were again detected simultaneously with Hakucho[85]. Again, no infrared bursts were observed[85]. The upper limits (at a 3σ level of confidence) for 15 s of integration are an order of magnitude below the integrated infrared flux values reported earlier[139,162].

If the infrared bursts[139,162] are real and are emitted isotropically, and for an assumed source distance of 10 kpc, the emitted energy in the infrared bursts is in the range of $\sim 6 \times 10^{37}$ ergs (burst 2, Fig. 30) to $\sim 3 \times 10^{38}$ ergs (burst 1, Fig. 30). The emitted energy in each type I X-ray burst from the Rapid Burster[127] is $\sim 10^{39}$ ergs, while the energy in a type II X-ray burst ranges from $\sim 10^{38}$ to $\sim 10^{41}$ ergs. The peak luminosities of the infrared bursts are $\sim 10^{37}$ ergs s^{-1}; the peak luminosities of both type I and type II X-ray bursts from the Rapid Burster are $\sim 10^{38}$ ergs s^{-1}.

The infrared bursts cannot be of thermal origin[139,162]. Apparao and Chitre[5] have suggested that they are due to a cyclotron maser instability and that they are associated with type I bursts (see also Kulkarni et al.[162]). They therefore suggest that similar bright infrared bursts should be, in general, observable from type I X-ray burst sources. There is some evidence that this is not the case (see Sect. 4.2.8).

It would be very valuable to obtain more simultaneous infrared and X-ray observations of the Rapid Burster. To date, infrared bursts have only been detected when no simultaneous X-ray observations were made[139,162]; they were not detected when simultaneous X-ray observations were made and type II X-ray bursts were observed[85,259].

In view of the null results described above, it is presently uncertain whether the reported infrared bursts are real and, if they are, whether they are associated with the X-ray bursts.

4.3.11 Radio Bursts from the Rapid Burster?

Calla et al.[30,31], have reported microwave bursts (at 4.1 GHz) from the direction of the Rapid Burster. Bursts were observed during 1979 April 4-16, August 20, September 18-21 and 1980 March 21. During 1979 April 14-16 the Rapid Burster was probably not in an active phase (see Fig. 28); during 1979 August 20, it was definitely X-ray burst-active[85]; and during 1979 September 18-21 it was probably not in an active phase since by 1979 August 23 the preceding burst-active phase had already almost ceased (M. Oda, private communication). It is not known whether the Rapid Burster was active on 1980 March 21.

The radio burst profiles are somewhat erratic, and burst durations varied from ∿8 s (on 1979 April 16) to ∿10 min (on 1979 August 20). Two bursts of ∿10 min duration with only ∿6 min separation between them were observed on 1979 August 20. The rise times of the bursts ranged from a few s to ∿90 s. Peak amplitudes ranged from ∿0.2 db to ∿3 db (refs. 30 and 31), where a peak amplitude of 0.25 db is estimated[253] to correpond to ∿270 Jy. On 1979 April 21, ten radio bursts were detected in about 1.3 h of observing time (O. Calla, private communication).

Simultaneous X-ray and radio (at 2695 MHz and 8085 MHz) observations of the Rapid Burster were made by Johnson et al.[137] in April 1977. The radio observations were made for a total of ∿10 h with the NRAO Green Bank interferometer and the X-ray observations with Ariel 5 and Copernicus. At this time the Rapid Burster was in an active phase (see Fig. 28); the two X-ray observatories detected a total of 64 X-ray bursts during the simultaneous radio observations. No radio bursts were detected (see Table 6).

One-sigma upper limits at both 2695 MHz and 8085 MHz were ∿20 mJy, which is ∿4 orders of magnitude smaller than the peak fluxes of the radio bursts reported by Calla et al.[30,31].

Simultaneous X-ray and radio (at 327 MHz) observations were also made during 1979 August 13-14 (ref. 253). The Rapid Burster was definitely in a burst-active phase[131] (see Fig. 28); at least two type II X-ray bursts were observed[131] during the ∿10.5 h of observation with the Ooty radio telescope. However, no radio bursts were observed. Upper limits to the peak radio flux densities were ∿1 Jy.

In view of these null results it is presently uncertain whether the reported radio bursts are real and, if so, whether they are associated with X-ray bursts. It would be useful to obtain further simultaneous radio and X-ray observations of the Rapid Burster.

4.4 Type II Bursts from Other Sources?

Type II bursts distinguish themselves from type I bursts in two ways: (i) the time scales of recurrence are two to three orders of magnitude shorter; and (ii) there is no strong spectral "softening" during burst decay (see Table 3). The "flare-burst-like" events observed from the X-ray pulsars GX 304-1 (ref. 229) and GX 301-2 (ref. 29) and from the X-ray binaries Cyg X-1 (ref. 40) and LMC X-4 (ref. 71) meet the phenomenological definition for type II bursts and, as suggested by Hoffman, Marshall and Lewin[127], they may be caused by the same mechanism as the type II bursts in the Rapid Burster (see Fig. 31). In any case, it seems likely that the "burst-like" events from these four sources and the type II bursts from the Rapid Burster are all due to instabilities in the accretion flow.

5. FAST TRANSIENTS (BURSTS?)

Many fast X-ray transient events of duration from several minutes up to a few hours have been reported[123,268,324,325]. Intensity profiles and spectral evolution are not known for any of the ~20 high galactic latitude events observed with Ariel 5 (K. Pounds, private communication and ref. 325) nor for the high galactic latitude event observed by Rappaport et al.[324] with SAS-3. It is unclear at this time whether these events are related to type I X-ray bursts. However, an event of ~600 s duration observed by Swank et al.[268] exhibited spectral characteristics and spectral evolution that are indistinguishable from an ordinary type I X-ray burst (see Sect. 4.2.6), and it seems highly likely that this event is generically related to type I bursts.

Hoffman et al.[123] have reported two events which may have been type I X-ray bursts[123] (Figs. 32-35). An event on 1977 February 7 lasted ~1500 s, and an event on 1977 June 28 lasted ~150 s. Both events were preceded by precursor pulses which lasted only a few seconds and which rose and fell in less than 0.4 s. The precursors were separated from the "main" events by several seconds, during which no X-rays (other than those due to background radiation) were detected. The spectra of the main events started out much softer than the spectra of the precursors. There are similarities between the two main events and ordinary type I X-ray bursts in both their temporal and spectral evolution. The spectra of the main events became harder as they approached maximum intensity and softened substantially as they decayed. In the main event of 1977 February 7, X-rays with energies greater than 10 keV were delayed by about 80 s relative to the 1.5-6 keV X-rays. A black-body fit to the spectral data of the main event of 1977 February 7 gives a maximum

temperature of 2.9×10^7 K (Fig. 35) and a radius of the emitting region of $\gtrsim 9$ km (under the assumption of a spherical surface and a source distance of 10 kpc). This is similar to the properties of many type I X-ray bursts (see Sects. 4.2.6 and 4.3.9). If the 1977 February 7 event came from a catalogued X-ray source, it was probably 4U1708-23 (see Fig. 2 of ref. 123).

As pointed out by Hoffman et al.[123], if the 1977 June 28 event came from a catalogued X-ray source it must have been MX1716-31 (ref. 213). This source was also the probable origin of a $\sim$10 min X-ray flare on another occasion[212], and ordinary type I X-ray bursts have also been detected from this source[241]. If MX1716-31 is the origin of the 1977 June 28 event, then the integrated energy flux was $\sim 6 \times 10^{-8}$ ergs cm^{-2} in the precursor and $\sim 3 \times 10^{-6}$ ergs cm^{-2} in the main event.

Extended SAS-3 observations, lasting for weeks and covering the large regions of the sky from which these events were seen, detected only these two. It thus seems that if these events are repetitive, the intervals are quite long. It might be possible to account for the durations, recurrence intervals and precursors in these events in terms of thermonuclear flashes that occur relatively deeply beneath the surfaces of slowly accreting neutron stars (see Sect. 6.3.3).

6. THEORY

Nearly all mechanisms that have been proposed to account for the X-ray burst phenomenon utilize accretion of matter onto a collapsed object (degenerate dwarf, neutron star or black hole). In every instance, the collapsed object serves at least one of two functions: its deep gravitational potential well allows the release of large amounts of gravitational energy in the form of X-radiation by the accreting matter, and its small dimensions

permit the X-ray emission to be released on the short time scale of an X-ray burst. The generic relations among the various proposed models are indicated schematically in Figure 36.

The proposed models can be broken down into two broad classes: (1) those invoking instabilities in the accretion flow onto a collapsed object; and (2) those that invoke thermonuclear flashes in the surface layers of an accreting neutron star. During the last few years, the greatest amount of progress has been achieved in developing the thermonuclear flash model, which has proved to be amenable to detailed numerical computations. As will be documented below, these calculations have been remarkably successful in accounting for the general properties of type I X-ray bursts. Moreover, the theoretical work to date strongly suggests that the characteristics of type I bursts should be capable of imparting substantial constraints upon the properties (e.g., masses, radii and internal temperatures) of the underlying neutron stars. However, as will be discussed in Sect. 6.2, it presently seems virtually certain that an accretion instability is responsible for type II bursts (see also Sect. 4.3.1). Hence, more theoretical work on such instabilities is presently called for.

6.1 Thermonuclear Flash Models for Type I Bursts

6.1.1 Historical Development

When binary X-ray pulsars were discovered in 1971 (refs. 193,260,279, 316), it was almost immediately recognized that these objects were probably neutron stars that were undergoing accretion from binary stellar companions. Soon thereafter, in 1973, Rosenbluth *et al.*[257] pointed out that nuclear fusion in the surface layers would be an independent source of energy that might be radiated from the neutron-star photosphere. A few years later, in 1975, Hansen and Van Horn[110] demonstrated that over a wide variety of conditions,

the nuclear burning ought to be unstable and should lead to thermonuclear flashes.

Hansen and Van Horn[110] noted that the energy released in such flashes might produce variable X-ray emission from the neutron star. However, they also discovered that the characteristic time scale for thermonuclear runaway was usually $\lesssim 1$ s. This was considerably shorter than most of the time scales of variability from X-ray sources that were then known (with the exception of the periodic pulses from some X-ray pulsars). Van Horn and Hansen[289] attempted to construct a hydrogen-flash model for the transient X-ray sources (which typically have rise times of a few days and decay time scales of weeks to months), but they were forced to resort to extremely low-mass ($\lesssim 0.15\ M_\odot$) neutron stars to get sufficiently thick hydrogen-rich envelopes and sufficiently long runaway time scales.

Following the discovery of X-ray bursts in 1975, a number of possible explanations for this phenomenon were soon advanced (see Fig. 36). Among the early proposals was the suggestion by Woosley and Taam[308] and Maraschi and Cavaliere[208] that X-ray bursts result from thermonuclear flashes on accreting neutron stars (see Sect. 4.1). This suggestion spurred more detailed investigations by Joss[141], Lamb and Lamb[165] and Taam and Picklum[275] into the physics of nuclear flashes on accreting neutron stars and their possible relation to X-ray bursts. Subsequently a number of authors, including Joss[142], Taam and Picklum[276], Joss and Li[148], Fujimoto, Hanawa and Miyaji[82], and Taam[274] have presented the results of detailed numerical computations of flashes of this type. Other discussions of various aspects of thermonuclear flashes on accreting neutron stars have been presented by Czerny and Jaroszynski[60], Ergma and Tutukov[72], Hoshi[130] and Barranco, Buchler and Livio[15].

6.1.2 The Overall Physical Picture

Consider a neutron star undergoing accretion from a binary stellar companion. The freshly accreted matter will be rich in hydrogen and/or helium. However, at depths greater than $\sim 10^4$ cm beneath the surface of the neutron star, the density is sufficiently high that nuclear statistical equilibrium will be swiftly achieved; the predominant nuclei will have maximal binding energies, with atomic weights of ~ 60. (Still deeper in the star, these nuclei dissolve into a fluid in which neutrons are the primary constituent.) Hence, the accreting matter must pass through a series of nuclear burning shells as it is gradually compressed by the accretion of still more material. If the core of the neutron star is sufficiently hot or the accretion rate is sufficiently high, the temperature in the surface layers will be high enough that the burning will proceed via thermonuclear reactions, rather than electron capture or pycnonuclear reactions (which are driven by high densities rather than high temperatures). A sketch of the resultant structure of the neutron-star surface layers is given in Figure 37.

It was first realized by Hansen and Van Horn[110] that these burning shells will tend to be unstable to thermal runaway. The instability, known as the "thin-shell instability," was first discovered in a different context by Schwarzschild and Härm[261]. The existence and strength of the instability are a direct result of the strong temperature dependence of the thermonuclear reaction rates. In the case of neutron-star envelopes, the instability is further enhanced by the partial degeneracy of the burning material. A cogent and thorough technical discussion of this type of instability has been given by Giannone and Wiegert[83] (see also ref. 15).

The p-p chains are insufficiently temperature-sensitive to produce a thermal runaway in the hydrogen-burning shell of a neutron star. The

instability of this shell is thus largely quenched by the saturation of the CNO cycle at very high reaction rates[141,165]. The saturation results from the appreciable lifetimes ($\sim 10^{2-3}$ s) of the beta-unstable nuclei ^{13}N, ^{14}O, ^{15}O and ^{17}F that participate in the cycle. For low neutron-star core temperatures ($\lesssim 1 \times 10^8$ K) the shell can in principle be unstable, but any runaways will be halted by the saturation effect before the release of a substantial amount of energy (see, however, the discussion of interacting hydrogen-helium shells in Sect. 6.1.3 below). The next shell inward is the helium-burning shell, which should be unstable over a wide range of conditions. It is uncertain whether there will be any other significant burning shells, as the matter might already burn to quite heavy elements in the helium shell[142,275]. However, if a carbon shell exists, it is very likely to be unstable also[275,308].

Dimensional analysis[141,165] indicates that the helium-burning flashes should have the following properties: (1) They should occur after the accumulation of 10^{21} g of fuel and release total energies of $\lesssim 10^{39}$ ergs per flash. (2) For accretion rates comparable with those observed in X-ray pulsars ($\lesssim 10^{17}$ g s^{-1}), the time interval between flashes should be $\sim 10^4$ s, very roughly. (3) The transport of energy through the surface layers should result in the emission of bursts of electromagnetic radiation from the neutron-star photosphere with rise times of ~ 0.1 s, peak luminosities of $\sim 10^{38}$ ergs s^{-1}, decay time scales of ~ 10 s, and peak black-body temperatures of $\sim 3 \times 10^7$ K (if a full 10^{39} ergs of energy is indeed released in a single flash).

Carbon-burning flashes, if they exist, would occur much deeper beneath the neutron-star surface ($\sim 10^4$ cm, compared to $\sim 10^2$ cm for the helium shell) and would result in the release of substantially more energy. Hence, the duration of a "burst" resulting from a carbon flash should be much longer than

for a helium flash[141], unless dynamical effects are generated in the outermost surface layers.

6.1.3 Numerical Models

The above estimates, though very crude, suggest that thermonuclear flashes on accreting neutron stars could account for the observed properties of type I burst sources. With this encouragement, detailed numerical computations of the evolution of the surface layers of an accreting neutron star have been carried out.

Joss[142] explored the evolution of the helium-burning shell (see also Hoshi[130]). In these calculations, the neutron star was chosen to have a mass of $M = 1.4\ M_{\odot}$ and a radius of $R = 6.6$ km. A simplified nuclear reaction network was used, incorporating the dominant reactions linking the nuclei from ^{4}He to ^{28}Si and allowing the release of most of the available nuclear energy. The accretion was assumed to be spherical and the star was taken to be nonrotating and unmagnetized, so that spherical symmetry could be assumed throughout the calculations. Moreover, the effects of hydrogen burning upon the structure of the surface layers was neglected. The importance of these assumptions and approximations will be discussed below.

Joss' models[142] contain two free parameters: the mass accretion rate, $\dot{m}$, and the core temperature of the neutron star, T_c. The values of $\dot{m}$ and T_c used in four models are indicated in Figure 38. If the core of the neutron star is in thermal equilibrium (i.e., if the heat flow into the core from the surface layers during thermonuclear flashes is just balanced by the heat lost from the core between flashes), then there is a unique relationship between $\dot{m}$ and T_c (ref. 165); the estimated locus of these equilibrium values, as given by Joss[142] (see also ref. 148), is shown in Figure 38. Three of the four models calculated by Joss[142] displayed thermonuclear flashes in the helium-burning

shell (see Figs. 39 through 41). The properties of these flashes were in good agreement with those expected from dimensional analysis[141,165]. More importantly, these calculations indicated that (1) a full $\sim 10^{21}$ g of matter accumulates on the neutron-star surface before each helium flash, (2) a flash consumes virtually all the available nuclear fuel and probably synthesizes mostly iron-peak elements, and (3) most of the energy of a flash is transported to the photosphere and lost as X-radiation, rather than carried inward to heat the interior of the star. These properties of the flashes had not been discerned prior to the performance of detailed evolutionary computations, at least partly because they depend upon the highly nonlinear characteristics of the flash growth and decay.

The behavior of the helium-burning shell was further explored by Joss and Li[148], who investigated the sensitivity of the flash properties to the assumed mass and radius of the neutron star. They argued that since each helium-burning flash apparently consumes virtually all the available nuclear fuel, the nuclear physics essentially factors out of the problem and most of the mass- and radius-dependence of the flash properties follow from a few basic physical considerations. Thus, the recurrence interval τ_R between flashes is just the amount of time required for the base of the helium-rich layer to reach the critical temperature and density for a flash to commence, which is roughly proportional to the surface area ($A = 4\pi R^2$) of the neutron star and to the scale height in its surface layers. The scale height, in turn, is roughly inversely proportional to the surface gravity $g = GM/R^2$. It then follows that

$$\tau_R \sim A\, g^{-1} \sim R^4\, M^{-1} . \qquad (6\text{-}1)$$

Similarly, the peak surface X-ray luminosity (L_{max}) following a flash just

scales as the Eddington limit[141], which is proportional to M but is independent of R; thus,

$$L_{max} \sim M \quad . \tag{6-2}$$

Finally, the time scale (τ_D) of decline of surface X-ray emission following a flash is roughly directly proportional to the energy released in the flash, which is in turn directly proportional to τ_R and inversely proportional to the rate ($\sim L_{max}$) at which that energy escapes the star; thus,

$$\tau_D \sim \tau_R / L_{max} \sim R^4 M^{-2} \quad . \tag{6-3}$$

Joss and Li[148] carried out numerical computations of the evolution of the helium-burning shell for neutron stars with a few different masses and radii (see Fig. 42) and fitted their results for τ_R, L_{max} and τ_B to power-law expressions in M and R. They obtained

$$\begin{aligned} \tau_R(\text{fit}) &\sim R^{3.1} M^{-0.5} \quad ; \\ L_{max}(\text{fit}) &\sim R^{0.1} M^{0.8} \quad ; \\ \tau_D(\text{fit}) &\sim R^{3.1} M^{-1.4} \quad . \end{aligned} \tag{6-4}$$

These expressions are in reasonably good agreement with relations (6-1) through (6-3). The existence of these simple scaling relations suggests the intriguing possibility that once the physics of neutron-star thermonuclear flashes is sufficiently well understood, it may be possible to deduce infor-

mation on the masses and radii of neutron stars from the observed properties of X-ray bursts that result from such flashes. (As noted by Joss and Li, however, these scaling relations should not be applied to the observational data until the remaining major uncertainties in the theoretical calculations have been resolved.) The indirect measurement of general relativistic effects from the burst properties may be even more powerful in this regard (see Sect. 5.1.4).

Joss and Li[148] also investigated the evolution of the helium-burning shell in models wherein the effects of an intense magnetic field upon the surface layers were taken into account. They argued that if the magnetic field is sufficiently strong to funnel the accretion onto the magnetic polar caps of the neutron star, then the effective accretion rate in the polar cap regions is enhanced by a factor of $\sim 10^3$ (for a fixed total accretion rate $\dot{m}$) and the instability of the nuclear burning shells should be reduced (see also refs. 141 and 275). The surface magnetic field strength, B, required to funnel the accretion is not well determined, but available estimates (see, e.g., Arons and Lea[8]) yield $B \approx 10^{12}$ G. Joss and Li[148] also incorporated into their model calculations the significant reductions in the radiative[322] and conductive[323] opacities that would be produced by magnetic fields in excess of $\sim 10^{12}$ G, and found that these effects further reduce the instability of the nuclear burning shells.

It has become increasingly clear that hydrogen burning can have a major influence on the behavior of the helium-burning shell[60,72,275]. The saturation of the CNO cycle by the non-negligible lifetimes of the beta-unstable nuclei that participate in the cycle limits the hydrogen-burning rates to such an extent that, at sufficiently high accretion rates ($\gtrsim 1 \times 10^{16}$ g s^{-1}), the hydrogen-burning shell is forced inward until it overlaps the helium-burning

shell. Taam and Picklum[276] and Taam[274] have carried out the first fully time-dependent computations of the evolution of the surface layers of a neutron star with a hydrogen-burning shell included and found that the hydrogen- and helium-burning shells can, indeed, interact in a complex way (see Fig. 43). In fact, in their models, the heating of the accreted material by the neutron-star core prior to a thermonuclear flash was negligible compared to the heating that resulted from hydrogen burning. However, this effect appears to have been a consequence of the low core temperatures chosen for the neutron star ($<10^8$ K); such cores would generally not be in thermal equilibrium with the nuclear burning shells, but they might represent the properties of an old neutron star that has begun to accrete matter during the past $\sim 10^{2-3}$ yr.

Fujimoto, Hanawa and Miyaji[82] have also studied the interaction between the hydrogen- and helium-burning shells. They argued that for neutron stars with low core temperatures there will be three modes of thermonuclear flashes: helium flashes followed by simultaneous helium burning and hydrogen burning when the two shells overlap at high accretion rates, pure helium flashes at intermediate accretion rates, and hydrogen flashes that ignite the helium-burning shell at low accretion rates. However, we note that due to the saturation of the CNO cycle, the rise in temperature ΔT due to a hydrogen flash is limited to

$$\Delta T \lesssim 10^8 \text{K} \left(\frac{X_{CNO}}{10^{-2}}\right) , \qquad (6\text{-}5)$$

where X_{CNO} is the fractional abundance by mass of CNO nuclei[9]. Hence, it seems that unless the abundances of the CNO nuclei in the accreting matter are substantially higher than their cosmic abundances, a hydrogen flash will usually be unable to fully ignite the helium shell and the third scenario

described by Fujimoto et al. will not be realized. Nonetheless, it has become apparent from all of the above work that the interactions between the hydrogen- and helium-burning shells may be very complex; it is very likely that still further complications will be uncovered by future work.

Fujimoto et al.[82] and Murakami et al.[234] have suggested that different "modes" of observed bursting behavior in 4U1608-52 (see Sect. 4.2.3) could be identified with changes in the character of the interaction between the hydrogen- and helium-burning shells as the accretion rates vary. However, in view of the great complexity of the observational data (see Chap. 4) and the remaining theoretical problems, we feel that such suggestions are presently very speculative. Our caution in this regard seems to gain support from 1980 observations of 4U1608-52 with the Hakucho satellite (M. Oda, personal communication), in which the bursting behavior does not fit into either of the "modes" identified by Murakami et al.[234].

Taam and Picklum[275] studied the thermal evolution of a carbon-burning shell in an accreting neutron star but did not carry their computations through a complete thermonuclear flash. Their models again assumed low core temperatures ($<10^8$ K) that would not be in thermal equilibrium with the surface nuclear burning shells.

6.1.4 General Relativistic Effects

The work by Swank et al.[268] and Hoffman, Lewin and Doty[120,121] showed that the spectra of X-ray bursts following peak luminosity could be well represented by those of black bodies. Utilizing the assumption of black-body spectra, Van Paradijs[291] demonstrated that in many cases the scale size of the X-ray emitting region is nearly constant; if the emitting region is a spherical surface, then its radius is ~7 km (see Sect. 4.2.6). This result lends compelling support to the idea that type I X-ray bursts are thermal emission from the photospheres of neutron stars.

However, it has become apparent that this argument is complicated by general relativistic corrections, such as the effect of gravitational redshift and time dilation upon the X-radiation emitted by the neutron-star photosphere[86,292]. The potential importance of general relativity can be seen by inspection of the parameter

$$\frac{2GM}{Rc^2} = 0.60 \left(\frac{M}{1.4M_\odot}\right) \left(\frac{R}{7\text{km}}\right)^{-1} . \qquad (6\text{-}6)$$

The left-hand side of this expression is just the ratio of the Schwarzschild radius of the neutron star ($2GM/c^2$) to its actual radius. For the indicated values of M and R, which have been used in many of the actual model calculations of thermonuclear flashes, it is evident that this parameter is not very much smaller than unity, so that general relativistic effects should be substantial.

It was shown by Goldman[86] and Van Paradijs[292] that when general relativistic corrections are included in determinations of the luminosities and effective black-body temperatures of X-ray bursts, one obtains, at least in principle, strong constraints on the masses and radii of the underlying neutron stars. If taken at face value, these constraints would, in turn, severely constrain the equation of state of matter at densities in excess of nuclear-matter densities ($\rho > 2 \times 10^{14}$ g cm^{-3}). However, such constraints cannot yet be taken seriously, as other complications, including possible violations of spherical symmetry (see Sect. 6.4) and deviations of the emitted spectrum from a simple black-body spectrum[273,298], may turn out to be important. Once these additional complexities have been untangled, the observed properties of type I bursts may prove to be a powerful probe of the basic properties of neutron stars.

General relativistic corrections to the equations of stellar structure and evolution may also play a significant role in determining the behavior of the thermonuclear flashes themselves. Some of these corrections have already been included in some calculations (e.g., those by Taam and Picklum[275,276], Czerny and Jaroszynski[60] and Taam[274]). However, no fully time-dependent model computations have yet included all of the relevant general relativistic corrections.

6.1.5 Future Work

We have just begun to grasp all of the intricacies of the thermonuclear flash model for type I bursts. The theoretical problems are fascinating, not only for their probable applications to X-ray burst sources and other observational phenomena, but also as investigations in fundamental physics and as a potentially powerful tool for probing the basic properties of neutron stars.

The only complete evolutionary computations of neutron-star thermonuclear flashes that have been carried out to date[142,148,274,276] relied on a number of simplifying assumptions and approximations, such as the assumption of spherical symmetry, the neglect of possible dynamical effects, and, in some cases, the assumption that the neutron-star core is in thermal equilibrium. These approximations will have to be relaxed in future studies before this phenomenon and its observational implications can be more fully understood.

Small but significant violations of spherical symmetry might result from accretion through a relatively weak ($\lesssim 10^{11}$ G) magnetic field or the residual angular momentum of the accreting matter. If thermonuclear flashes result in X-ray bursts, such violations could be the key to the observed complexities in burst structure and recurrence patterns (see Sects. 4.2.3 and 4.2.4). For example, a thermonuclear flash that ignites on one portion of the neutron-star

surface may propagate around the star, in a pattern that varies from flash to flash and from one star to another[142]. A thorough investigation of such possibilities will eventually require two- or three-dimensional numerical computations, which will be much more difficult than the computations of spherically symmetric models that have been attempted to date.

Complexities in radiative transfer in the outer surface layers of the neutron star and possible mass ejection from the photosphere near the peak of a burst may also substantially complicate the observational properties of X-ray bursts and render their physical interpretation much more difficult. There are indications that the Eddington limit is exceeded by as much as a factor of ~10 near the peak of some type I bursts (refs. 86,103,121; see Sect. 4.2.6); if this is so, some mass ejection probably occurs. Some preliminary results on deviations from black-body emission by a hot neutron-star atmosphere have been reported[273,298], but much work in these areas remains to be done.

The importance of thermal equilibrium of the neutron-star core has been only tentatively explored (see Fig. 38). If there is a change in the average accretion rate, the thermal inertia of the core is sufficient to require the elapse of $\sim 10^{2-3}$ yr for thermal equilibrium to be reestablished[165]. Thus departures from thermal equilibrium are entirely possible, and they could have a substantial effect upon the behavior of the nuclear burning shells.

6.2 Accretion-Instability Models for Type II Bursts

Since the discovery of X-ray bursts, a number of theoretical mechanisms have been proposed that relied on instabilities associated with accretion onto a collapsed object (refs. 10,91,113,129,163,201,237,267,302,317,319). Much of the early work in this area was thoroughly reviewed by Lamb and Lamb[164]. For the reasons discussed in Sects. 6.1 and 6.3.1, it now seems likely that type I

bursts are caused by thermonuclear flashes rather than an accretion instability. However, it is also evident from the properties of the Rapid Burster that its type II bursts are, in fact, the result of an accretion instability[127] (see Sects. 4.3 and 6.3.2), and more theoretical work on such instabilities is needed.

Some of the earlier proposals[91,163,267] for accretion instabilities involved spherical accretion onto a collapsed object. Grindlay's model[91] was developed following an early suggestion by Grindlay and Gursky[95] that 3U/MXB1820-30, was associated with a massive black hole in the globular cluster NGC6624 (see Sects. 3.3 and 4.1). This model entails a purely thermal instability that does not require the presence of a magnetic field, so that the central collapsed object could be a black hole; moreover, the requisite mass of the collapsed object was well in excess of the probable maximum stable mass of a white dwarf or neutron star. However, as discussed in Sects. 3.3 and 4.1, the phenomenological reasons for favoring the idea of a massive black hole have disappeared. Moreover, Cowie, Ostriker and Stark[58] have placed rather severe physical constraints on models of this general type, and it now seems unlikely that any such model will prove to be viable.

Several models that involve the angular momentum of the accreting matter, as well as an intense magnetic field from the collapsed object, have also been advanced[10,113,129,267,317,319]. In principle, such models appear to be more promising to develop into a completely satisfactory model for type II bursts. However, the presence of nonspherical accretion substantially complicates the relevant physics, and it seems clear that none of the models advanced to date will be entirely adequate. Other models[201,302], which invoke instabilities in an accretion disk surrounding a collapsed object, are presently both rather primitive and rather far removed from observational tests. However, Wheeler's

model[302], which requires the presence of a collapsed object with a mass of $\sim 10\ M_\odot$ (almost certainly greater than the maximum stable mass of a neutron star), might be eliminated if the neutron-star nature of the Rapid Burster is accepted (see Sects. 4.3.1, 4.3.9 and 6.3.2).

6.3 Theory versus Observation

6.3.1 Type I X-Ray Bursts

The results of the numerical calculations of thermonuclear flashes (see Figs. 38-43) strongly support the conjecture that type I bursts result from such flashes. In particular, the typical burst rise times, decay time scales, peak luminosities, total emitted energies, spectral properties, low-energy "tails", and recurrence intervals (see Sect. 4.2) are reproduced remarkably well by such calculations.

However, there are some difficulties with this model. It does not predict the observed complex recurrence patterns and burst structures (e.g., the double peaks shown in Fig. 13), which vary from one burst source to another and often vary with time in a single source. Another problem for the model is the narrow range of persistent X-ray luminosities (and, presumably, a correspondingly narrow range of accretion rates) for which bursting behavior has been observed in some sources (see Sects. 4.2.2 and 4.2.4). It is quite possible that these complexities will be better understood when some of the approximations of the present model calculations are relaxed (see Sect. 6.1.5).

A particularly severe problem for the nuclear flash model is the ratio, α, of time-averaged persistent X-ray luminosity to time-averaged burst luminosity from the observed burst sources (see Sect. 4.2.5). In this model, α should just be the ratio of the gravitational energy released by accretion (more or less continuously) to the nuclear energy released in the flashes.

For helium-burning flashes, the numerical value of α should thus be[141,165]

$$\alpha \approx 100 \left(\frac{M}{M_\odot}\right) \left(\frac{R}{10\text{km}}\right)^{-1} \quad . \tag{6-7}$$

However, some type I burst sources have reported values of α significantly less than 100; one such case is 4U1608-52, which displayed two bursts separated by an interval of only ten minutes and a correspondingly small upper limit of $\alpha < 2.5$ during that interval[235] (see Sect. 4.2.5). Moreover, as discussed in Sect. 4.2.4, in some sources the recurrence intervals have been observed to increase (decrease) when the persistent luminosity increased (decreased), which is opposite to the trend expected from this model.

If the nuclear flash model for type I bursts is correct, it is possible that the observed values of α are sometimes (perhaps always) reduced by the storage of nuclear fuel during burst-inactive phases[165]. Such a "battery" mechanism may be provided by large-scale violations of spherical symmetry (see Sect. 6.1.5), so that only a fraction of the surface of the neutron star participates in each flash, or from fluctuations resulting from the interaction between the hydrogen- and helium-burning shells (e.g., fluctuations in the amount of hydrogen entrained into the convection zone generated by a helium flash). Even in the absence of any fluctuations, the entrainment of hydrogen into a helium-burning flash could, in principle, reduce the value of α by up to a factor of $\sqrt{5}$ (due to proton captures onto the heavier nuclei being synthesized and a concomitant increase in the energy yield per unit mass); the calculations by Taam and Picklum[276] and Taam[274] do not indicate any reduction in α-values by this effect, but more complete hydrogen-burning reaction networks might yield different results[9,300,315]. It has also been suggested that the accretion-driven luminosity is emitted

anisotropically and/or largely shifted to photon energies $\lesssim$1 keV; Milgrom[232] has proposed a specific mechanism that could produce both of these effects and thereby reduce the observed values of α by up to a factor of $\sqrt{2}$ (see Sect. 6.4).

In some cases, α-values considerably larger than 10^2 have been observed during burst-inactive periods in some sources. However, in the context of the nuclear-flash model, it will probably not be difficult to account for large α-values. For example, such values might result from episodes when the nuclear burning shells become relatively stable and the bursting phenomenon is intermittently suppressed, and/or from one or more inefficiencies in the nuclear flash process, such as loss of some flash energy to the core of the neutron star and partial burning of the relevant nuclear fuel between flashes.

6.3.2 Type II Bursts and The Rapid Burster

It is important to realize that the type II bursts from the Rapid Burster almost certainly cannot be the result of thermonuclear flashes (see Sect. 4.3.1). Hoffman, Marshall and Lewin[127] were the first to propose that the type I bursts from the Rapid Burster are the result of thermonuclear flashes on an accreting neutron star, while the type II bursts are the result of an unstable accretion flow onto the same object (see Sect. 6.2 for a discussion of the various proposed instabilities that may produce the type II bursts).

6.3.3 The Fast X-Ray Transients

The morphology of some of the fast X-ray transients is suggestively similar to that of ordinary type I X-ray bursts[123] (see Chap. 5). Joss[145] suggested that the fast transients may be the result of helium-burning flashes relatively deep within the surface layers of very slowly accreting neutron stars ($\dot{M} \lesssim 10^{15}$ g s^{-1}). If this picture is correct, one would expect outbursts from the fast transients to recur, but only on time scales of weeks

or longer. Moreover, the low accretion rate should result in a relatively large temperature contrast between the nuclear flashing shell and the outermost surface layers of the neutron star, so that the precursors observed in some fast transients (see Chap. 5) might be the result of shock heating of the outer surface layers. However, detailed numerical computations of deep helium-burning flashes have yet to be carried out, and in the interim the above scenario must be regarded as highly speculative.

6.3.4 Relation to Binary X-Ray Pulsars and the Ages of Burst Sources

Let us accept, for the sake of discussion, that type I bursts can be understood as thermonuclear flashes on accreting neutron stars. Since X-ray pulsars are also widely believed to be accreting neutron stars, it is then puzzling, at first sight, that these objects do not also display bursting behavior. However, the strong magnetic field ($\gtrsim 10^{12}$ G; see ref. 8) that funnels the accretion onto the magnetic polar caps of an X-ray pulsar will also enhance the efficiency of radiative and conductive heat transport within and above its nuclear burning shells. Moreover, the heat released by accretion will have a much greater influence upon the inner burning shells if the freshly accreted matter is confined to the polar caps, rather than spread uniformly over the neutron-star surface (see Sect. 6.1.3). These effects should reduce the instability of the nuclear burning shells of an X-ray pulsar against thermonuclear flashes[142,148,275]. Evolutionary models of the helium-burning shell in the presence of an intense magnetic field confirm the assertion that such fields reduce the instability of the shell[148].

With this picture, we can also understand why the persistent X-ray flux from type I burst sources is unpulsed: those neutron stars whose magnetic fields are too weak to funnel the accreting matter may be precisely those that can undergo thermonuclear flashes[142,148,225]. If the magnetic field was

originally as strong as in an X-ray pulsar but has since decayed, then the neutron star must be fairly old (probably older than 10^7 yr; see Sect. 2.1 and refs. 77, 258). The lack of X-ray eclipses in burst sources may also reflect membership in relatively old binary systems[149] and may result from X-ray beaming effects that set in after the neutron-star magnetic field has decayed (see Sects. 2.2 and 6.4 and ref. 232). The concentration of X-ray burst sources in the direction of the galactic center (see Fig. 5) and the identification of several of them with globular clusters (see Chap. 3) may well be other manifestations of membership in an older galactic population than the X-ray pulsars, which are distributed through the disk of the galaxy and whose binary companion stars are often of early spectral type.

6.4 The Highly-Compact-Binary Model for Galactic Bulge Sources

If the X-ray burst sources are a physical subset of the larger class of galactic bulge sources, the conclusion seems inescapable that all of these sources derive their X-ray luminosities, directly or indirectly, by accretion of matter onto a collapsed object which, in the case of the burst sources, is evidently a neutron star. If this is the case, then the observed X-ray luminosities (up to $\sim 10^{38}$ ergs s^{-1}) require accretion rates as high as $\sim 10^{18}$ g s^{-1}. Such accretion rates, in turn, seem to require the presence of close-binary companion stars to supply the accreting matter (provided that very massive black holes are excluded; see Sects. 3.3 and 4.1). Many of the ideas related to the basic concept of galactic bulge sources as binary stellar systems have been mentioned in earlier chapters, but for the sake of clarity we shall collect and elaborate upon these ideas in this section.

The faintness of the optical counterparts of most of these sources (see Sect. 4.2.7) rules out giant, supergiant, or early-type main sequence stellar

companions. It therefore seems likely that many of the companion stars, with perhaps only a few exceptions, are low-mass ($\lesssim 0.5\ M_\odot$) main-sequence dwarfs or degenerate dwarfs[149] (see Sect. 4.2.7c). It is, moreover, possible that such a star could only transfer sufficient mass to the collapsed star if it fills its critical potential lobe, in which case the orbital separation would be $\lesssim 10^6$ km and the orbital period $\lesssim 0.3$ days (see Fig. 17). For such highly compact binary systems, the mass transfer could be effected through the decay of the orbit due to gravitational radiation, possibly augmented by a self-excited stellar wind and/or the evolution of the companion (which could be the evolved remnant of a more massive star).

The properties of such systems can be reconciled with the observational characteristics of most of the galactic bulge sources[149]. In particular, the faintness of the optical counterparts is a natural consequence of the intrinsic faintness of the companion star; in fact, most of the very blue light that is seen results from reprocessing of X-radiation within the system, rather than from the intrinsic luminosity of the companion (see Sect. 4.2.7).

The lack of observed X-ray eclipses (see Sect. 2.2) is a bit harder to understand. Due to the small size of the companion compared to the dimensions of the system, the probability of observing eclipses in any one system is only

$$P_{eq} \approx 0.2\ \left(\frac{1+q}{10}\right)^{-1/3} \quad (q > 1), \qquad (6\text{-}8)$$

where q is the ratio of the mass of the X-ray star to that of its companion and it is assumed that the companion star fills its Roche lobe[149]. However, the a priori probability is quite high ($\gtrsim 99$ percent; cf. ref. 149) for having detected eclipses in at least one of the twenty galactic bulge sources for which adequate observations are available (see Sect. 2.2). As first suggested

by Milgrom[232], the companion may be largely shielded from the X-radiation by an accretion disk surrounding the collapsed star, which may account for this lack of eclipsing behavior. Moreover, the shielding of the companion from most of the X-radiation may account for the general lack of optical photometric variability at the orbital period (see Sect. 4.2.7). As was pointed out in Sect. 4.2.7, the observed properties of the X-ray pulsar 4U1626-67 provide indirect but persuasive evidence in favor of the highly-compact-binary model for the galactic bulge sources. There is evidence that some of the spectrally "soft" X-ray transients have somewhat more massive companions ($\gtrsim 0.5\ M_\odot$; see Sect. 4.2.7e), but it is possible that their transient nature results from an instability in the mass transfer process that is, in turn, causally related to these relatively high masses[256].

If the surface magnetic field of a neutron star has largely decayed away, as is probable for neutron stars in systems with ages of $\gtrsim 10^9$ yr (refs. 77,258), then the accretion disk may extend downward all the way to the surface of the neutron star[232]. When this occurs, up to $\sim 1/2$ the gravitational potential energy may be released in the disk rather than on the surface of the neutron star. The relatively large X-radiating surface area of the inner disk plus neutron star may then account for the "soft" X-ray spectra of the galactic bulge sources compared to those of the X-ray pulsars, whose magnetic fields are evidently strong enough to funnel the accretion flow onto the magnetic polar caps of the neutron star.

A highly compact binary stellar system of the type described above may evolve from a cataclysmic-variable system, wherein a degenerate dwarf accretes matter until it exceeds the Chandrasekhar limiting mass ($\sim 1.4\ M_\odot$), at which time it undergoes a dynamical collapse to form a neutron star[106,149,288]. It is conceivable that the formation of a neutron star under such circumstances

could be relatively "quiet," resulting in the ejection of sufficiently little mass to leave the system gravitationally bound (see, e.g., ref. 32). This scenario and the subsequent evolution of the binary systems have most recently been discussed by Li et al.[198]. It is plausible that a sufficient rate of mass transfer can be driven by the decay of the orbit due to gravitational radiation, but more detailed numerical calculations now in progress[256] indicate that the evolutionary history of the system is substantially influenced by the thermal evolution of the companion star. Much more work on the evolution of such systems remains to be done.

We note that the evolution of the X-ray sources in globular clusters is likely to be somewhat different from those of other galactic bulge sources. It is possible that many or all of the galactic bulge sources outside globular clusters are primordial binaries, but the observational statistics suggest that the globular cluster X-ray sources are binary systems formed by capture rather than primordial binaries (see Chap. 3). We also note that some of the non-bursting galactic bulge sources might conceivably contain black holes with masses of the order of a few solar masses, formed when a neutron star accretes sufficient matter to exceed its maximum stable mass[146]. (Most current theoretical estimates place the maximum stable mass of a neutron star at $\sim 2\ M_\odot$.) However, there is presently no compelling theoretical or observational evidence for the existence of black holes of any mass in any of the galactic bulge sources.

7. CONCLUDING REMARKS

The past several years have witnessed an enormous increase in observational and theoretical information on the galactic bulge X-ray sources in general, and on the X-ray burst sources in particular. In the preceding chapters, we have attempted to distill from this information those aspects

which seem to have the greatest relevance to the continued development of our understanding of the nature of these sources. We have undoubtedly failed in some respects. However, we hope that, at a minimum, the material we have compiled will serve to supply the interested reader with both an overview and a fairly comprehensive bibliography from which more detailed information might be obtained.

The basic character of the galactic bulge sources now seems clear. They are collapsed objects of roughly solar mass, probably neutron stars in most cases, which are accreting matter from low-mass stellar companions. Type I bursts very likely result from thermonuclear flashes in the surface layers of some of these neutron stars, while the type II bursts from the Rapid Burster almost certainly result from an instability in the accretion flow onto a neutron star.

There are, however, a number of outstanding phenomenological and theoretical problems. What is the prior evolutionary history of the binary stellar systems that become galactic bulge sources? How do the globular cluster X-ray sources differ in character and genealogy from other galactic bulge sources? Are the fast X-ray transients, as well as the type I X-ray bursts, the result of thermonuclear flashes on neutron stars? What mechanisms are responsible for the long-term transient outbursts in the Rapid Burster and several other galactic bulge sources? What is the nature of the accretion instability that is operative in the Rapid Burster? Why is this instability not comparably active in any other known X-ray burst source or X-ray pulsar? Has the same instability ever, in fact, been observed in any other X-ray source? This list of problems is hardly more than illustrative; a complete list of the unanswered questions raised in the preceding chapters would be very much longer.

Nonetheless, we have come a remarkably long way. Five years prior to the time of this writing, the galactic bulge sources were a complete enigma and X-ray bursts were unknown. Now, we seem not only to be on our way to a satisfying understanding of these phenomena, but also to have gained a new and powerful observational handle on the fundamental properties of neutron stars and of the interacting binary systems in which they are often contained.

ACKNOWLEDGEMENTS

Some portions of this review were adopted (and updated) from previous ones written by WHGL (refs. 174,175), by PCJ (refs. 143,144) and by WHGL in collaboration with George W. Clark (refs. 176,177).

We are grateful to Ewa Basinska, Claude Canizares, George Clark, Lynn Cominsky, Josh Grindlay, Jeff McClintock, Bruno Rossi and Jan van Paradijs for their valuable comments on this manuscript, and we thank Susan Black and Maggie Carracino for their assistance and patience in preparing this manuscript. This work was supported by the National Aeronautics and Space Administration under contract NAS5-24441 and grant NSG-7643 and by the National Science Foundation under grant AST78-21993.

REFERENCES

1. Abramenko, A.N., Gershberg, R.E., Pavlenko, E.P. et al. 1978, M.N.R.A.S. 184, 27P.

2. Alcock, C., and Hatchett, S. 1978, Ap. J. 222, 456.

3. Amnuel, P.R. and Guseinov, O.H., 1979, Astrophys. Space. Sc. 63, 131.

4. Apparao, K.M.V., Bradt, H.V., Dower, R.G., et al. 1978, Nature 271, 225.

5. Apparao, K.M.V. and Chitre, S.M. 1980, submitted to Astrophys. Space Sc.

6. Apparao, K.M.V., Chitre, S.M., Ashok, N.M. and Kulkarni, P.V. 1979, IAU Circular 3344.

7. Apparao, K. and Narranan. 1978, Private communication, SAS-3 data.

8. Arons, J., and Lea, S.M. 1980, Ap. J. 235, 1016.

9. Ayasli, S., and Joss, P.C. 1980, manuscript in preparation.

10. Baan, W. 1977, Ap. J. 214, 245; and 1979, Ap. J. 227, 987.

11. Bahcall, J.N. and Ostriker, J.P. 1975, Nature 256, 23.

12. Bahcall, J.N. and Wolf, R.A. 1976, Ap. J. 209, 214.

13. Bahcall, N.A. and Hausman, M.A. 1977, Ap. J. 213, 93.

14. Bahcall, N.A., Lasker, B.M. and Wamsteker, W. 1977, Ap. J. 213, L105.

15. Barranco, M., Buchler, J.R., and Livio, M. 1980, preprint.

16. Basinska, E., Lewin, W.H.G., Cominsky, L., et al. 1980, Ap. J. 241, Oct. 15 (in press).

17. Becker, R.H., Pravdo, S.H., Serlemitsos, P.J. and Swank, J.H. 1976, IAU Circular 2953.

18. Becker, R.H., Smith, B.W., Swank, J.H. et al. 1977, Ap. J. 216, L101.

19. Belian, R.D., Conner, J.P. and Evans, W.D. 1972, Ap. J. 171 L87.

20. Belian, R.D., Conner, J.P. and Evans, W.D. 1976, IAU Circ. No. 2969.

21. Belian, R.D., Conner, J.P. and Evans, W.D. 1976, Bull. Am. Astron. Soc. 8, No. 2, p. 396.

22. Belian, R.D., Conner, J.P. and Evans, W.D. 1976, Ap. J. 206, L135.

23. Belian, R.D., Conner, J.P. and Evans, W.D. 1976, Ap. J. 207, L33.

24. Bernacca, P.L., Bianchini, A., Walker, A., et al. 1979, M.N.R.A.S. 186, 287.

25. Birmingham Group (Ariel V). 1976, IAU Circ. No. 2929.

26. Birmingham Group (Ariel V). 1976, IAU Circ. No. 2934.

27. Bond, H.E. 1977, IAU Circ. No. 3085.

28. Bradt, H., Doxsey, R.E. and Jernigan, J.G. 1979, in "Advances in Space Exploration", Proceedings of IAU/COSPAR Symposium on X-Ray Astronomy, Innsbruck, Austria, May 1978. ed. W.A. Baity and L.E. Peterson (Oxford: Pergamon), Vol. 3, p3.

29. Bradt, H., Kelley, R., and Petro, L. Proceedings of NATO Advanced Study Institute, Cape Sounion, Greece, June 1979 (in press).

30. Calla, O.P.N., Barathy, S., Snagal, A.K. et al. 1980, IAU Circ. Nos. 3458 and 3467.

31. Calla, O.P.N., Bhandari, S.M., Deshpande, M.R. and Vats Hari O.M. 1979, IAU Circ. No. 3347.

32. Canal, R., and Schatzman, E. 1976, Astron. Astrophys. 46, 229.

33. Canizares, C.R. 1975, Ap.J. 201, 589.

34. Canizares, C.R. 1976, Ap. J. 207, L101.

35. Canizares, C.R., Grindlay, J.E., Hiltner, W.A., et al. 1978, Ap.J. 224, 39.

36. Canizares, C.R., McClintock, J.E. and Grindlay, J.E. 1979, IAU Circular 3362.

37. Canizares, C.R., McClintock, J.E. and Grindlay, J.E. 1979, Ap. J. 234, 556.

38. Canizares, C.R., McClintock, J.E. and Grindlay, J.E. 1980, Ap. J. 236, L55.

39. Canizares, C.R. and Neighbours, J.E. 1975, Ap.J. 199, L97.

40. Canizares, C.R. and Oda, M. 1977, Ap. J. 214, L119.

41. Carpenter, G.F., Skinner, G.K., Wilson, A.M. and Willmore, A.P. 1976, Nature 262, 473.

42. Clark, G.W. 1975, Ap.J. 199, L143.

43. Clark, G.W. 1976, IAU Circ. No. 2907.

44. Clark, G.W. 1976, IAU Circ. No. 2922.

45. Clark, G.W. 1976, IAU Circ. No. 2932.

46. Clark, G.W., Jernigan, G., Bradt, H., et al. 1976, Ap. J. 207, L105.

47. Clark, G.W. and Li, F.K. 1977, IAU Circ. No. 3090.

48. Clark, G.W. and Li, F.K. 1977, IAU Circ. No. 3092.

49. Clark, G.W., Li, F.K., Canizares, C.R. et al. 1977, M.N.R.A.S. 179, 651.

50. Clark, G.W., Markert, T.H. and Li, F.K. 1975, Ap. J. 199, L93.

51. Cominsky, L., Forman, W., Jones, C. and Tananbaum, H. 1977, Ap.J. 211, L9.

52. Cominsky, L., Jernigan, J.G., Ossman, W., et al. 1980, Ap.J., Dec. 15 (in press).

53. Cominsky, L., Jones, C., Forman, W. and Tananbaum, H. 1978, Ap. J. 224, 46.

54. Cominsky, L., Lewin, W.H.G., Ossman, W., et al. 1980, manuscript in preparation.

55. Conner, J.P., Evans, W.D. and Belian, R.D. 1969, Ap. J. 157, L157.

56. Cooke, B.A., Ricketts, M.J., Maccacaro, T. et al. 1978, M.N.R.A.S. 182, 489 (2A Catalogue).

57. Cordova, F.A., Garmire, G.P. and Lewin, W.H.G. 1979, Nature 278, 529.

58. Cowie, L.L., Ostriker, J.P. and Stark, A.A. 1978, Ap. J. 226, 1041.

59. Cruddace, R.G., Fritz, G., Shulman, S., et al. 1978, Ap. J. 222, L95.

60. Czerny, M., and Jaroszyński, M. 979, Submitted to Acta Astronomica.

61. Davidsen, A. 1975, IAU Circ. No. 2824.

62. Davidsen, A., Malina, R., Smith, H. et al. 1974, Ap. J. 193, L25.

63. Doty, J. 1976, IAU Circ. No. 2922.

64. Dower, R.G., Apparao, K.M.V., Bradt, H.V. et al. 1978, Nature 273, 364.

65. Doxsey, R.E. 1975, IAU Circ. No. 2820.

66. Doxsey, R.E., Apparao, K.M.V., Bradt, H. et al. 1977, Nature 269, 112.

67. Doxsey, R.E., Bradt, H., Gursky, H. et al. 1978, Ap. J. 221, L53.

68. Doxsey, R., Clark, G.W. and Li, F. 1977, IAU Circ. No. 3094.

69. Doxsey, R.E., Grindlay, J., Griffiths, R. et al. 1978, Ap. J. 228, L67.

70. Duldig, M., Greenhill, J., Thomas, R. et al. 1977, IAU Circ. No. 3108.

71. Epstein, A., Delvaille, J., Helmken, H. et al. 1977, Ap. J. 216, 103.

72. Eryma, E.V., and Tutukov, A.V. 1980, Astron. Astrophys. 84, 123.

73. Evans, W.D., Belian, R.D. and Conner, J.P. 1976, Ap. J. 207, L91.

74. Fabbiano, G. and Branduardi, G. 1979, Ap. J. 227, 294.

75. Fabian, A.C., Pringle, J.E. and Rees, M.J. 1975, M.N.R.A.S. 172, 15P.

76. Fall, S.M. and Malkan, M.A. 1978, M.N.R.A.S. 185, 899.

77. Flowers, E. and Ruderman, M. 1977, Ap. J. 215, 302.

78. Forman, W. and Jones, C. 1976, Ap. J. 207, L177.

79. Forman, W., Jones, C., Cominsky, L., et al. 1978, Ap. J. Suppl. 38, No. 4, page 357 (4U Catalogue).

80. Forman, W., Jones, C. and Tananbaum, H. 1976, Ap. J. 208, 849.

81. Friedman, H. 1978, talk presented at HEAD/AAS Meeting, San Diego, California.

82. Fujimoto, M., Hanawa, T. and Miyaji, S. 1980, preprint.

83. Giannone, P. and Weigert, A. 1967, Zs. Astrophs. 67, 41.

84. Glass, I.S. 1978, Nature 273, 35.

85. Glass, I.S. and Oda, M., private communication.

86. Goldman, Y. 1979, Astron. Astrophys. 78, L15.

87. Griffiths, R.E., Gursky, H., Schwartz, D.A. et al. 1978, Nature 276, 247.

88. Griffiths, R., Johnston, M., Bradt, H. et al. 1978, IAU Circ. No. 3190.

89. Grindlay, J. 1977, IAU Circ. No. 3101.

90. Grindlay, J. 1978, IAU Circ. No. 3229.

91. Grindlay, J.E. 1978, Ap. J. 221, 234.

92. Grindlay, J.E. 1978, Ap. J. 224, L107.

93. Grindlay, J.E. in Proceedings of the HEAD/AAS Meeting, in Cambridge, Mass., January 1980 (in press).

94. Grindlay, J. and Gursky, H. 1976, IAU Circ. No. 2932.

95. Grindlay, J. and Gursky, H. 1976, Ap. J. 205, L131.

96. Grindlay, J.E. and Gursky, H. 1976, Ap. J. 209, L61.

97. Grindlay, J.E. and Gursky, H. 1977, Ap. J. 218, L117.

98. Grindlay, J., Gursky, H., Schnopper, H. et al. 1976, Ap. J. 205, L127.

99. Grindlay, J. and Heise, J. 1976, IAU Circ. No. 2879.

100. Grindlay, J., Hertz, P., Branduardi, G. et al. 1979, to be submitted to Ap. J.

101. Grindlay, J.E. and Liller, W. 1977, Ap. J. 216, L105.

102. Grindlay, J.E. and Liller, W. 1978, Ap. J. 220, L127.

103. Grindlay, J., Marshall, H., Hertz, P. et al. 1979, submitted to Ap. J. (Lett).

104. Grindlay, J., McClintock, J., Canizares, C. and Van Paradijs, J. 1978, IAU Circ. No. 3230.

105. Grindlay, J.E., McClintock, J.E., Canizares, C.R. et al. 1978, Nature 274, 567.

106. Gursky, H. 1976, in "IAU Symposium No. 73," ed. P. Eggleton, S. Mitton and J. Whelan (Dordrecht: Reidel), p. 19.

107. Gursky, H., Bradt, H., Schwartz, D.A. et al. 1978, Ap. J. 223, 973.

108. Hackwell, J.A., Gehrz, R.D., Grasdalen, G.L. et al. 1979, IAU Circ. No. 3331.

109. Hackwell, J.A., Gehrz, R.D., Grasdalen, G.L. et al. 1979, Ap. J. 233, L115.

110. Hansen, C.J. and Van Horn, H.M. 1975, Ap. J. 195, 735.

111. Hearn, D. 1976, IAU Circ. No. 2925.

112. Heise, J. and Grindlay, J. 1976, IAU Circ. No. 2929.

113. Henriksen, R.N. 1976, Ap. J. 210, L19.

114. Hills, J.G. 1975, Astron. J. 80, 1075.

115. Hjellming, R.M. 1979, IAU Circ. No. 3369.

116. Hoffman, J. 1976, IAU Circ. No. 2946.

117. Hoffman, J. 1976, IAU Circ. No. 295[illegible]

118. Hoffman, J.A., Cominsky, L. and Lewin, W.H.G. 1980, Ap. J. 240, L27.

119. Hoffman, J., Doty, J. and Lewin, W.H.G. 1977, IAU Circ. No. 3025.

120. Hoffman, J.A., Lewin, W.H.G. and Doty, J. 1977, Ap. J. 217, L23.

121. Hoffman, J.A., Lewin, W.H.G. and Doty, J. 1977, M.N.R.A.S. 179, 57P.

122. Hoffman, J., Lewin, W.H.G., Doty, J. et al. 1976, Ap. J. 210, L13.

123. Hoffman, J.A., Lewin, W.H.G., Doty, J. et al. 1978, Ap. J. 221, L57.

124. Hoffman, J., Lewin, W.H.G., Marshall, H. et al. 1978, IAU Circ. No. 3190.

125. Hoffman, J.A., Lewin, W.H.G., Primini, F.A., et al. 1979, Ap.J. 233, L51.

126. Hoffman, J.A., Marshall, H. and Lewin, W.H.G. 1977, IAU Circ. No. 3117.

127. Hoffman, J.A., Marshall, H.L. and Lewin, W.H.G. 1978, Nature 271, 630.

128. Hoffman, J.A., Wheaton, W.A., Primini, F.A. et al. 1978, Nature, 276, 587.

129. Horiuchi, R., Kadonaga, T. and Tsuimatsu, A. 1980, submitted to Prog. Theor. Phys.

130. Hoshi, R. 1980, preprint.

131. Inoue, H., Koyama, K., Makishima, K. et al. 1980, Nature 283, 358.

132. Jernigan, J.G., Apparao, K.M.V., Bradt, H.V. et al. 1977, Nature 270, 321.

133. Jernigan, J.G., Apparao, K.M.V., Bradt, H.V. et al. 1977, Nature 272, 701.

134. Jernigan, J.G. and Clark, G.W. 1979, Ap. J. 231, L125.

135. Jernigan, J.G., McClintock, J., Marshall, H. et al. 1978, IAU Circ. No. 3204.

136. Johnson, H.M. 1976, Ap. J. 208, 706.

137. Johnson, H.M., Catura, R.C., Lamb, R.A. et al. 1978, Ap. J. 222, 664.

138. Johnston, M.D., Bradt, H.V. and Doxsey, R.E. 1979, Ap. J. 233, 514.

139. Jones, A.W., Selby, M.J., Mountain, C.M. et al. 1980, Nature 283, 550.

140. Jones, C. and Forman, W. 1976, IAU Circ. No. 2913.

141. Joss, P.C. 1977, Nature 270, 310.

142. Joss, P.C. 1978, Ap. J. 225, L123.

143. Joss, P.C. 1979, Comments on Astrophys. 8, 109.

144. Joss, P.C. 1980. Annals N.Y. Acad. Science 336, 479. (Proceedings of the Ninth Texas Symposium on Relativistic Astrophysics, Munich, West Germany).

145. Joss, P.C. 1979, in "Compact Galactic X-Ray Sources," ed. D. Pines and F. Lamb (Urbana, Illinois: Physics Dept., Univ. of Illinois), p. 89.

146. Joss, P.C. 1980, in Proceedings of the HEAD/AAS Meeting, Cambridge, Massachusetts, January 1980 (in press).

147. Joss, P.C., Avni, Y. and Rappaport, S. 1978, Ap. J. 221, 645.

148. Joss, P.C. and Li, F.K. 1980, Ap. J., 238, 287.

149. Joss, P.C. and Rappaport, S.A. 1979, Astron. and Astroph. 71, 217.

150. Joss, P.C., Ricker, G.R., Mayer, W. and Hoffman, J. 1977, IAU Circ. No. 3108.

151. Kaluzienski, L. 1977, Ph.D. Thesis, University of Maryland.

152. Kaluzienski, L. and Holt, S. 1977, IAU Circ. Nos. 3099, 3108, 3129 and 3349.

153. Kaluzienski, L. and Holt, S. 1979, IAU Circ. Nos. 3360 and 3362.

154. Kaluzienski, L.J., Holt, S., Boldt, E.A. and Serlemitsos, P.J. 1975, IAU Circ. No. 2859.

155. Kaluzienski, L.J., Holt, S.S. and Swank, J.H. 1980, preprint.

156. Katz, J.I. 1975, Nature 253, 698.

157. Kelley, R., Rappaport, S. and Petre, R. 1980, Ap. J. (in press).

158. Kellogg, E., Gursky, H., Murray, S. et al. 1971, Ap. J. 169, L99.

159. King, I.R. 1966, Astron. J. 71, 64.

160. Kleinmann, D.E., Kleinmann, S.G. and Wright, E.L. 1976, Ap.J. 210, L83.

161. Kondo, I., Inoue, H., Koyama, K. et al. 1980, ISAS Research Note 109.

162. Kulkarni, P.V., Ashok, N.M., Apparao, K.M.V. and Chitre, S.M. 1979, Nature 280, 819.

163. Lamb, F.K., Fabian, A.C., Pringle, J.E. and Lamb, D.Q. 1977, Ap. J. 217, 197.

164. Lamb, D.Q. and Lamb, F.K. 1977, Annals N.Y. Acad. Sci. 302, 261.

165. Lamb, D.Q. and Lamb, F.K. 1978, Ap. J. 220, 291.

166. Lewin, W.H.G. 1976, IAU Circ. No. 2911.

167. Lewin, W.H.G. 1976, IAU Circ. No. 2918.

168. Lewin, W.H.G. 1976, IAU Circ. No. 2922.

169. Lewin, W.H.G. 1977, IAU Circ. No. 3078.

170. Lewin, W.H.G. 1977, American Scientist 65, No. 5, p. 605.

171. Lewin, W.H.G. 1977, M.N.R.A.S. 179, 43.

172. Lewin, W.H.G. 1977, Annals N.Y. Acad. Sc. 302, 210 (Proceedings of the Eighth Texas Symposium on Relativistic Astrophysics, Boston, Mass).

173. Lewin, W.H.G. 1978, IAU Circ. No. 3193.

174. Lewin, W.H.G. 1979, in "Advances in Space Exploration", (Proceedings of IAU/COSPAR Symposium on X-Ray Astronomy Innsbruck, Austria, May 1978) ed. W.A. Baity and L.E. Petersen. (Oxford: Pergamon), Vol. 3, p. 133.

175. Lewin, W.H.G. 1980, in "Globular Clusters", (Proceedings of Globular Cluster Meeting held in Cambridge, England, August 1976) ed. D. Hanes and B. Madore, (Cambridge, England: Cambridge University Press), p. 315.

176. Lewin, W.H.G. and Clark, G.W., in "Symposium on the Results and Future Prospects of X-Ray Astronomy 1979 August 3-4, Tokyo", (Tokyo: ISAS, Univ. of Tokyo), p. 3.

177. Lewin, W.H.G. and Clark, G.W. 1980. Annals N.Y. Acad. Sc. 336, 451. (Proceedings of the Ninth Texas Symposium on Relativistic Astrophysics, Munich, West Germany).

178. Lewin, W.H.G., Cominsky, L. and Van Paradijs, J. 1978, IAU Circ. No. 3308.

179. Lewin, W.H.G., Cominsky, L., Walker, A.R. and Robertson, S.C. 1980, Nature 287, 27.

180. Lewin, W.H.G., Doty, J., Clark, G.W. et al. 1976, Ap. J. 207, L95.

181. Lewin, W.H.G., Doty, J., Hoffman, J.A. and Li, F.K. 1976, IAU Circ. No. 2984.

182. Lewin, W.H.G. and Hoffman, J.A. 1977, IAU Circ. No. 3079.

183. Lewin, W.H.G., Hoffman, J.A. and Doty, J. 1976, IAU Circ. No. 2994.

184. Lewin, W.H.G., Hoffman, J.A. and Doty, J. 1977, IAU Circ. No. 3039.

185. Lewin, W.H.G., Hoffman, J.A. and Doty, J. 1977, IAU Circ. No. 3087.

186. Lewin, W.H.G., Hoffman, J.A., Doty, J. et al. 1977, Nature 267, 28.

187. Lewin, W.H.G., Hoffman, J.A., Doty, J. et al. 1976, M.N.R.A.S. 177, 83P.

188. Lewin, W.H.G., Hoffman, J.A., Doty, J. et al. 1977, IAU Circ. No. 3075.

189. Lewin, W.H.G., Hoffman, J.A., Marshall, H. et al. 1978, IAU Circ. No. 3190.

190. Lewin, W.H.G. and Joss, P.C. 1977, Nature 270, 211.

191. Lewin, W.H.G., Li, F.K., Hoffman, J.A. et al. 1976, M.N.R.A.S. 177, 93P.

192. Lewin, W.H.G., Marshall, H. and Cominsky, L. 1978, IAU Circ. No. 3211.

193. Lewin, W.H.G., McClintock, J.E. and Ricker, G.R. 1971, Ap. J. 169, L17.

194. Lewin, W.H.G., Van Paradijs, J., Cominsky, L., and Holzner, S. 1980, M.N.R.A.S. 193, 15.

195. Li, F. 1976, IAU Circ. No. 2936.

196. Li, F.K. and Clark, G.W. 1977, IAU Circ. No. 3095.

197. Li, F.K. and Clark, G.W. 1980, manuscript in preparation.

198. Li, F.K., Joss, P.C., McClintock, J.E. et al. 1980, Ap. J. 240, 628.

199. Li, F. and Lewin, W.H.G. 1976, IAU Circ. No. 2983.

200. Li, F.K., Lewin, W.H.G., Clark, G.W. et al. 1977, M.N.R.A.S. 179, 21P.

201. Liang, E.P.T. 1977, Ap. J. 211, L67 and Ap. J. 218, 243.

202. Lightman, A.P., Press, W.H. and Odenwald, S.F. 1978, Ap. J. 219, 629.

203. Liller, M.H. and Carney, B.W. 1978, Ap. J. 224, 383.

204. Liller, W. 1976, IAU Circ. No. 2929.

205. Liller, W. 1976, IAU Circ. No. 2936.

206. Liller, W. 1977, Ap. J. 213, L21.

207. Liller, W. 1979, IAU Circ. No. 3366.

208. Maraschi, L. and Cavaliere, A. 1977, in "Highlights in Astronomy" Vol. 4, Part I, p. 127.

209. Margon, B. 1980, IAU Circ. No. 3478.

210. Margon, B. and Whitter, K.B. 1978, IAU Circ. No. 3246.

211. Markert, T., Backman, D.E., Canizares, C.R, et al. 1975, Nature 257, 32.

212. Markert, T.H., Backman, D. and McClintock, J. 1976, Ap. J. 208, L115.

213. Markert, T.H., Bradt, H.V., Clark, G.W. et al. 1975, IAU Circ. No. 2765.

214. Markert, T., Canizares, C.R. and Clark, G.W. et al. 1977, Ap. J. 218, 801.

215. Marshall, F.J. 1979, IAU Circ. No. 3336.

216. Marshall, H. and Lewin, W.H.G. 1978, IAU Circ. No. 3208.

217. Marshall, H., Li, F. and Rappaport, S. 1977, IAU Circ. No. 3134.

218. Marshall, H.L., Ulmer, M., Hoffman, J.A. et al. 1979, Ap. J. 227, 555.

219. Mason, K.O., Bell-Burnell, S.J. and White, N.E. 1976, Nature 262, 474.

220. Mason, K.O., Middleditch, J., Nelson, J.E. and White, N.E. 1980, Nature Phys. Sc. (in press).

221. Matilsky, T., Bradt, H., Buff, J. et al. 1976, Ap. J. 210, L127.

222. Matsuoka, M., Inoue, H., Koyama, K. et al. 1980, ISAS Res. Note 94, submitted to Ap. J. (Letters).

223. McClintock, J.E. 1977, IAU Circ. No. 3084.

224. McClintock, J.E. 1977, IAU Circ. No. 3088.

225. McClintock, J.E., Canizares, C. and Backman, D.E. 1978, Ap. J. 223, L75.

226. McClintock, J.E., Canizares, C.R., Bradt, H.V. et al. 1977, Nature 270, 320.

227. McClintock, J.E., Canizares, C., Li, F.K. and Grindlay, J. 1980, Ap. J. 235, L81.

228. McClintock, J.E., Canizares, C.R., Van Paradijs, J. et al. 1979, Nature 279, 47.

229. McClintock, J.E., Rappaport, S., Nugent, J. and Li, F.K. 1977, Ap. J. 216, L15.

230. McClintock, J.E. and Remillard, R.A. 1980, preprint CSR-HLA-80-17, submitted to Ap. J.

231. Middleditch, J., Mason, K.O., Nelson, J. and White, N. 1980, Ap. J. (in press).

232. Milgrom, M. 1978, Astron. Astrophys. 67, L25.

233. Mook, D., Kurtz, M., Weed, J. and Johns, M. 1978, IAU Circ. No. 3251.

234. Murakami, T., Inoue, H., Koyama, K. et al. 1980, ISAS Research Note 106, submitted to Ap. J. (Letters).

235. Murakami, T., Inoue, H., Koyama, K. et al. 1980, ISAS Research Note 105, submitted to Nature.

236. Murdin, P., Penston, M.J., Penston, M.V. et al. 1974, M.N.R.A.S. 169, 25.

237. Neugebauer, M. and Tsurutani, B.T. 1976, Ap. J. 226, 494.

238. Oda, M. 1979, IAU Circ. No. 3349.

239. Oda, M. 1979, IAU Circ. No. 3366.

240. Oda, M. 1979, IAU Circ. No. 3392.

241. Oda, M., 1980, in Proceedings of the HEAD/AAS Meeting, Cambridge, Mass., January 1980 (in press).

242. Oda, M. and the Hakucho Team, 1980, IAU Circ. No. 3481.

243. Oke, J.B. 1977, Ap. J. 217, 181.

244. Oke, J.B. and Greenstein, J.L. 1977, Ap. J. 211, 872.

245. Ostriker, J.P., Rees, M.J. and Silk, J. 1970, Astrophys. Lett. 6, 179.

246. Ostriker, J.P., Spitzer, L. and Chevalier, R.A. 1972, Ap. J. 176, L51.

247. Paczyński, B. and Jaroszyński, M. 1978, Acta Astron. 28, 111.

248. Parsignault, D. and Grindlay, J.E. 1978, Ap. J. 225, 970.

249. Pedersen, H., Lub, J., Oda, M. et al. 1980, to be submitted to Ap. J. (Letters).

250. Pedersen, H., Oda, M., Hakucho Team et al. 1979, IAU Circ. No. 3399.

251. Peterson, C.J. 1976, Astron. J. 81, 617.

252. Peterson, C.J. and King, I.R. 1975, Astron. J. 80, 427.

253. Pramesh Rao, A. and Venugopal, V.R. 1980, preprint.

254. Press, W.H. and Teukolsky, S.A. 1977, Ap. J. 213, 183.

255. Proctor, R.J., Skinner, G.K. and Willmore, A.P. 1978, M.N.R.A.S. 185, 745.

256. Rappaport, S., Joss, P.C. and Webbink, R. 1980, manuscript in preparation.

257. Rosenbluth, M.N., Ruderman, M., Dyson, F. et al. 1973, Ap. J. 184, 907.

258. Ruderman, M. 1972, Ann. Rev. Astron. Astrophys. 10, 427.

259. Sato, S., Kawara, K., Kobayashi, Y. et al. 1980, preprint.

260. Schreier, E., Levinson, R., Gursky, H. et al. 1972, Ap. J. 172, L79.

261. Schwarzschild, M. and Harm, R. 1965, Ap. J. 142, 855.

262. Seitzer, P., Smith, G. and Ross, B. 1979, IAU Circ. No. 3372.

263. Seitzer, P., Tuohy, I.R., Mason, K.O. et al. 1979, IAU Circ. No. 3406.

264. Shapiro, S.L. 1977, Ap. J. 217, 281.

265. Share, G., Wood, K., Yentis, D. et al. 1978, IAU Circ. No. 3190.

266. Silk, J. and Arons, J. 1975, Ap. J. 200, L131.

267. Svestka, J. 1976, Astrophys. Space Sc. 45, 21.

268. Swank, J.H., Becker, R.H., Boldt, E.A. et al. 1977, Ap. J. 212, L73.

269. Swank, J.H., Becker, R.H., Boldt, E.A. et al. 1978, M.N.R.A.S. 182, 349.

270. Swank, J.H., Becker, R., Pravdo, S. and Serlemitsos, P.J. 1977, IAU Circ. No. 2963.

271. Swank, J., Becker, R., Pravdo, S. et al. 1976, IAU Circ. No. 3000.

272. Swank, J.H., Becker, R.H., Pravdo, S.H. et al. 1976, IAU Circ. No. 3010.

273. Swank, J.H., Eardley, D.M. and Serlemitsos, P.J. 1979, preprint.

274. Taam, R.E. 1980, preprint.

275. Taam, R.E. and Picklum, R.E. 1978, Ap. J. 224, 210.

276. Taam, R.E. and Picklum, R.E. 1979, Ap. J. 233, 327.

277. Takagishi, K., Nagareda, K., Matsuoka, M. et al. 1978, ISAS Research Note 60, preprint CSR-P-78-31.

278. Tananbaum, H., Chaisson, L.J., Forman, W. et al. 1976, Ap. J. 209, L125.

279. Tananbaum, H., Gursky, H., Kellogg, E.M. et al. 1972, Ap. J. 174, L143.

280. Tawara, Y. 1980, Ph.D. Thesis Univ. of Tokyo, ISAS Research Note 103.

281. Thomas, R.M., Duldig, M.L., Haynes, R.F. et al. 1979, M.N.R.A.S. 187, 299.

282. Thorstensen, J., Charles, P. and Bowyer, S. 1978, IAU Circ. No. 3253.

283. Thorstensen, J., Charles, P. and Bowyer, S. 1978, Ap. J. 220, L131.

284. Thorstensen, J., Charles, P., Bowyer, S. et al. 1979, Ap. J. 233, L57.

285. Thorstensen, J., Charles, P.A., Bowyer, S. et al., talks presented at the HEAD/AAS Meeting in San Diego, California, 1978 and at the HEAD/AAS Meeting in Cambridge, Mass., January 1980.

286. Ulmer, M.P., Hjellming, R.M., Lewin, W.H.G. et al. 1978, Nature 276, 799.

287. Ulmer, M.P., Lewin, W.H.G., Hoffman, J.A. et al. 1977, Ap. J. 214, L11.

288. Van den Heuvel, E.P.J. 1977, Annals N.Y. Acad. Sc. 302, 14.

289. Van Horn, H.M. and Hansen, C.J. 1974, Ap. J. 191, 479.

290. Van Paradijs, J. 1978, IAU Circ. No. 3197.

291. Van Paradijs, J. 1978, Nature 274, 650.

292. Van Paradijs, J. 1979, Ap. J. 234, 609.

293. Van Paradijs, J. 1980, IAU Circ. No. 3487.

294. Van Paradijs, J., Cominsky, L. and Lewin, W.H.G. 1978, IAU Circ. No. 3294.

295. Van Paradijs, J., Cominsky, L. and Lewin, W.H.G. 1979, M.N.R.A.S. 189, 387.

296. Van Paradijs, J., Joss, P.C., Cominsky, L. and Lewin, W.H.G. 1979, Nature 280, 375.

297. Van Paradijs, J. and Lewin, W.H.G. 1978, Nature 276, 249.

298. Van Paradijs, J., Rybicki, G. and Lamb, D.Q. 1980, talk presented at the HEAD/AAS Meeting, Cambridge, Mass., January 1980, Abstract in Bull. Amer. Astron. Soc. 11, 788.

299. Van Paradijs, J., Verbunt, F., Van der Linden, T. et al. 1980, preprint.

300. Wallace, R.K. and Woosley, S.E. 1980, preprint.

301. Watson, M.G. 1976, M.N.R.A.S. 176, 19P.

302. Wheeler, J.C. 1977, Ap. J. 214, 560.

303. Whelan, J., Ward, M.J., Allen, D.A. et al. 1977, M.N.R.A.S. 180, 657.

304. White, N.E. and Burnell, S. 1977, IAU Circ. No. 3067.

305. White, N.E., Mason, K.O., Carpenter, G.F. and Skinner, G.K. 1978, M.N.R.A.S. 184, 1P.

306. Willmore, A.P., Mason, K.O., Sanford, P.W. et al. 1974, M.N.R.A.S. 169, 7.

307. Wilson, A.M., Carpenter, G.F., Eyles, C.J. et al. 1977, Ap. J. 215, L111.

308. Woosley, S.E. and Taam, R.E. 1976, Nature 263, 101.

309. Wyckoff, S. 1979, IAU Circ. No. 3386.

310. 1978, IAU Circ. No. 3243.

311. Oda, M. 1980, IAU Circ. No. 3506.

312. Grindlay, J. 1980, IAU Circ. No. 3506.

313. Terzan, A. 1971, Astron. Astrophys. 12, 477.

314. Sztajno, M., Basinska, E., Cominsky, L. and Lewin, W.H.G. 1980, manuscript in preparation.

315. Ergma, E.V., and Kudrjashov, A.D. 1980, preprint.

316. Giacconi, R., Gursky, H., Kellogg, E. et al. 1971, Ap. J. 167, L67.

317. Apparao, K.M.V. and Chitre, S.M. 1979, Astrophys. Space Sci. 63, 125.

318. Brecher, K., Morrison, P. and Sadun, A. 1977, Ap. J. 217, L139.

319. Joss, P.C. and Rappaport, S. 1977, Nature 265, 222.

320. Cowley, A.P., Crampton, D. and Hutchings, J.B. 1979, Ap. J. 231, 539.

321. Crampton, D. and Cowley, A.P. 1980, Astron. Soc. Pac. 92, 147.

322. Lodenquai, J., Canuto, V., Ruderman, M. and Tsuruta, S. 1974, Ap. J. 190, 141.

323. Canuto, V. 1970, Ap. J. 159, 641.

324. Rappaport, S., Buff, J., Clark, G. et al. 1976, Ap. J. 206, L139.

325. Pounds, K., talk presented at the AAS/HEAD Meeting, San Diego, September, 1978.

326. Mason, K.O., Middleditch, J., Nelson, J.E. et al. 1981, Ap. J. (in press).

327. Lewin, W.H.G., Van Paradijs, J., Oda, M. and Pounds, K. 1979, IAU Circ. No. 3334.

328. Lewin, W.H.G., Cominsky, L. and Oda, M. 1979, IAU Circ. No. 3420.

329. Lewin, W.H.G. and Cominsky, L. 1979, IAU Circ. No. 3428.

FIGURE CAPTIONS

Figure 1. Histogram of the optically identified compact galactic X-ray sources (with $L_X > 10^{34}$ ergs s^{-1}) as a function of L_X/L_{opt}. There seem to be two classes: (i) the massive binaries (at left) with an O or B stellar companion, indicated by ■ ; (ii) the galactic bulge sources (on the right) which, in general, are optically faint objects that show no normal stellar absorption lines in their spectra (at maximum light), indicated by ▲. Several objects in this class are type I X-ray burst sources, indicated by ● . Several of the sources on the right are known low-mass close-binary systems (see Sects. 4.2.2 and 4.2.7). It is very likely that the galactic bulge sources, as a class, are low-mass close-binary systems. This figure was provided by J.E. McClintock, who used refs. 28, 38, 136, and 284. The optical identification of 1916-05 is not firm[285].

Figure 2. Log-log plot of the core radius r_c (in parsec), versus the central core brightness (B) for 69 globular clusters. The grid lines are loci of constant core mass ($M_c=Br_c^2$) and core density ($\rho_c=M_c/r_c^3$). The core densities have a range of $\sim 10^5$. The globular clusters that contain X-ray sources (except NGC6712) have relatively high core densities (see text). Not all X-ray clusters are indicated (see Table 1). This figure is from F.K. Li, Ph.D. thesis.

Figure 3. The discovery of X-ray bursts. Detection of an X-ray burst from a source located in the globular cluster NGC6624. The integration intervals are 1 s. This is one of two bursts from the same source detected on 1975 September 28 with the Astronomical Netherlands Satellite. This figure is from Grindlay et al.[98]

Figure 4. The discovery of X-ray bursts. Each dot shows the location of an X-ray flare event (with a 3σ level of confidence) observed with the Vela 5B satellite between May 1969 and August 1970. Many, but definitely not all, of these events are probably type I X-ray bursts (see text). Note the strong concentration of events in the constellation Norma near the galactic plane (galactic longitude ≈330°). These are probably type I X-ray bursts from the transient/burst source 4U1608-52 and/or from 4U/MXB1636-53 (see Figure 5). This figure is from Belian, Conner and Evans[23].

Figure 5. Sky map (galactic coordinates) of the 31 type I X-ray burst sources listed in Table 4 (based on data available as of September 1, 1980). There are at least 6 more detected burst sources that are probably within 30° of the galactic center (unpublished SAS-3 data). Their positions are poorly known and they are not shown here. The many burst events observed by the Los Alamos group are also not shown here (see text and Fig. 4). At least 26 but possibly all 31 burst sources shown here emit type I bursts.

Figure 6. Composite profile (X-ray flux versus time), in five X-ray energy channels of seven type I X-ray bursts from MXB1728-34. The bursts are plotted full-scale on the left. On the right, the vertical scale is expanded and the horizontal scale extended to show the enhanced level of radiation in the lower energy channels after the bursts. The pre-burst flux levels are indicated with dashed lines. The data are binned in 0.83-s intervals, and the tic marks on the abscissa show 10-s intervals. Note that the burst duration decreases rapidly with increasing X-ray energy, indicating cooling of the burst emission region (see text). This figure is from Hoffman, Lewin and Doty[121].

Figure 7. Profiles of type I X-ray bursts from five different sources (SAS-3 data). Note again (as in Fig. 6) that the gradual decay (burst "tail") persists longer at low energies than at high energies, indicating cooling of the burst emission region (see text). This figure is from Lewin and Joss[190].

Figure 8. Profiles of six type I X-ray bursts from 4U/MXB1636-53. The bursts have similar shapes except for the third one (c), which does not show the narrow feature in the 1.2-3 keV channel that is evident in the other bursts. This burst occurred unusually soon (2.7 h) after the preceding burst. Intervals between the other bursts range from 9.5 h to 12.2 h. This figure is from Hoffman, Lewin and Doty[120].

Figure 9: Profiles of five type I X-ray bursts from the transient X-ray source MXB1659-29. The burst intervals (≈2.5 h) were the most regular of all burst sources reported to date. This figure is from Lewin and Clark[176,177] (see also ref. 54).

Figure 10. Profiles of type I X-ray bursts from three burst sources located within a degree of the galactic center. MXB1743-29 produced bursts at intervals of ≈35 h; they all showed double (sometimes triple) peaks at high energies (see also Fig. 13). The burst intervals of MXB1742-29 were ≈10 h. MXB1743-28 was seen only once when it produced three type I bursts in quick succession with intervals of ≈17 min and ≈4 min. This figure is from Lewin et al.[187].

Figure 11. Profiles of five type I X-ray bursts from 4U/MXB1735-44. The burst profiles are all similar. Note the evidence of cooling during burst decay. Burst intervals from this source are highly irregular. This figure is from Lewin et al.[194]

Figure 12. Lower curve: High time resolution (10 ms) profile from the HEAO A1 detectors during the first part of a type I X-ray burst from MXB1728-34. Upper curve: Combined data from the A1 (5-17 keV) and A2 MED (2-15 keV) detectors in 80 ms bins. This figure is from Hoffman et al.[125].

Figure 13. Profiles of type I X-ray bursts from three different sources, all showing a characteristic multiple-peaked structure (see text). The spectrum from MXB1743-29 (this source is located near the galactic center) is highly cut-off below 3 keV due to interstellar absorption. The burst source MXB1650-08 is located in the globular cluster NGC6712. This figure is from Hoffman, Cominsky and Lewin[118].

Figure 14. Average spectra, in three time intervals, of a very long (≈600 s) type I X-ray burst from XB1724-30 which is probably the burst source located in Terzan 2 (ref. 103). Time zero is near the burst onset. The solid curves show the best fits to black-body spectra. The values for kT are ≈0.9 keV (0-20 s), ≈2.3 keV (40-70 s) and ≈1.2 keV (150-440 s). Under the assumption of a spherical emitting surface and a source distance of 10 kpc the best-fit black-body radii were ≈100 km during the first 20 s of the burst and ≈15 km during the remainder of the burst. This figure is from Swank et al. [268].

Figure 15. The optical brightening of the transient X-ray source Cen X-4. (a) The Palomar observatory sky survey blue print showing Cen X-4 in its quiescent state. (b) The discovery plate obtained by M. Liller at the prime focus of the CTIO 4 m telescope on 1979 May 19. This figure is from Canizares, McClintock and Grindlay[38].

Figure 16. Spectra in the blue (3500-5000 Å) of the counterparts of three type I X-ray burst sources. Several emission lines are identified (top). The spectra are believed to be due to X-ray heating of an accretion disk, which accounts for why they are devoid of normal stellar absorption lines (see text). The spectra 2B and 3B (of 4U/MXB1735-44) were taken on consecutive nights: 8B and 9B (of MXB1659-29) were taken only a few hours apart. Spectral variability over hours to days were observed[37]. This figure is from Canizares, McClintock and Grindlay[37].

Figure 17. Highly-compact-binary model for the X-ray pulsar 4U1626-67. The Figure is drawn to scale for a companion star of mass $\sim$0.1 $M_\odot$, a neutron star of mass $\sim$1 $M_\odot$ and an orbital separation of $\sim$1 light second (which is appropriate to a main-sequence dwarf companion). This figure is from Li et al.[198] (see also refs. 149 and 231).

Figure 18. Optical and X-ray bursts simultaneously observed from 4U/MXB1636-53. In observations of this kind, the X-rays act as a probe that illuminates the surroundings of the X-ray star. These surroundings reveal their size and structure by the delayed emission (in response to the X-ray heating) of visible light (see text). In this source the optical response is delayed by $\sim$3.5 s relative to the X-rays. This figure is from Pedersen et al.[249].

Figure 19. Blowup of a prominent X-ray/optical flare from the pulsar 4U1626-67. (This event is not a type I X-ray burst, and 4U1626-67 is not a burst source.) During the flare the X-ray flux increased by a factor of ~3 while the optical flux increased by only ~50%. The duration of the optical flare is about 1.5 minutes longer than that of the X-ray flare. X-ray and optical fluxes from the source prior to the flare are indicated by horizontal dashed lines (background counting rates have been subtracted). It is most likely that the optical emission comes from the reprocessing of X-rays in an accretion disk surrounding the X-ray star. The optical response to X-ray bursts (see Fig. 18) is similar. This figure is from McClintock et al.[227].

Figure 20. Infrared photograph of Liller I, the highly reddened globular cluster in which the Rapid Burster (MXB1730-335) is located. This is a 60 minute exposure with the 4-meter reflector of CTIO. The pass band of the filter is 6900-8900 Å. This figure is from Liller[206].

Figure 21. Type II X-ray bursts from the Rapid Burster (MXB1730-335). These are ~24 minute stretches of data from eight different orbits of the SAS-3 observatory on 1976 March 2-3, when this unique object was discovered[180]. Bursts with durations in excess of ~15 s show "flux saturation" (i.e., flat tops). This is also apparent in the very long bursts shown in Figure 24. Note the strong correlation between the integrated counts in a

burst and the duration of the quiescent period that follows (see Fig. 25). The arrow indicates a type I burst from MXB1728-34. This figure is from Lewin[172].

Figure 22. Discovery of type I X-ray bursts from the Rapid Burster (MXB1730-335) (see Table 3). The type I bursts (marked as "special") occur independently of the sequence of the rapidly repetitive type II bursts (numbered separately). This figure is from Hoffman, Marshall and Lewin[127].

Figure 23. Spectral information for the data shown in Figure 22a. Note that the type I ("special") burst spectra soften during burst decay; this softening is absent in the type II bursts. This figure is from Hoffman, Marshall and Lewin[127].

Figure 24. Type II X-ray bursts from the Rapid Burster (MXB1730-335), as observed with SAS-3 between 1979 March 3 and 5. The bursts labelled I and III last ≈400 s and ≈250 s, respectively. About five months later, many more of these very long type II bursts were observed with Hakucho[131]. The type I burst indicated with an arrow is from MXB1728-34. This figure is from Basinska et al.[16] (see also ref. 215).

Figure 25. Log-log plots of the integrated type II X-ray burst energy, E, versus the waiting time, Δt_2, to the next burst, for some of the data indicated with arrows in the left part of Figure 26. The data points would follow a straight line with slope 45° if the

relation between E and Δt were strictly linear. See Section 4.3.4 for the definitions of modes I and II. This figure is from Marshall et al.[218].

Figure 26. Integrated energy in each type II X-ray burst (abscissa) versus the time in UT of its occurrence (ordinate). Each dot represents one type II burst from the Rapid Burster (MXB1730-335). D is the distance to the source in kpc. Two different burst patterns are distinguishable (see also Fig. 27). This figure is from Marshall et al.[218].

Figure 27. Distribution of integrated energies in type II X-ray bursts from the Rapid Burster (MXB1730-335). (a) Data from an ~8 hour period in March 1976 (indicated in Figure 26). Note the double peaked distribution. (b) Data from a ~17 hour period in April 1976 (indicated in Figure 26). This figure is from Marshall et al.[218].

Figure 28. Complete record of observations of the Rapid Burster (MXB1730-335). The scale of the horizontal axis is in fractions of a year; the months of the year are also indicated. Periods of X-ray coverage where bursts were not observed are indicated by open rectangles, while burst active periods are marked by filled rectangles. Only a few (one or two) bursts were observed during periods marked by open rectangles with one or two diagonal lines. These bursts were probably type I bursts from the nearby source MXB1728-34. Data

are from Uhuru, Copernicus, ANS, SAS-3, Ariel 5, HEAO-1, Einstein and Hakucho (see Table 4 for references). The eight vertical dashed lines indicate observing periods of less than one day during which no bursts were observed. The line marked "a" represents a ~7 h period during which the source may have been burst-active, however, this is very uncertain[305]. The source may have been burst-active during the period marked "b", however, this is somewhat uncertain[305]. During the period marked "c" (from about mid August to September 26, 1980), observations of the Rapid Burster were made intermittently with ~3 day intervals; no burst activity was observed (M. Oda, private communication). This figure was prepared by Ewa Basinska; it is an updated version of one published previously by Grindlay and Gursky[97].

Figure 29. Top: Composite profile of 18 type II X-ray bursts from the Rapid Burster (MXB1730-335), chosen to be of similar duration (~34-45 s). The expanded vertical scale on the right shows the growth of an enhancement of the X-ray emission after these bursts (see text). Counting rates prior to the bursts are indicated by dashed lines. This figure is from Marshall et al.[218]. Bottom: Superposition of the counting rates from the Rapid Burster during 60 burst-free intervals, synchronized to the onset of the first burst after each interval. The counting rates just prior to the bursts are indicated by dashed lines. An enhancement is clearly visible in the 3 lowest energy channels; it drops rapidly just before the onset of the burst (see text). This figure is from Van Paradijs, Cominsky and Lewin[295].

Figure 30. Left: Profiles of six infrared (1.6 μm) bursts which may have come from the Rapid Burster (MXB1730-335), as reported by Kulkarni et al.[162] (see text). The ordinate is marked in units of 10^{-16} W cm^{-2} μm^{-1}. Right: Profiles of two infrared (2.2 μm) bursts which may also have come from the Rapid Burster, as reported by Jones et al.[139]. The bursts are accompanied by seven brief flashes (see text). The feature at A is an artifact. The ordinate is marked in units of 10^{-12} W m^{-2} μm^{-1}.

Figure 31. Profiles of a flare event (type II burst?) from GX301-2, observed with SAS-3. The underlying low-level X-ray flux is the persistent flux from GX301-2, modulated by the collimator response due to spacecraft rotation. This figure is from Bradt, Kelley and Petro[29].

Figure 32. Profiles of the early portion of the 1977 February 7 event, as observed with the SAS-3 Center Slat detectors. A precursor is clearly visible but shows no obvious spectral evolution. After the precursor the signal drops back to its original level before the "main" event begins. The delay between the precursor and the rise of the "main" event increases with energy and has a duration of ~80 s in the 8-35 keV channel. Thus, in this energy channel the "main" event rises near t~115 s (off scale); the rise is shown in Figure 33. The "main" event displays significant spectral softening during its decay (see Figs. 33 and 35). This figure is a modified version

of one shown by Hoffman et al.[123]

Figure 33. (a) and (b) Profiles of the complete 1977 February 7 event, which lasted ~1500 s. Note the distinct spectral softening during the decay of the "main" event. The precursor is not visible in (b) because of the lumping of the data in coarse time bins. (c) Composite profile of type I X-ray bursts from MXB1728-34 (see also Fig. 6). The resemblance between the event shown in (b) and the type I X-ray bursts is striking. This figure is from Hoffman et al.[123].

Figure 34. (a) Profiles of the 1976 June 28, event in coarse (~7.5 s) time bins. (b) The onset of the event shown on an expanded time scale in 0.83 s time bins. A precursor is clearly visible. The "main" event rises later at high energies, as in the February 1977 event (see Figs. 32 and 33). The 1σ error bars shown include counting statistics and the uncertainty in the deconvolution of the collimator transmission. This event probably came from MX1716-31 (see the entry for XB1715-32 in Table 4). This Figure is from Hoffman et al.[123].

Figure 35. The evolution of the ratios of X-ray fluxes in different spectral channels with time for (a) the 1977 February 7 event, (b) the 1976 June 28 event and (c) a composite X-ray burst from MXB1728-34. All cases display initial spectral hardening and subsequent softening. The "c" with an arrow (right) in each case represents the corresponding ratio for the Crab Nebula.

The spectral evolution during the decay of these three profiles is strikingly similar. This suggests that the events of June 1976 and February 1977 are generically related to type I X-ray bursts. This figure is from Hoffman et al.[123].

Figure 36. Generic relations among the various proposed mechanisms for X-ray bursts. "Magnetospheric" instabilities (cf. refs. 10, 113,129,163,237,267,317,319) rely in part on the intense magnetic field of the collapsed object, which must therefore be a degenerate dwarf or neutron star. "Purely thermal" instabilities[91] depend only upon the character of the heating and cooling rates of the accreting matter, and hence could conceivably be associated with accretion onto a massive black hole. Other proposed mechanisms[201,302] invoke instabilities in an accretion disk surrounding a collapsed object. Thermonuclear flashes near the surface of a neutron star[208,308] also rely on the existence of accretion, but only indirectly. The present evidence strongly favors thermonuclear flashes as the cause of type I bursts and one or another accretion instability as the cause of type II bursts (see text).

Figure 37. Schematic sketch of the surface layers of an accreting neutron star. This figure is from Joss[143].

Figure 38. Mass accretion rates ($\dot{m}$) and core temperatures (T_c) for the evolutionary models of the helium-burning shell by Joss[142]. Points 1 through 4 denote the parameter values used in four

models. All models assume a neutron-star mass of 1.4 $M_\odot$, a radius of 6.6 km, no magnetic field and spherical symmetry. The solid curve passing through points 1, 3, and 4 is the estimated locus of parameter values for which the core of the neutron star is in thermal equilibrium (see text). Models 1, 2 and 3 all displayed thermonuclear flashes in the helium-burning shell; the hatched region denotes the range of parameter values for which flashes may be expected. The helium-burning shell in model 4 did not display flashes; the shell evidently becomes thermally stable at high values of T_c and $\dot{m}$ (ref. 142; see text). The behavior of the helium-burning shell at low values of T_c and $\dot{m}$ remains unexplored, but it is anticipated that flashing behavior will disappear at very low values of T_c and $\dot{m}$ ($T_c < 10^8$ K and $\dot{m} < 10^{15}$ g s^{-1}; ref. 165). Also unexplored is the behavior of the helium-burning shell for parameter values far from the equilibrium curve (the upper left-hand and lower right-hand corners of the figure). This figure is from Joss[143].

Figure 39. (a) The behavior of the surface luminosity L following a thermonuclear flash in model 1 by Joss[142] (see Fig. 38). (b) Same for model 3. In each case, time t = 0 is at the start of accretion onto the neutron-star surface, the dashed line denotes the level of persistent accretion-driven luminosity, and the effective black-body temperature (T_e) is indicated at a few points. The properties of these luminosity variations are in remarkably good agreement with the typical properties of

observed X-ray bursts (see text). (c) The surface luminosity behavior for model 4. No flashes occur at the high core temperature and accretion rate of this model, so that the nuclear energy generation rate does not vary greatly and never produces more than a small perturbation on the accretion-driven luminosity. This figure is from Joss[143].

Figure 40. The decline from maximum X-ray luminosity in model 1 by Joss[142], on time scales longer than those shown in Figure 39. L_a is the level of persistent accretion-driven luminosity from the neutron-star surface, so that $(L-L_a)$ is the excess luminosity due to the thermonuclear flash. The initial decline is well fitted by an exponential decay (dashed line) with a time constant of $\tau \approx 3$ s. However, for times greater than $\sim$20 s after the burst peak, the decay time scale becomes much longer; 100 s after the peak, the local best-fit time constant is $\tau \approx$ 60 s. This "tail" of relatively soft X-rays (black-body temperature $\approx 1.3 \times 10^7$ K) contains $\sim$10% of the total burst emission. These properties are similar to those of soft X-ray "tails" in many observed X-ray burst sources (see Sects. 4.2.3 and 4.2.6). This figure is from Joss[144].

Figure 41. Structure of the surface layers of model 1 by Joss[142] prior to and during the first helium-burning flash, which begins near time t_0. M is the total mass of the neutron star and m(r) is the mass enclosed within a sphere of radius r, with r = 0 at the stellar center; thus (M-m) is the total mass of the surface

layers above level r. T is the temperature (left-hand scale), ρ the density (right-hand scale), and Y the fractional abundance of helium by mass (left-hand scale). The hatched regions indicate the extent of the convection zone generated by the flash. (a) Just prior to the flash; (b) near the start of the flash; (c) at the time when ~60% of the available fuel has been consumed; and (d) near the time of peak shell-burning temperature and peak surface luminosity. This figure is from Joss[142].

Figure 42. Temporal evolution of the first X-ray burst from model 1 by Joss[142], with neutron-star mass M = 1.41 $M_\odot$ and radius R = 6.57 km. The notation is the same as in Figure 39. (b) Same as (a), but for a model by Joss and Li[148] which has the same parameters as model 1 except that R = 13.15 km. (c) Same as (a), but for a model[148] which has the same parameters as model 1 except that M = 0.705 $M_\odot$. Note that (a) has a different time scale than (b) and (c). The differences among these three models can be largely explained by simple scaling arguments[148] (see text). This figure is from Joss and Li[148].

Figure 43. The behavior of the surface luminosity, L_s, following a thermonuclear flash in model 2 by Taam [274]. The parameters of the model are indicated. The accreting material is assumed to have an initial heavy-element abundance of 0.004 by mass. Time t=0 is at the start of accretion onto the neutron-star surface, L_{acc} is the level of the persistent accretion-driven

luminosity, and the effective temperature (T_e) is indicated at a few points. The flash is driven by helium burning, but the entrainment of hydrogen into the flash has a strong effect upon its properties (ref. 274; see text). This figure is from Taam[274].

TABLE 1

GLOBULAR CLUSTER X-RAY SOURCES

		R_c (arc sec)	Burst Source?	References**
47 Tuc	1E002151-7221.5	29	No bursts observed	100
NGC1851	MX0513-40	7	Yes	14,48,76, 134,196,211
Terzan 2	4U1722-30 1E172420-3045.6	7	Yes	92,103,268
Liller 1	MXB1730-335	7	Yes	67,180,206, 218
Terzan 1	1732-303		Yes (only bursts observed)	311,312,313
Terzan 5	1745-248		Yes (only bursts observed)	311,312,313
NGC6441	4U1746-37	9	Probably	50,134,196
NGC6624	4U1820-30	6	Yes	35,46,79,96, 134,136
NGC6712	A/4U1850-08	49	Almost Certainly	51,56,66, 134,197,272
NGC7078	4U2131+11	10	No bursts observed	79,134,136
*Kron 3	4U0026-73		No bursts observed	79,92
*NGC6440	MX1746-20		No bursts observed	79,136,211

*These two associations are uncertain. According to J. Grindlay (private communication) his earlier tentative identification of 4U0026-73 with Kron 3 is almost certainly incorrect.

**For more detailed references and for accurate source locations, see Table 4 and ref. 28.

TABLE 2

UPPER LIMITS TO PERIODICITIES IN THE PERSISTENT EMISSION FROM TYPE I BURST SOURCES*

Source	Upper limits (90% confidence) to pulsed fraction in percent, for periods in the ranges listed		
	2 ms-2 s	1.6 s-66 s	66 s-10^3 s
1636-53		1.9	3.5
1659-29		3.5	9.5
1728-34		3.6	9.2
1735-44	8	1.9	13.0
1820-30	1.5**	1.5	1.5†
1837+05		1.1	6.1
1916-05		1.3	15

*Most of the data in this table are from Cominsky et al.[52]. Upper limits of ~3% in the range ~2 ms to 2 s were found for seven bright sources (not burst sources) near the galactic center (see text).

**F.K. Li, private communication.

†Period range 66-200 s.

TABLE 3

CLASSIFICATION OF X-RAY BURSTS*

Type I (~30 sources)

- burst intervals of hours - days (longer?)
- Distinct spectral "softening" during burst decay
  - o Cooling of a "black body" during decay**
  - o Thermonuclear flashes on a neutron star
  - o Energy source is nuclear energy

Type II (Rapid Burster + others?)

- Burst intervals of sec - min
- No distinct spectral softening during burst decay
  - o "Black-body" radiation with no significant cooling during decay
  - o Instability in accretion flow onto a neutron star
  - o Energy source is gravitational potential energy

---

*This classification was introduced by Hoffman, Marshall and Lewin[127]. It was based on the two phenomenological differences listed under the solid dots. The characteristics listed under the open circles are interpretations (see e.g., refs. 127,142,144,218).

**Gray bodies with an emissivity of > 0.1 are allowed. This would increase the size of the emitting regions by a factor <3 (refs. 120, 121, 268, 273, 291, 292).

TABLE 4
September 1, 1980

Burst Source				Assoc. Persistent Source				4U Catalog Intensity		Comments	References
Name	α(1958)δ (degrees)	ℓ^{II} b^{II} (degrees)	Pos Acc (deg^2)	Names	(1958) h m s	(1958) ° ′	error circle radius (arcsec)	Average or Maximum Vela	Max Vela		
MXB 0512 40 (in NGC 1851)				2S0512 400 2A0512 399 4U0513 40	05 12 28 7	40 05 53	20	18	7		48 50 56 78 79 101 134 140 174 175 177 186 190 196 296
XB 06?? + ??		200 -5	~ 8 × 8	4U0614 + 09? or 4U0621 + 11? star?	06 21 38 06 14 22 3	11 46 48 09 09 25	3	120 2 1	5	1 burst observed	62 54 79 174 175 186 190 236 269 306 see Fig 5
MXB 0??? ??		263 -14	~ 24 × 24	?						Ten 4U sources in error box 1 Type I burst observed	63 171 172 174 175 186 190 see Fig 5
MXB 147?− 6?		315 -4	~24 × 24	?						Many 4U sources in error box 1 Type I burst observed	7 177 220 see Fig 5
XB 1455 21 (blue star)			~ 1	Cen X−4 star	14 55 19 5	-31 28 07	5			Transient	19 36 38 55 115 153 155 207 222 239 262 293 299 309
1535 29?				4U1535 29?	15 35 53	-29 13 12		200	> 10	Only 1 burst-like event May not be a Type I burst source	79
XB 1608 52 (star)				MX1608-52 4U1608-52 2S1608-523 star	16 08 51 16 08 52 2	-52 18 02 -52 17 43	20 ± 0 5	10^3	~ 25	Transient	4 21 22 23 47 68 70 78 89 94 96 102 152 154 171 172 174 175 177 181 195 214 234 235 238 278
4U1636 53 (blue star)				4U1636-53 2S1636-536 star	16 36 56 2	-53 39 15	3	250	2	15 optical bursts observed 5 of which simultaneously with X Ray bursts	37 79 107 119 120 132 174 175 177 186 190 224 226 249 250 277 281 291 296 306 307
MXB1659 29 (blue star)				4U1704 30? H1658 298 star	16 58 55 5	-29 52 26	5	3 1 80	> 15	Transient Star visible in summer 1978 (X Ray high state) not in summer 1979 X Rays undetectable Bursts not observed when persistent source in high state	37 54 69 88 90 172 173 174 175 177 183 186 189 190 265 291 296 297
XB1702 42				4U1702 42 2S1702 424	17 02 40 4	-42 57 58	30	30	3		79 133 172 174 175 177 217 241 272
MXB 1715 32	258 9 -32 1	354 2 +3 1	~ 0 1	MX 1716 31 2S1715 321	17 15 31 9	-32 07 15	60	~ 2000 ~ 15	~1001		123 212 213 241
XB1724 30 (in Terzan 2)				4U1722 30 1E 1724 20 −3045 6	17 24 20	-30 45 36	5	7			79 92 93 103 174 175 177 268 291
MXB1728 34				4U1728 33 2S1728 337	17 28 39 6	-33 47 52	30	150	5	Some bursts have two peaks at high energy X Rays	25 41 81 84 118 121 122 124 125 132 168 171 172 174 175 177 181 190 206 296 307
MXB1730 335 Rapid Burster (in Liller 1)				H1730-333	17 30 07 4	-33 20 34		~ 50 (Type II bursts	> 10	Type I and Type II bursts Recurrent transient with period of ~ 6 months IR and radio bursts reported	6 16 25 30 31 41 67 97 111 112 117 124 126 127 128 131 135 137 139 150 160 168 170 171 172 174 175 177 178 180 181 182 186 188 190 192 204 205 206 215 216 218 219 240 241 253 259 280 287 294 296 297 304 305 307
XB1732 30 (in Terzan 1 ?)	263 0 -30 3	357 6 +1 2	~ 0 8	Terzan 1?	17 32 35	-30 26 18				Only bursts observed no persistent emission Source probably in Terzan 1	311 312 313

MXB1735-44 (blue star)				4U1735 44 2S 1735 444 star	17 35 19 0	-44 25 19	3	210	1 7	2 optical bursts observed one of which simultaneously with X-Ray burst Burst intervals very erratic	27 37 79 104 105 107 132 174 175 177 186 188 190 194 223 225 228 291 296 297 307
MXB1742 29	255 7	-29 6	359 5	-0 4	0 34	A1742 294? 2S1742 294? in GCX (4U1743 29)	17 42 53 6	-29 29 50	30	90 40	> 2 5	Association with transient persistent source is possible but uncertain in view of high source density in Gal Center region	26 44 57 59 79 133 158 167 171 172 174 175 184 186 187 255
MXB1743 28	265 9	-28 5	0 5	+ 0 0	0 28	in GCX (4U1743 29)				40	5	Three bursts observed in quick succession (~4 min and 17 min apart)	57 59 116 118 158 171 172 184 186 187 255 291
MXB1743 29	265 75	-29 02	359 98	-0 16	0 09	A1742 289? in GCX (4U1743 29)	17 42 26 4	-28 59 55	25	2×10^3 40	> 200 5	Association with transient persistent source is possible but uncertain in view of high source density in Gal Center region	44 57 59 158 166 167 171 172 174 175 184 186 187 190 255 291
	either one of two positions												
	265 58	-29 29	359 67	-0 17	0 09								
XB1744 26				~ 2×10^3	4U 1744 26 GX 3 + 1 2S1744 265	17 44 49 1	-25 32 50	4	600	3		28 79 311
XB1745-24 (in Terzan 5)	266 3	-24 8	3 8	+ 1 7	~ 05	Terzan 5	17 45 0 1	-24 45 52 1				Only bursts observed no persistent emission	311 312 313
MXB1746 37 (in NGC 6441)				~ '	4U1746 37 2S1746 370		17 46 48 8	-37 02 25	30	40	1 5	Association with persistent source probable not certain (see Table 2)	50 79 98 134 174 175 177 186
XB 180? - 2?			4	-4	~ 4	?						No catalogued persistent source in error box Globular cluster NGC 6553 is in error box	172 174 175 177 186 190 272 see Fig 5
MXB1820-30 (in NGC 6624)					4U1820 30 2S1820-303		18 20 27 7	-30 23 11	20	320	3 > 10	Bursts only observed when persistent source in low state	34 35 38 43 45 46 49 50 79 80 98 99 101 134 136 137 171 172 174 175 177 181 186 190 203 286 297 307
XB 183? - 2?			11	-8	~ 8 × 8	4U1831 23?	18 31 47	-23 12 18		6		4U1831 23 is the only known persistent source in the large error box of burst source Association uncertain 4 Globular clusters in error box	17 171 172 174 175 177 186 190 see Fig 5
MXB1837 + 05 (blue star)					4U1837 + 04 Ser X 1 2S1837 - 049 star		18 37 29 6	04 59 2'	~ 3	280	2	Blue star (mg ~ 19 2) within 2" of ~ 18 5 magn star Burst intervals very erratic	' 24 61 65 66 79 80 108 109 137 171 172 174 175 177 179 181 186 190 199 200 210 270 277 282 286 290 291
MXB1850-08 (in NGC 6712)				< 0 3	A1850-08 4U1850-08 2S1850-087		18 50 2' 9	-08 45 54	~ 30	9		Association almost certain (see Table 2)	51 56 66 79 118 134 172 174 175 177 190 197 272
MXB1906 + 00					4U1857 + 01 A1905 + 00 2S1905 + 000		19 05 54 9	00 05 37	35	4 1 ± 1			56 66 75 137 171 172 174 175 177 181 186 190 191 199 277 291 296
Aql MXB XB 1908 + 00 (blue star)					4U 1908 + 00 Aql X 1 2S 1905 + 005 star		19 08 42 9	00 30 05	2		10^3	Transient Reanalysis of SAS 3 data shows that Aql MXB is almost certainly Aql X 1	28 65 171 172 174 175 177 181 186 190 191 242 283
MXB1916-05					4U1915-05 2S1916-053		19 16 08 5	-05 19 5'	20	20	2	Optical identification tentative (ref 285)	' 18 66 79 172 174 175 177 185 186 190 272 277 285 291 296
XB 2??? + 3?			79	-9	~ 50	?						4U 2058 + 32 2104 + 31 and 2120 + 32 (all very weak) in large error region of burst source	174 175 177 186 190 see Fig 5

TABLE 5

RATIOS OF OPTICAL (B BAND) TO X-RAY ENERGY FOR PERSISTENT EMISSION AND FOR BURSTS.

Values in parentheses have been corrected for interstellar extinction.

	E_{opt}/E_x			
	Persistent	Burst	X-ray band	References
4U/MXB1735-44	$1.3 \pm 0.1 \times 10^{-4}$	$2.0 \pm 0.6 \times 10^{-5}$*	2.5 - 10 keV	105,226,228
	$(<4 \times 10^{-4})$	$(<5 \times 10^{-5})$*		249
MXB1837+05+ = Ser X-1	$2.2 \pm 0.4 \times 10^{-5}$	$2.8 \pm 0.9 \times 10^{-6}$*	1.2 - 12 keV	109
4U/MXB1636-53	$\sim 5.0 \times 10^{-4}$	$\sim 1.4 \times 10^{-4}$**	1 - 25 keV	249
	$(>2 \times 10^{-3})$	$(>5 \times 10^{-4})$**		249

* ~10 s integration.

** ~10 s integration at maximum flux in the burst of 1979 June 28 (shown in Figure 18).

+The interstellar extinction in the B band for Ser X-1 is very uncertain (see ref. 179).

TABLE 6

From Johnson et al. (ref. 137)

SUMMARY OF RADIO AND X-RAY OBSERVATIONS OF X-RAY BURST SOURCES

SOURCE, UT 1977 SATELLITE	CENTER OF RADIO MAP [α(1950), δ(1950)]	RADIO OBSERVATIONS—ALL 30 s INTEGRATIONS				RADIO OBSERVATIONS—30 s INTEGRATIONS CONTAINING BURSTS		X-RAY OBSERVATIONS		
		Frequency (MHz)	Total n**	Strongest Image in Map (mJy)	Synthesized Beam (")	Strongest Image in Map (mJy)	Synthesized Beam (")	Total Number of X-ray Bursts	Flux Density of Steady Source (mJy)	Time-integrated Flux Density* of Individual Bursts (mJy s)
MXB 1730−335										
Apr 23, 24, 27										
Ariel 5, Copernicus.....	17h30m07s0	2695	599	3 ± 2	26 × 4.1	9 ± 9	33 × 4.4	31		
	−33°21′17″	8085	584	5 ± 3	8.6 × 1.4	8 ± 12	10 × 1.4	33	< 0.016†	0.7–3
MXB 1820−30										
Apr 25, 26, 28										
Copernicus.....	18h20m30s0	2695	583	4 ± 2	25 × 4.4	...	...	0		
	−30°23′00″	8085	571	4 ± 3	8.2 × 1.5	...	...	0	0.33	...
MXB 1837+05										
Jun 12, 13, 14										
SAS 3.....	18h37m29s8	2695	1573	2 ± 1	23 × 4.9	9 ± 35	38 × 6.4	2		
	+04°50′23″	8085	1531	2 ± 2	7.4 × 1.6	20 ± 50	200 × 1.5	2	0.25	3–6
MXB 1906+00										
Jun 15, 16, 17										
SAS 3.....	19h05m54s9	2695	1496	2 ± 1	28 × 4.9	...	...	0		
	+00°05′37″	8085	1438	2 ± 2	8.6 × 1.8	...	...	0	0.010	..

* Values indicate observed range of flux densities integrated over the burst duration.

† Upper limit obtained by White *et al.* (ref. 305)

** n is the number of integrations.

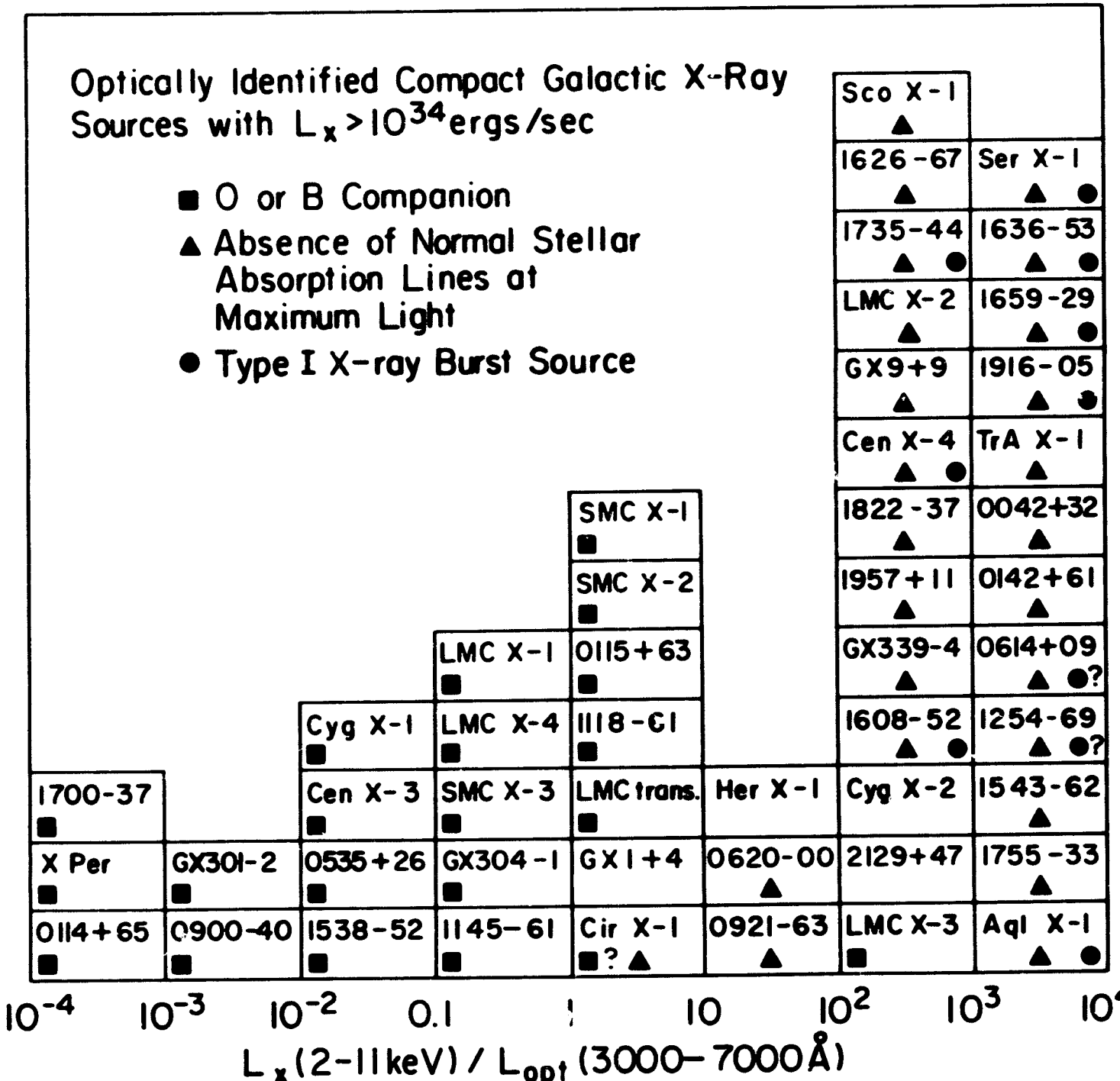
Optically Identified Compact Galactic X-Ray Sources with $L_x > 10^{34}$ ergs/sec
■ O or B Companion
▲ Absence of Normal Stellar Absorption Lines at Maximum Light
● Type I X-ray Burst Source
Sco X-1
1626-67
Ser X-1
1735-44
1636-53
LMC X-2
1659-29
GX9+9
1916-05
Cen X-4
TrA X-1
SMC X-1
1822-37
0042+32
SMC X-2
1957+11
0142+61
LMC X-1
0115+63
GX339-4
0614+09
Cyg X-1
LMC X-4
1118-61
1608-52
1254-69
1700-37
Cen X-3
SMC X-3
LMC trans.
Her X-1
Cyg X-2
1543-62
X Per
GX301-2
0535+26
GX304-1
GX1+4
0620-00
2129+47
1755-33
0114+65
0900-40
1538-52
1145-61
Cir X-1
0921-63
LMC X-3
Aql X-1
10^{-4}
10^{-3}
10^{-2}
0.1
1
10
10^2
10^3
10^4
L_x(2-11keV) / L_{opt} (3000-7000Å)

Figure 1

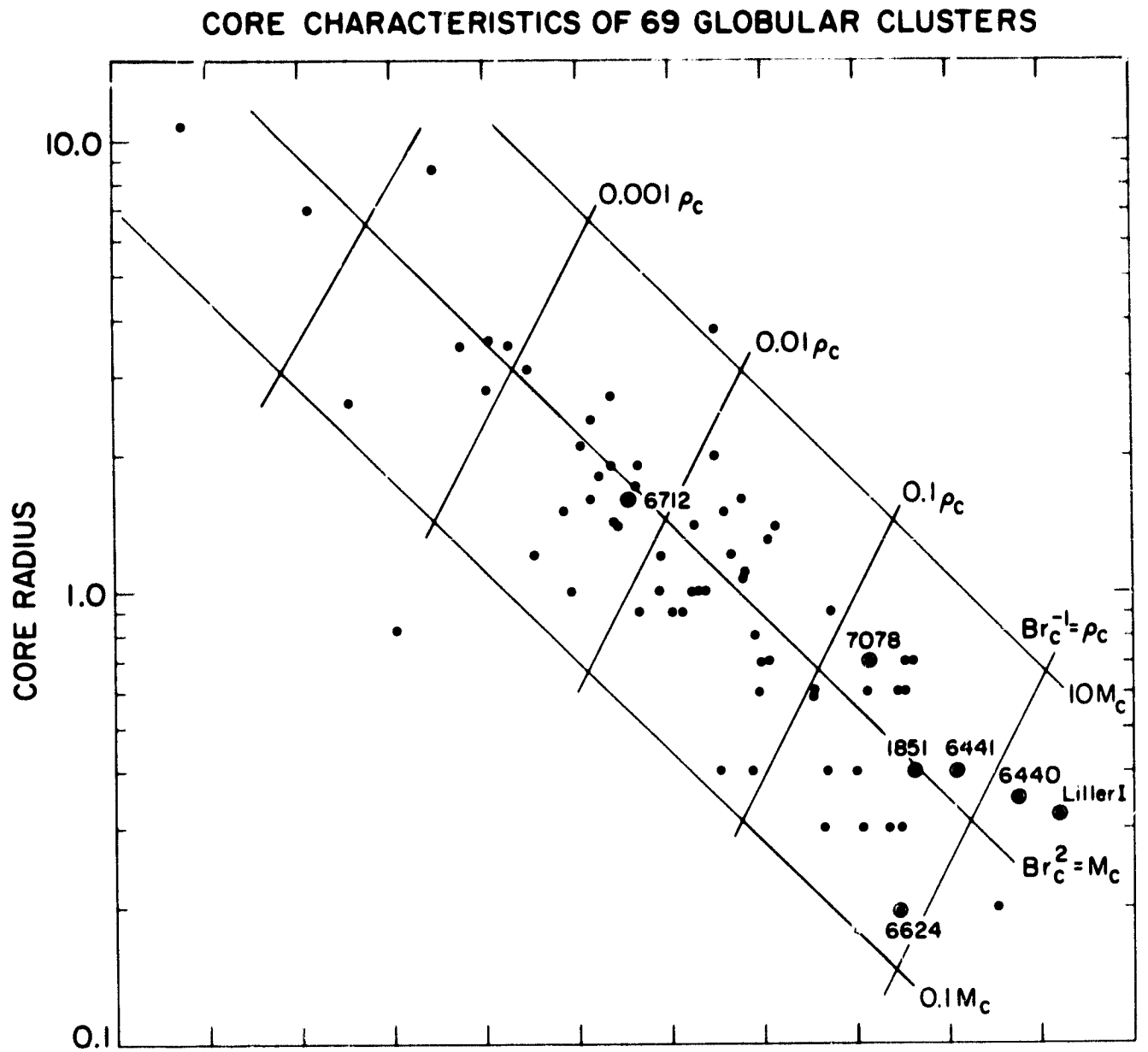
CORE CHARACTERISTICS OF 69 GLOBULAR CLUSTERS
10.0
1.0
0.1
CORE RADIUS
0.001 ρc
0.01 ρc
0.1 ρc
6712
7078
1851
6441
6440
Liller I
6624
Br_c^-1 = ρc
10Mc
Br_c^2 = Mc
0.1Mc
14
13
12
11
10
9
8
7
6
5
4
3
CENTRAL BRIGHTNESS (MAG/SQ ARC MIN)

Figure 2

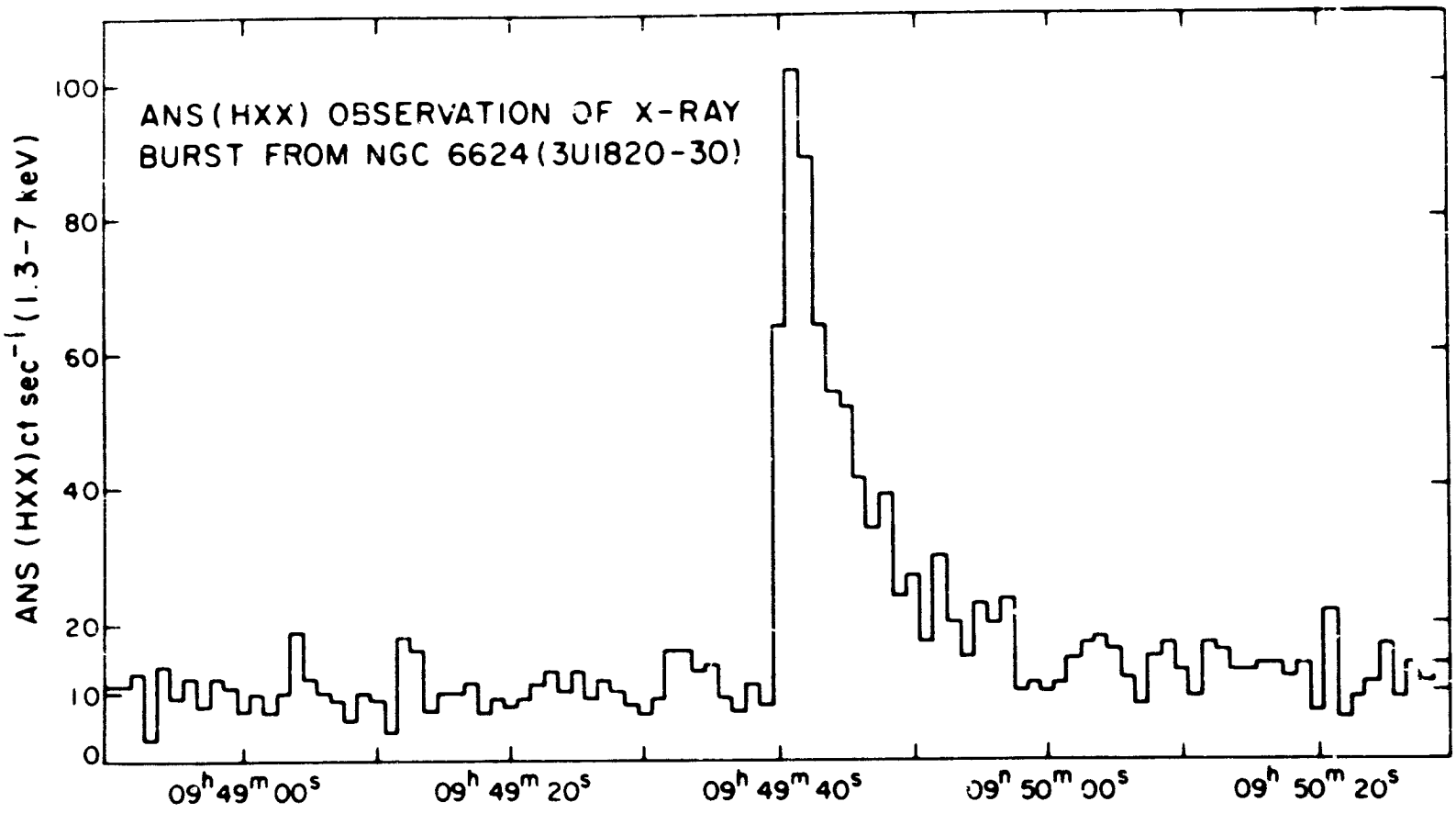
ANS(HXX) OSSERVATION OF X-RAY
BURST FROM NGC 6624(3U1820-30)
ANS (HXX)ct sec^{-1}(1.3-7 keV)
100
80
60
40
20
10
0
09^{h}49^{m}00^s
09^{h}49^{m}20^s
09^{h}49^{m}40^s
09^{h}50^{m}00^s
09^{h}50^{m}20^s

Figure 3

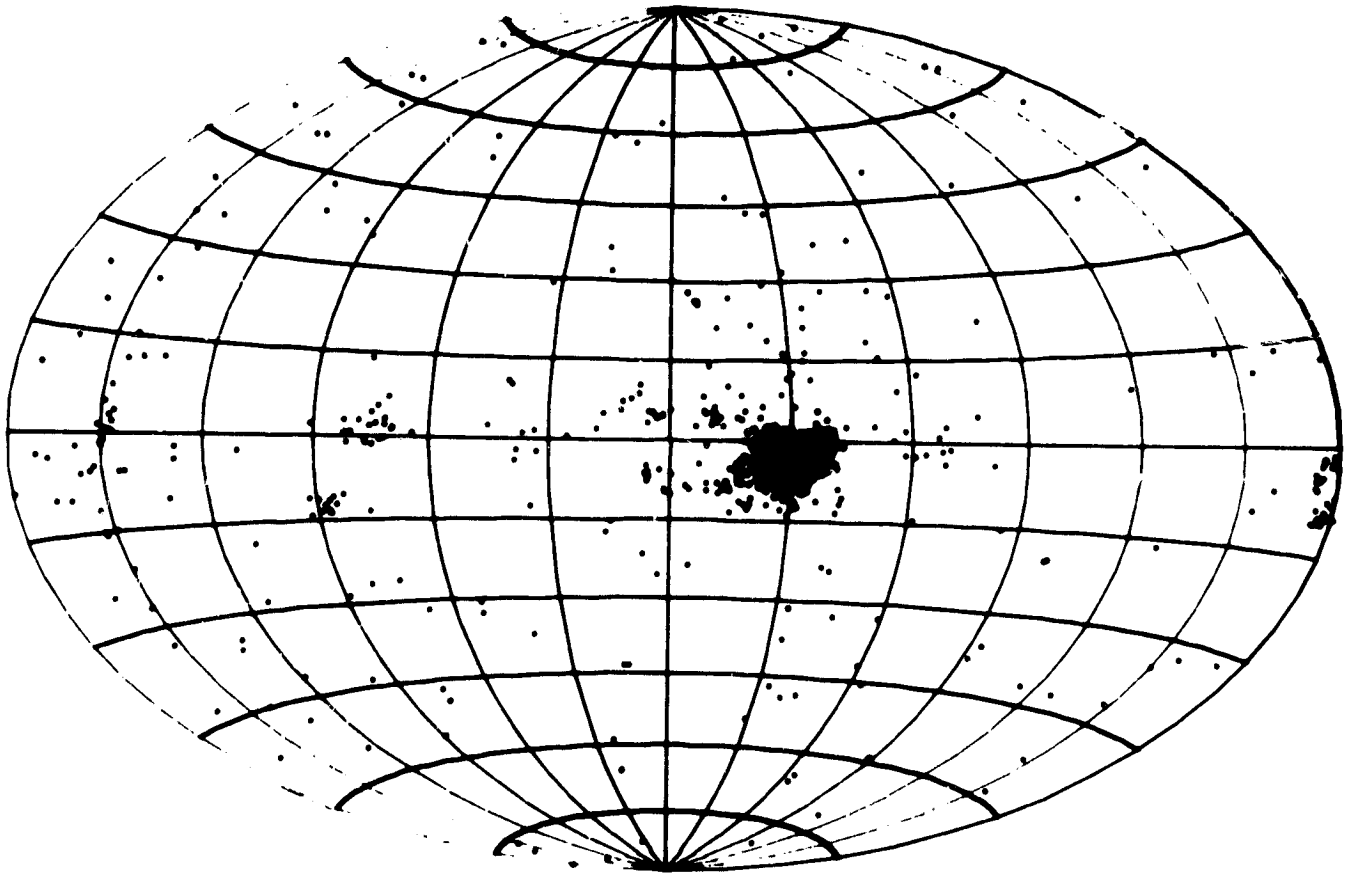

GALACTIC COORDINATES SATELLITE 58
EQUAL AREA PROJECTION

Figure 4

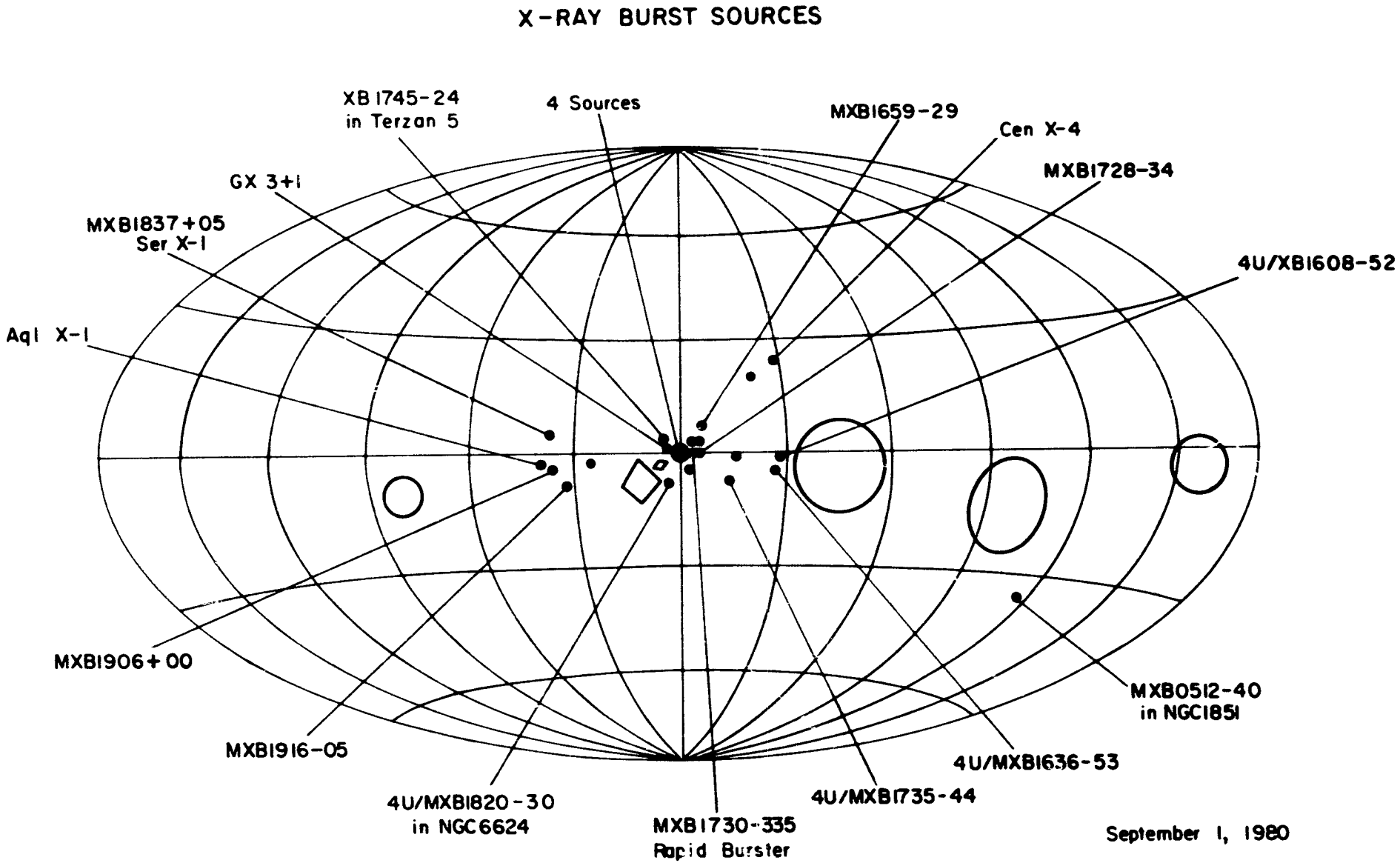
X-RAY BURST SOURCES
XB 1745-24
in Terzan 5
4 Sources
MXB1659-29
Cen X-4
MXB1728-34
GX 3+1
MXB1837+05
Ser X-1
4U/XB1608-52
Aql X-1
MXB1906+00
MXB0512-40
in NGC1851
MXB1916-05
4U/MXB1636-53
4U/MXB1735-44
4U/MXB1820-30
in NGC6624
MXB1730-335
Rapid Burster
September 1, 1980

Figure 5

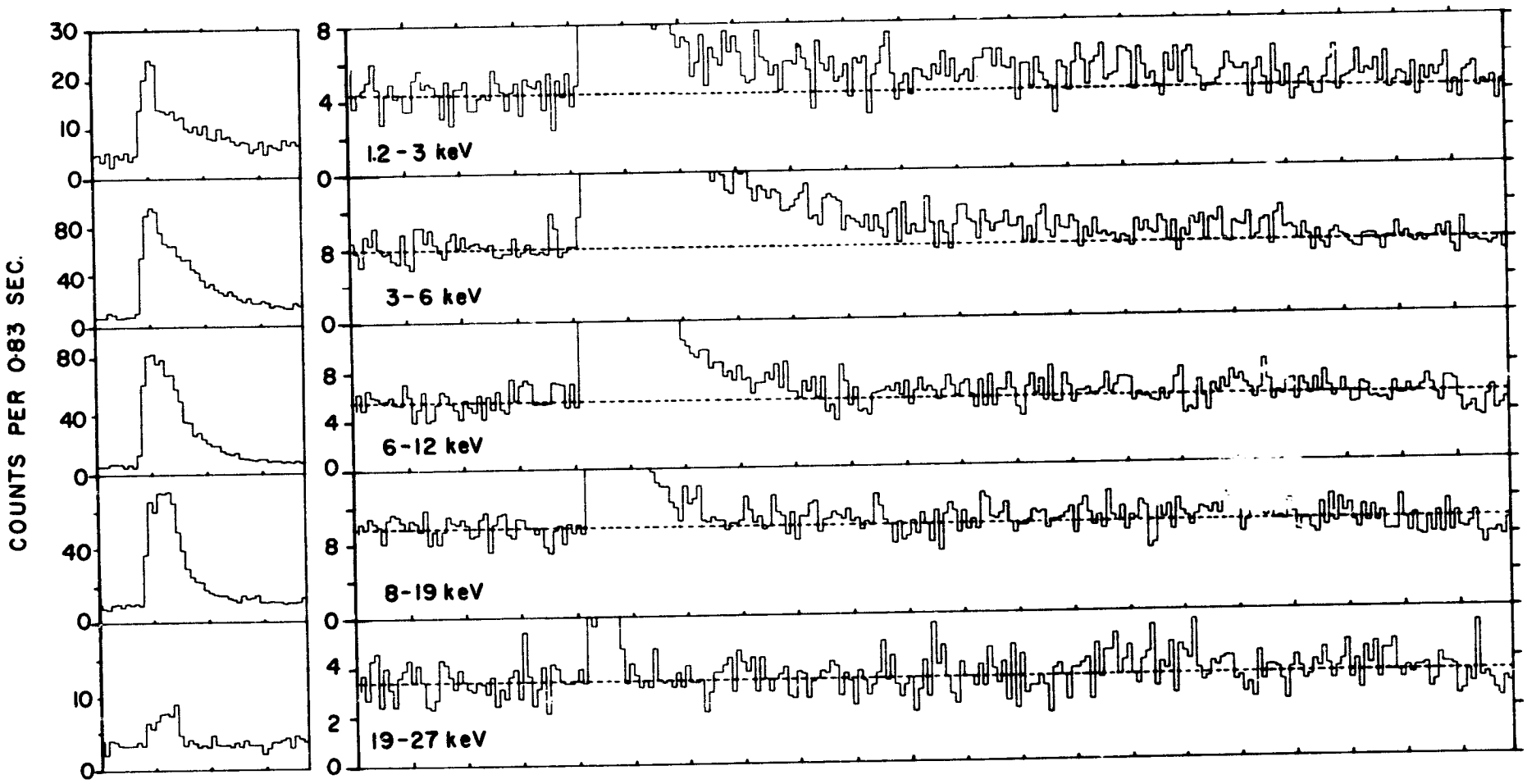
MXB1728-34 7-BURST COMPOSITE (June - July, 1976)
COUNTS PER 0·83 SEC.
1.2 - 3 keV
3 - 6 keV
6 - 12 keV
8 - 19 keV
19 - 27 keV
TIME (10 sec.)

Figure 6

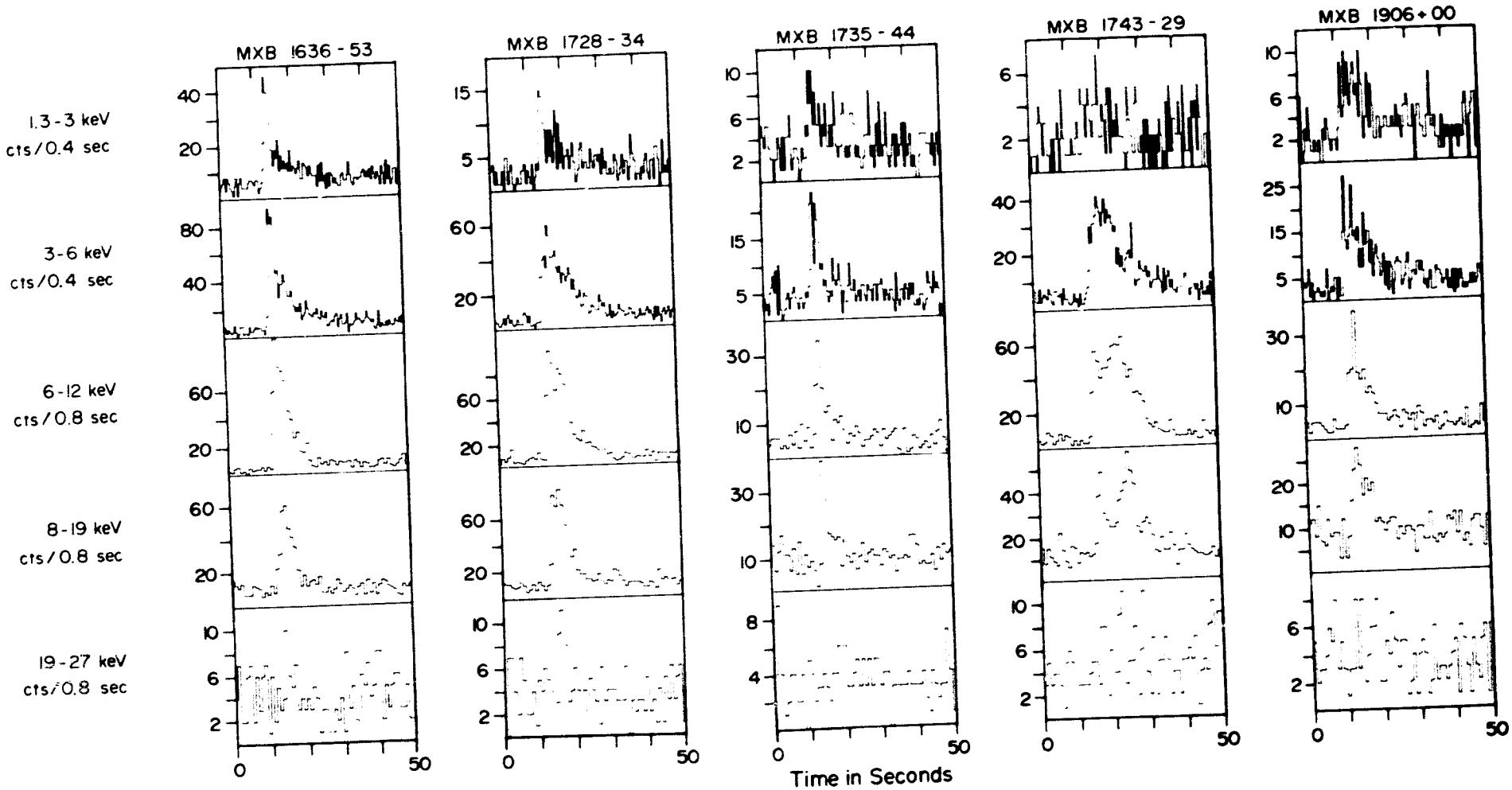
MXB 1636 - 53
MXB 1728 - 34
MXB 1735 - 44
MXB 1743 - 29
MXB 1906 + 00
1.3 - 3 keV
cts / 0.4 sec
3 - 6 keV
cts / 0.4 sec
6 - 12 keV
cts / 0.8 sec
8 - 19 keV
cts / 0.8 sec
19 - 27 keV
cts / 0.8 sec
0
50
Time in Seconds

Figure 7

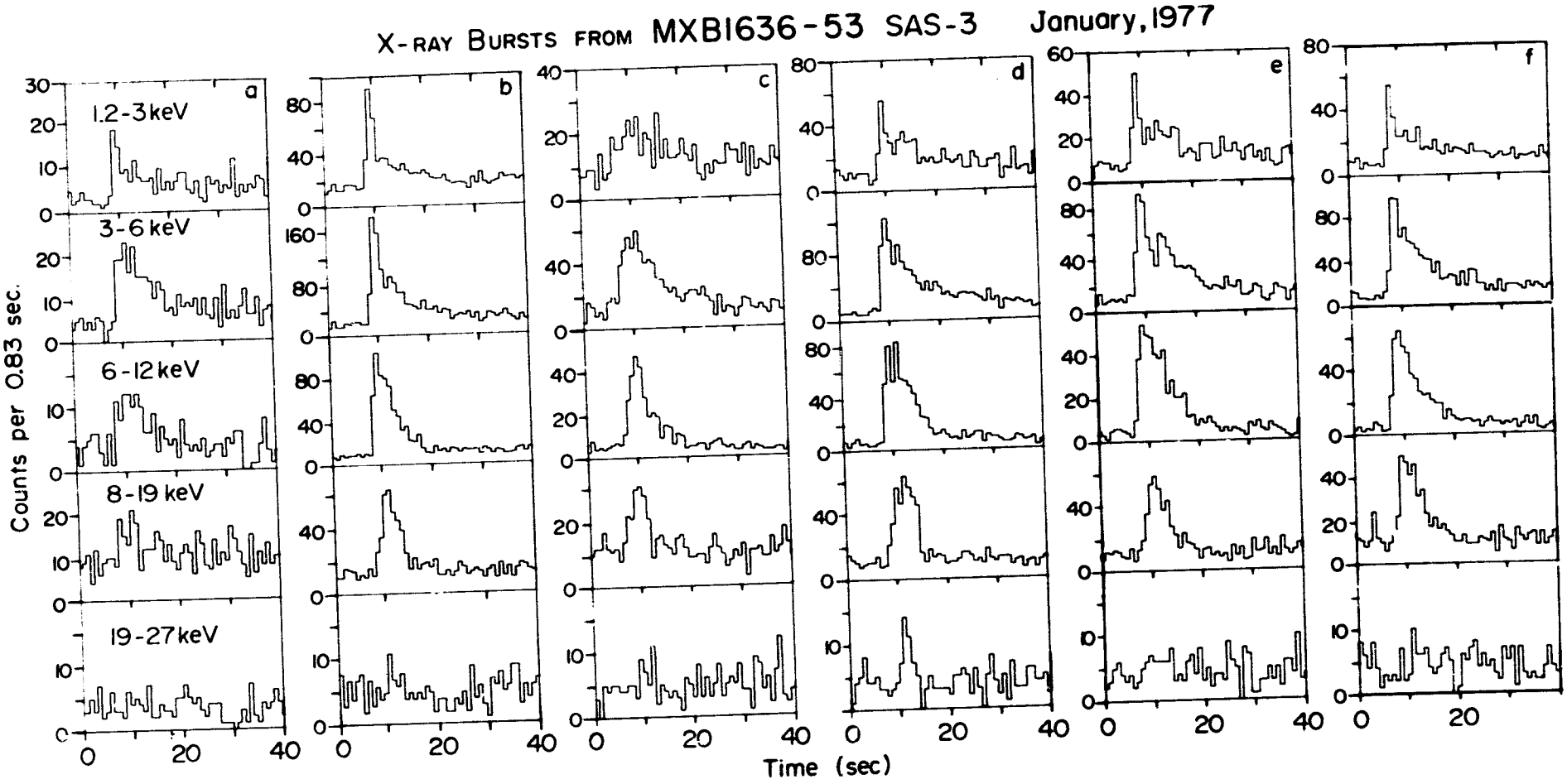
X-RAY BURSTS FROM MXB1636-53 SAS-3 January, 1977
1.2-3 keV
3-6 keV
6-12 keV
8-19 keV
19-27 keV
a
b
c
d
e
f
Counts per 0.83 sec.
Time (sec)

Figure 8

SAS-3 OBSERVATIONS OF MXB 1659-29

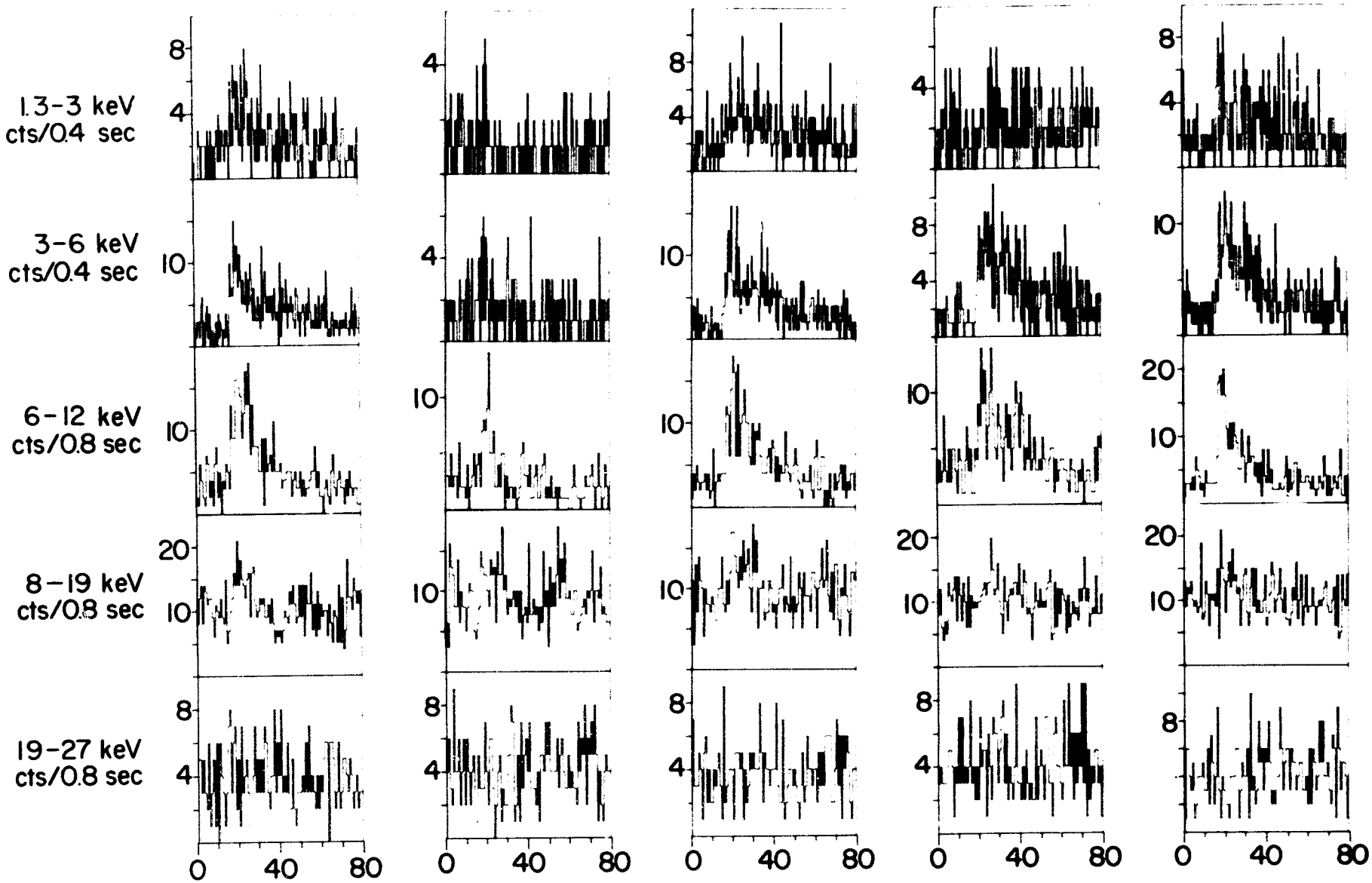

Figure 9

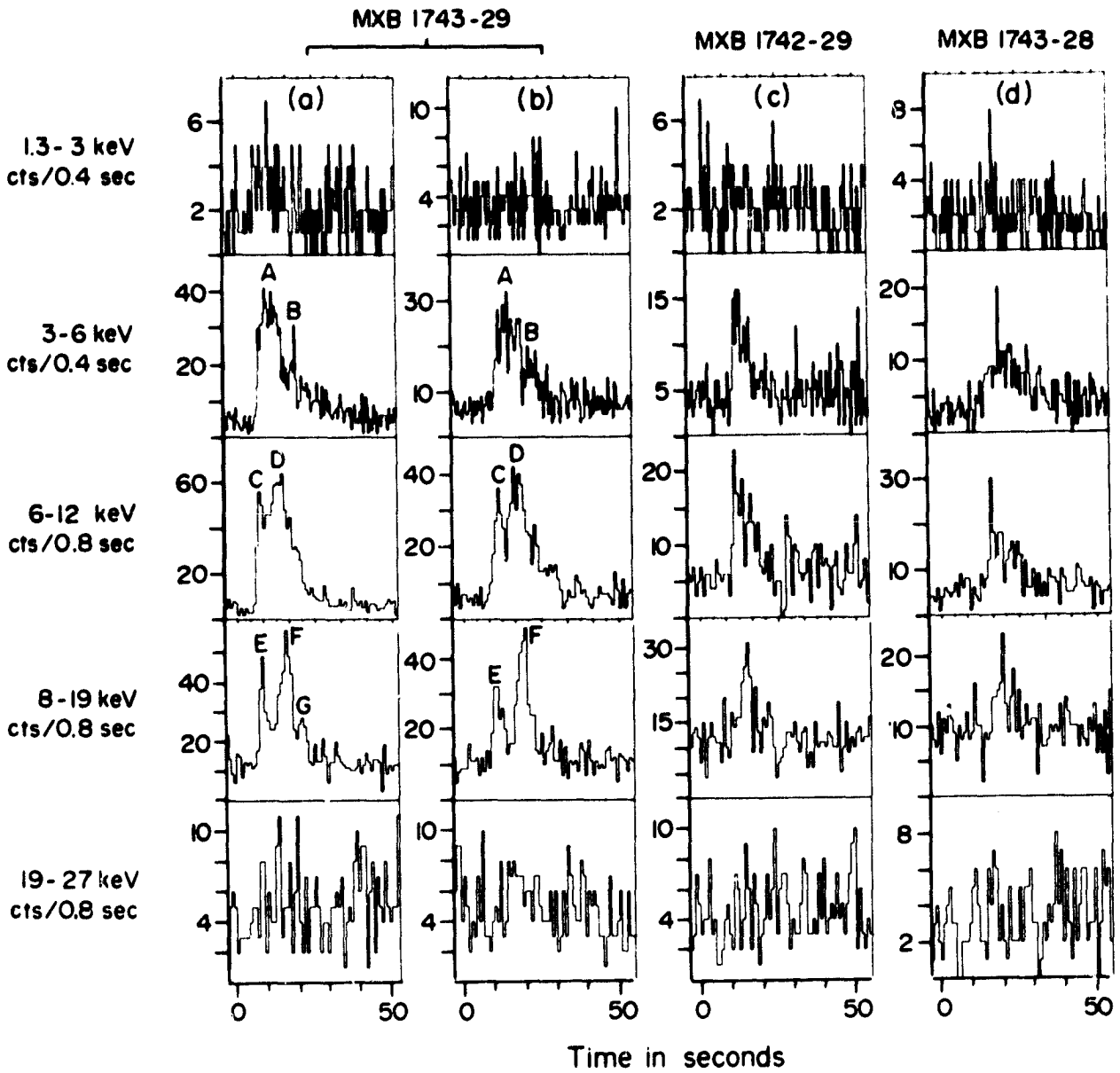
MXB 1743-29
MXB 1742-29
MXB 1743-28
(a)
(b)
(c)
(d)
1.3-3 keV
cts/0.4 sec
3-6 keV
cts/0.4 sec
6-12 keV
cts/0.8 sec
8-19 keV
cts/0.8 sec
19-27 keV
cts/0.8 sec
A
B
C
D
E
F
G
0
50
Time in seconds

Figure 10

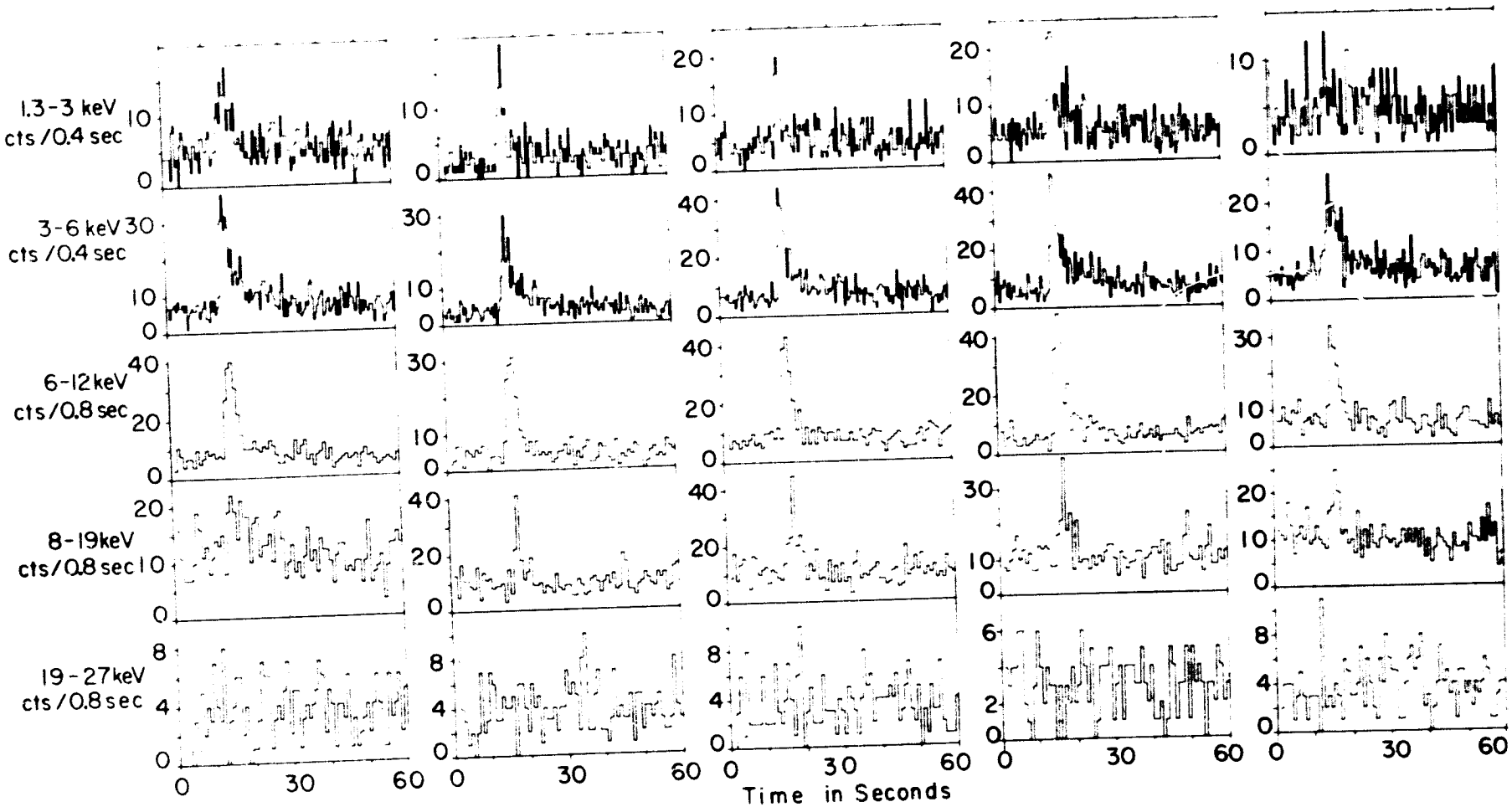
SAS-3 OBSERVATIONS OF MXB1735-44
1.3-3 keV
cts/0.4 sec
3-6 keV
cts/0.4 sec
6-12 keV
cts/0.8 sec
8-19 keV
cts/0.8 sec
19-27 keV
cts/0.8 sec
Time in Seconds

Figure 11

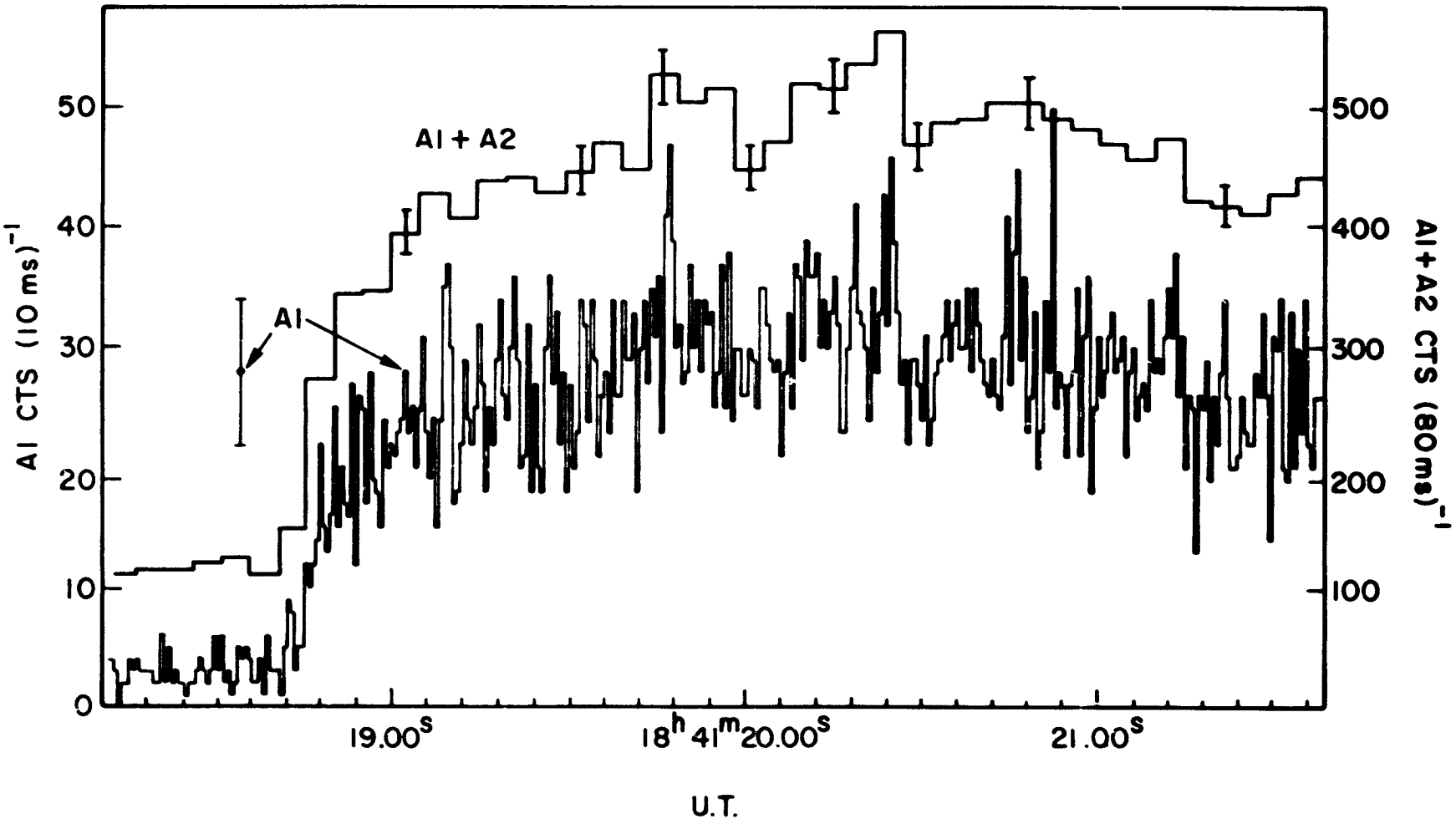
A1 + A2
A1
A1 CTS (10 ms)$^{-1}$
A1+A2 CTS (80 ms)$^{-1}$
0
10
20
30
40
50
100
200
300
400
500
19.00^{s}
18^{h} 41^{m}20.00^{s}
21.00^{s}
U.T.

Figure 12

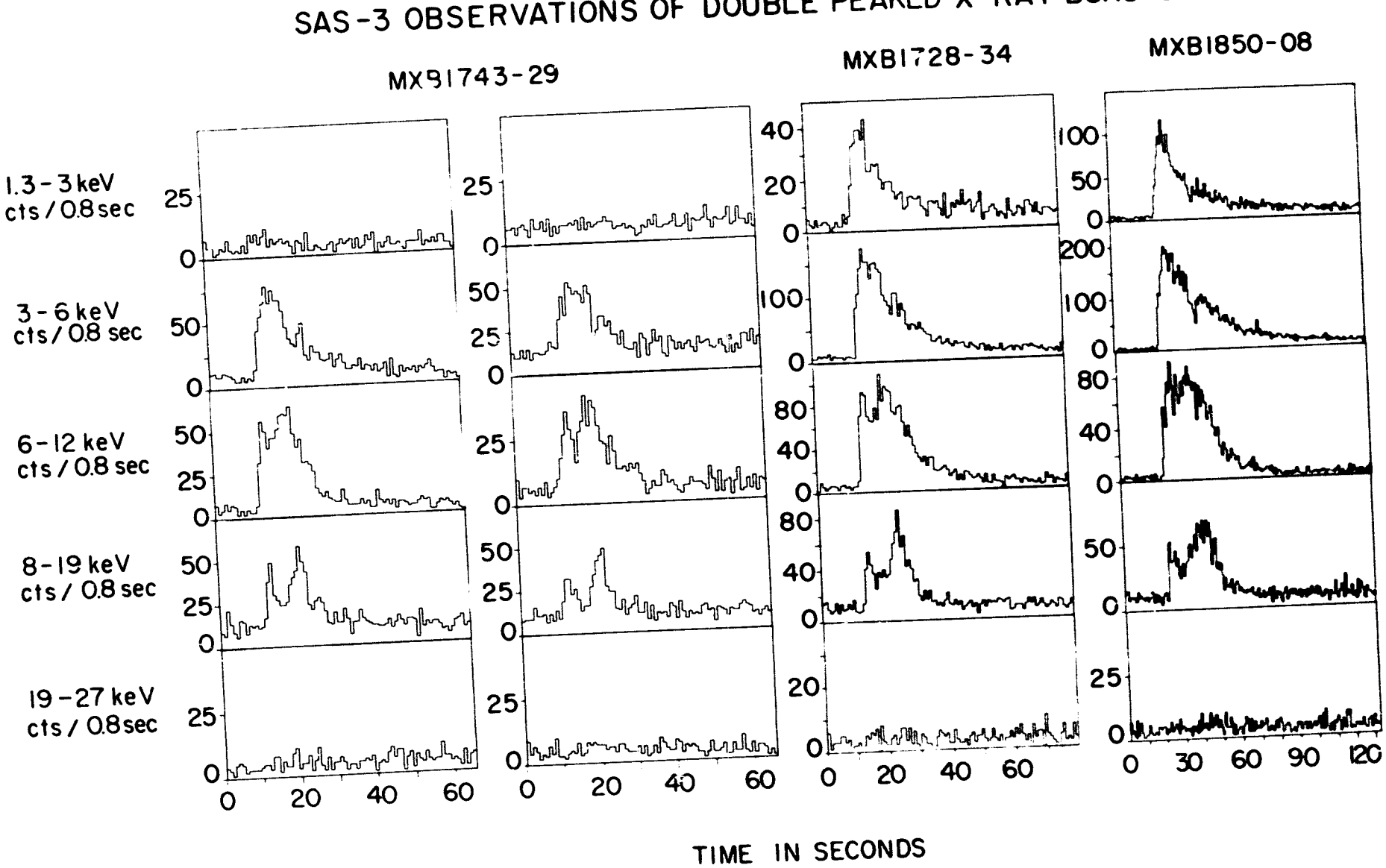
SAS-3 OBSERVATIONS OF DOUBLE PEAKED X-RAY BURSTS
MX91743-29
MXB1728-34
MXB1850-08
1.3-3 keV cts / 0.8 sec
3-6 keV cts / 0.8 sec
6-12 keV cts / 0.8 sec
8-19 keV cts / 0.8 sec
19-27 keV cts / 0.8 sec
TIME IN SECONDS

Figure 13

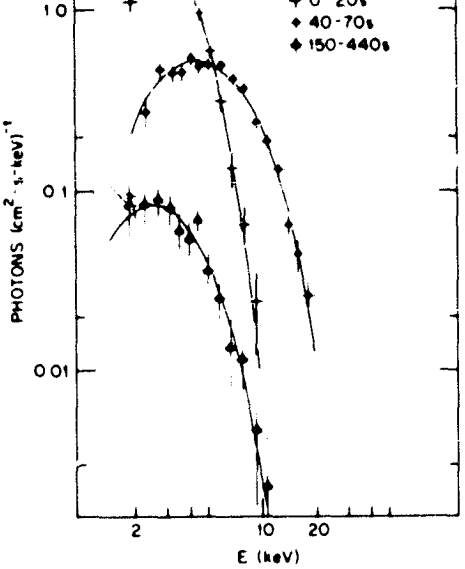

Figure 14

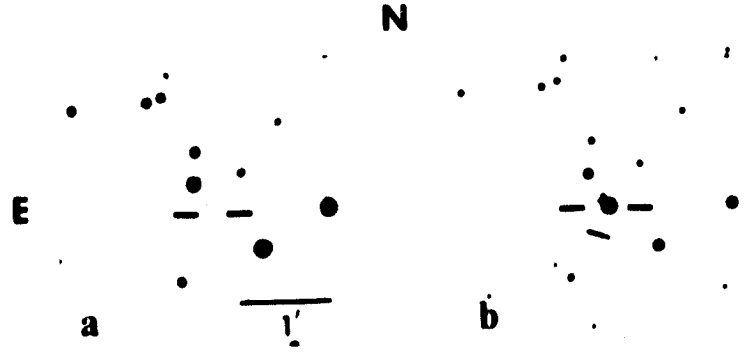

Figure 15

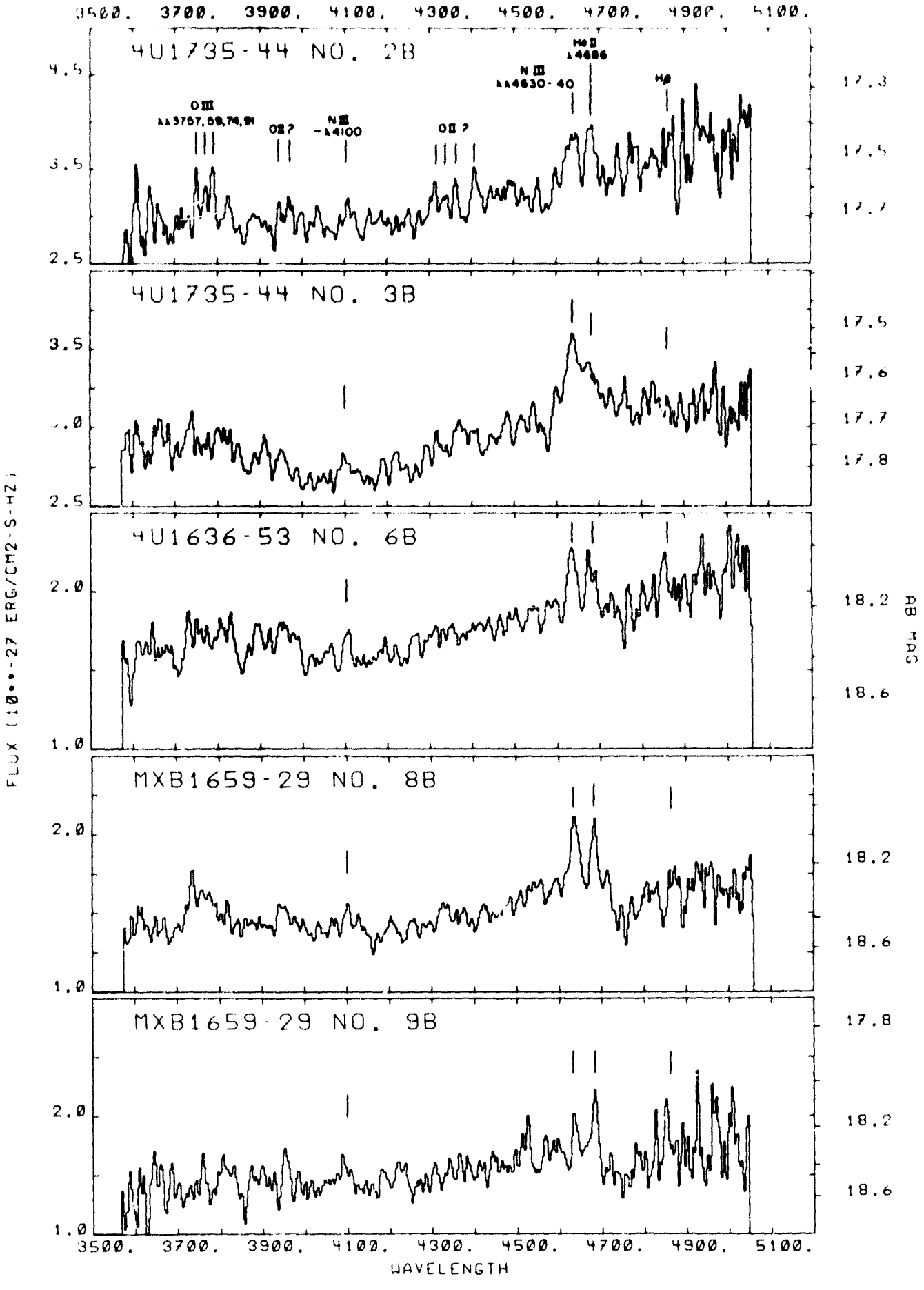
4U1735-44 NO. 2B
4U1735-44 NO. 3B
4U1636-53 NO. 6B
MXB1659-29 NO. 8B
MXB1659-29 NO. 9B
OIII λλ3757,59,74,91
OII ?
NIII ~λ4100
OII ?
NIII λλ4630-40
HeII λ4686
Hβ
FLUX (10**-27 ERG/CM2-S-HZ)
AB MAG
WAVELENGTH
3500. 3700. 3900. 4100. 4300. 4500. 4700. 4900. 5100.

Figure 16

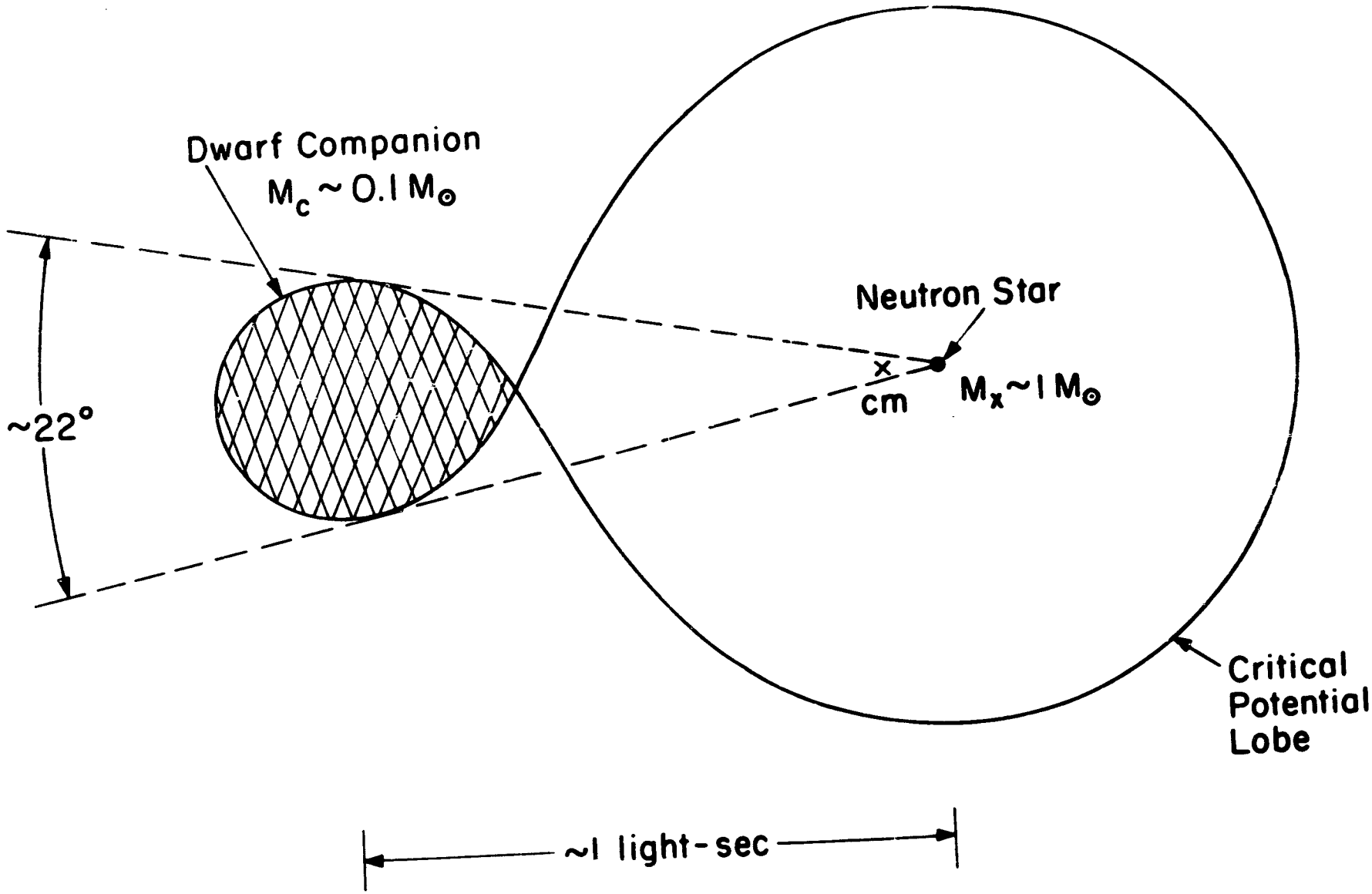
Dwarf Companion
$M_c \sim 0.1\,M_\odot$
Neutron Star
x
cm
$M_x \sim 1\,M_\odot$
~22°
Critical
Potential
Lobe
~1 light-sec

Figure 17

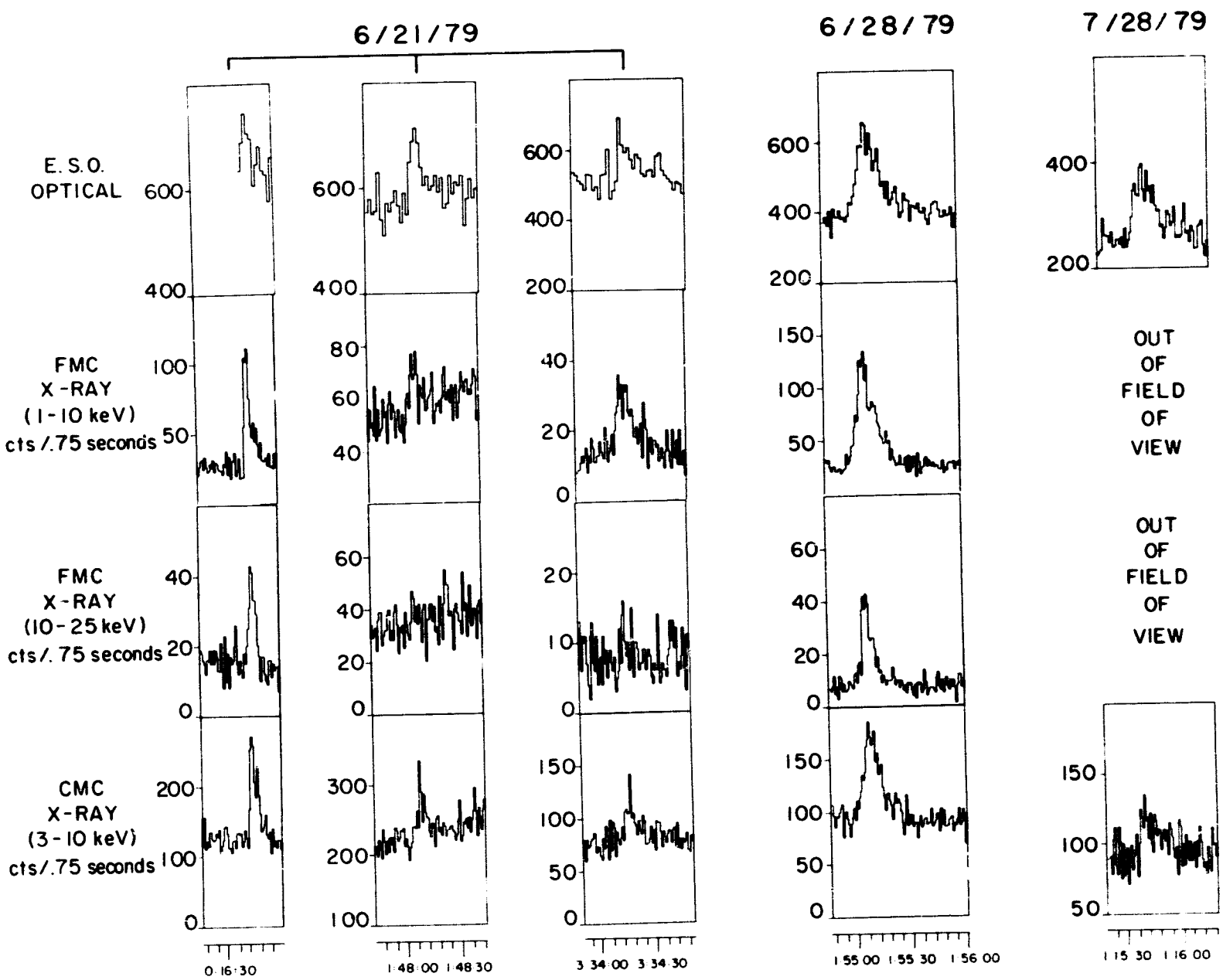
E. S. O. / HAKUCHO OBSERVATIONS OF MXB1636-53
6/21/79
6/28/79
7/28/79
E. S. O. OPTICAL
FMC X-RAY (1-10 keV) cts/.75 seconds
FMC X-RAY (10-25 keV) cts/.75 seconds
CMC X-RAY (3-10 keV) cts/.75 seconds
OUT OF FIELD OF VIEW
OUT OF FIELD OF VIEW
0 16 30
1 48 00
1 48 30
3 34 00
3 34 30
1 55 00
1 55 30
1 56 00
1 15 30
1 16 00

Figure 18

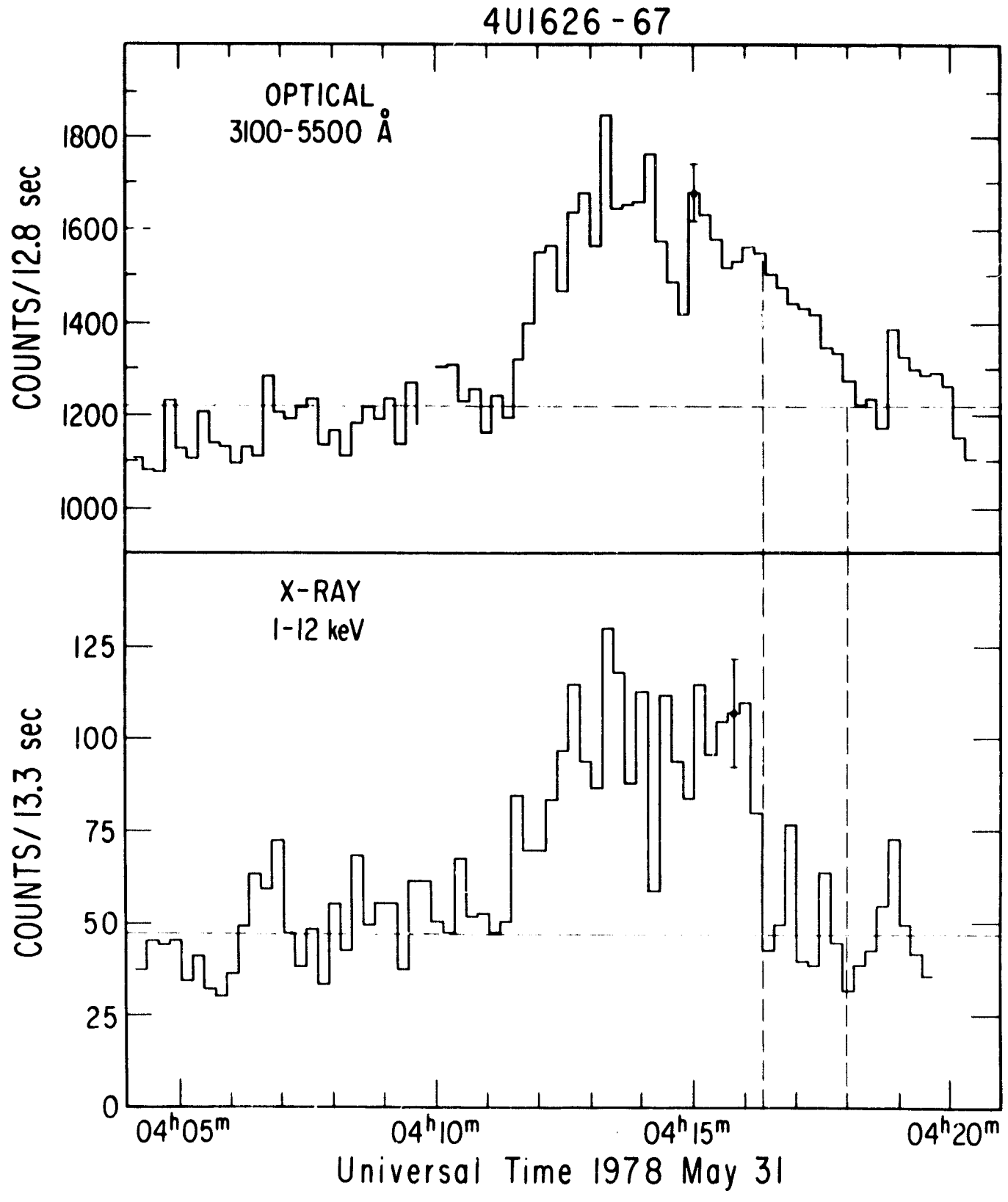
4U1626-67
OPTICAL
3100-5500 Å
COUNTS/12.8 sec
1800
1600
1400
1200
1000
X-RAY
1-12 keV
COUNTS/13.3 sec
125
100
75
50
25
0
04h05m
04h10m
04h15m
04h20m
Universal Time 1978 May 31

Figure 19

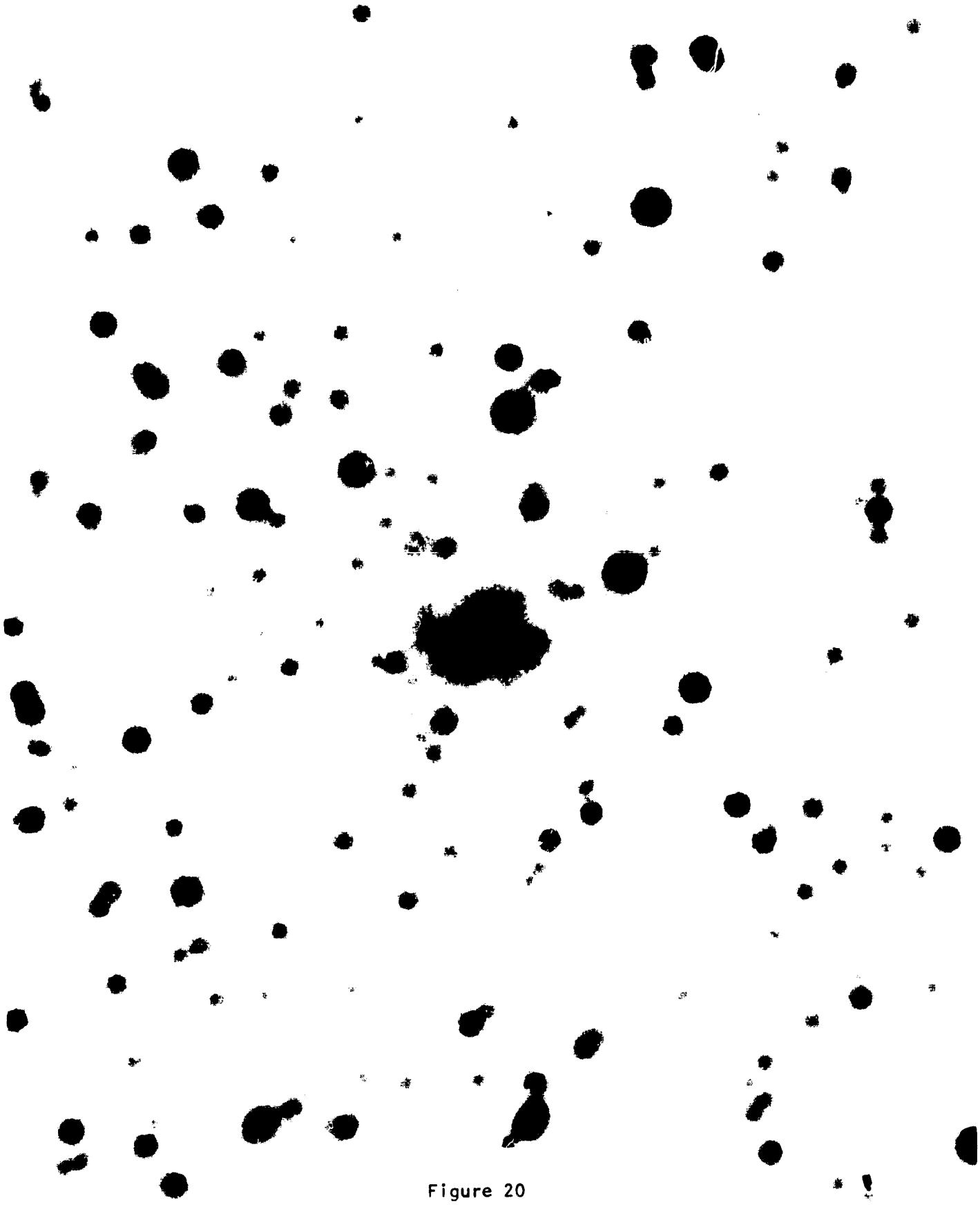

Figure 20

ORIGINAL PAGE IS
OF POOR QUALITY

SAS-3 OBSERVATIONS OF RAPIDLY REPETITIVE X-RAY BURSTS FROM MXB 1730-335

24-minute snapshots from 8 orbits on March 2/3, 1976

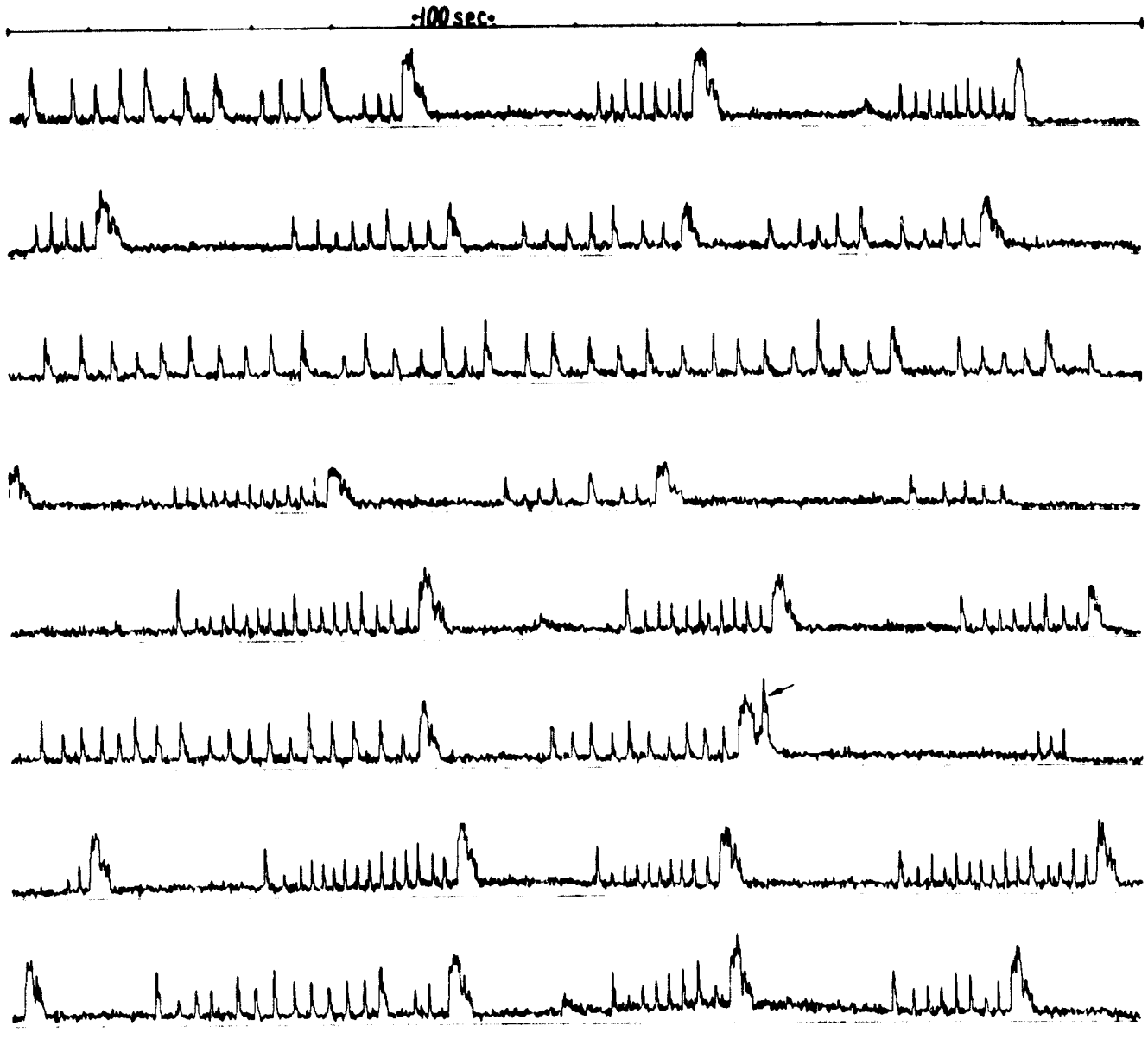

Figure 21

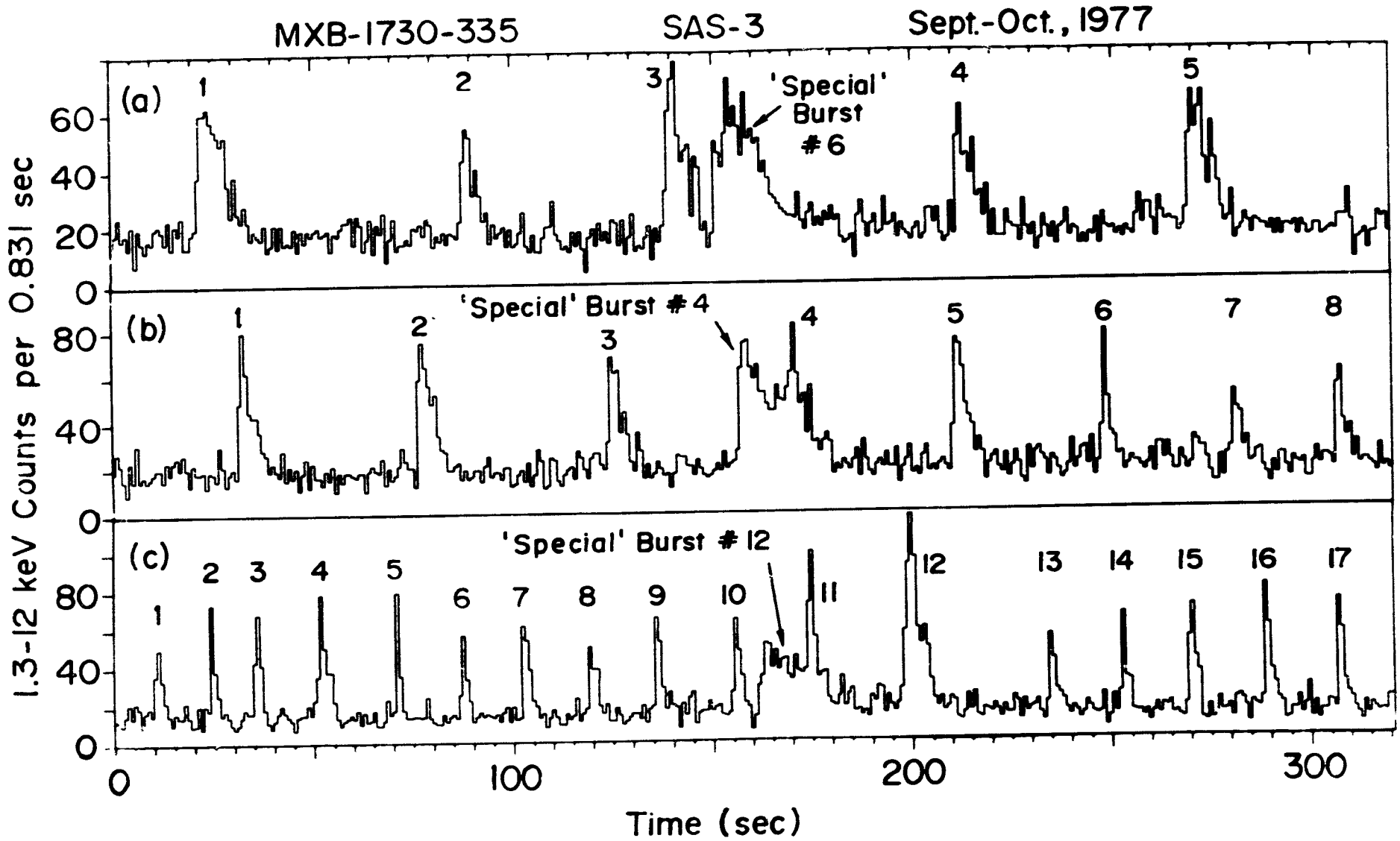
MXB-1730-335
SAS-3
Sept.-Oct., 1977
(a)
'Special' Burst #6
(b)
'Special' Burst #4
(c)
'Special' Burst #12
1.3-12 keV Counts per 0.831 sec
Time (sec)
0
100
200
300

Figure 22

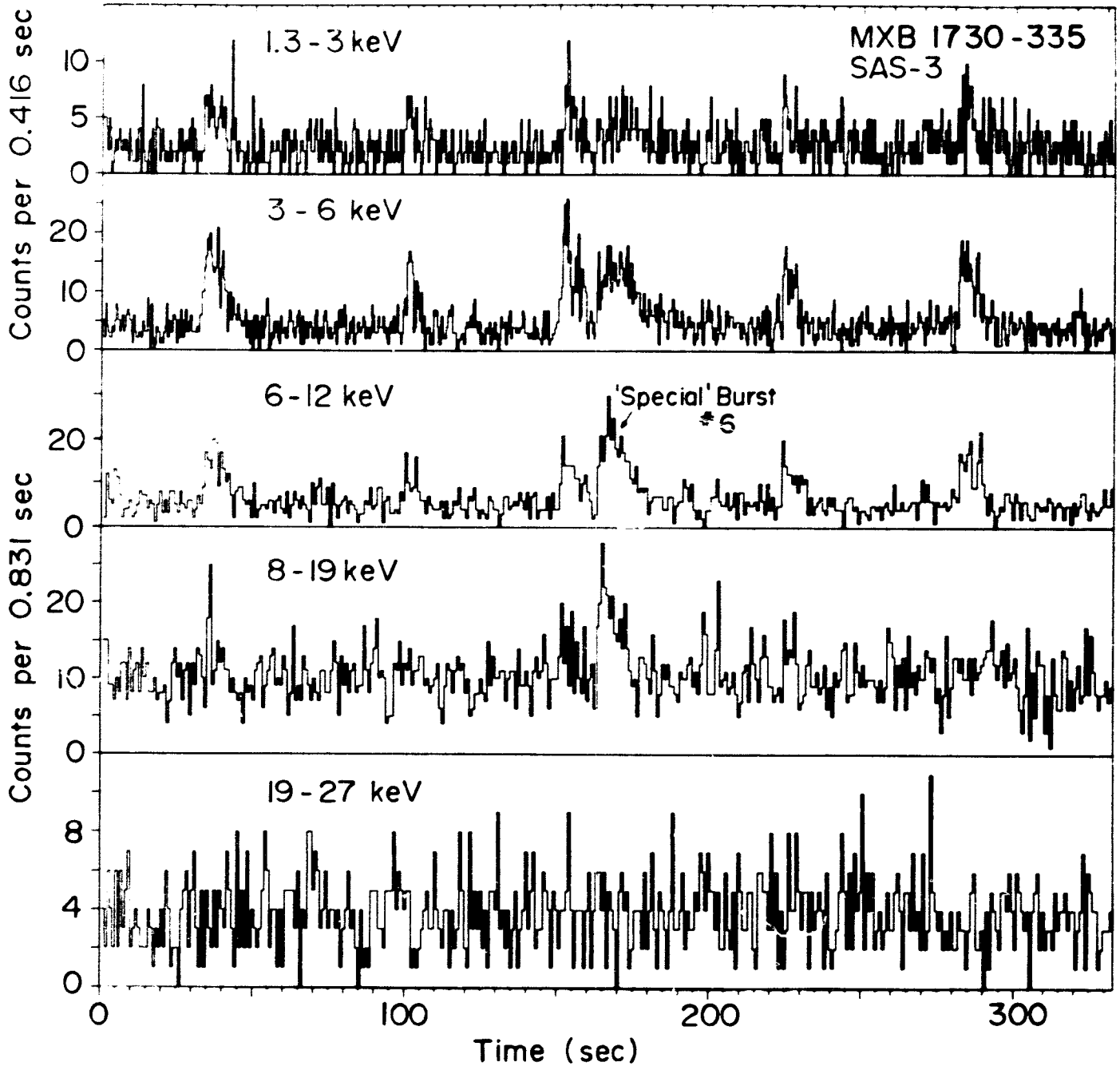
MXB 1730-335
SAS-3
1.3 - 3 keV
3 - 6 keV
6 - 12 keV
'Special' Burst
#6
8 - 19 keV
19 - 27 keV
Counts per 0.416 sec
Counts per 0.831 sec
Time (sec)
0
100
200
300

Figure 23

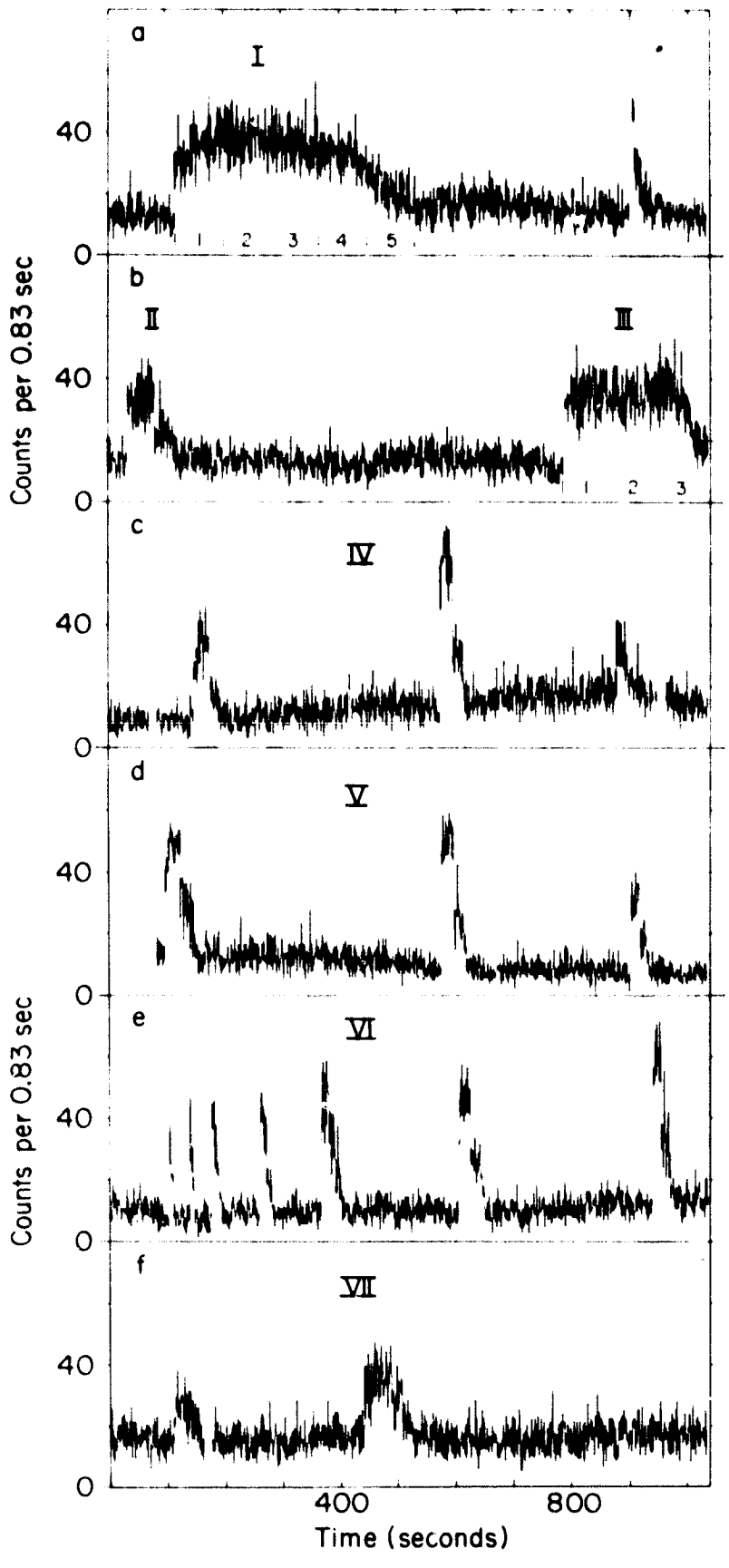
SAS-3 OBSERVATIONS OF MXB 1730-335
a
I
b
II
III
c
IV
d
V
e
VI
f
VII
1 2 3 4 5
1 2 3
40
0
Counts per 0.83 sec
400
800
Time (seconds)

Figure 24

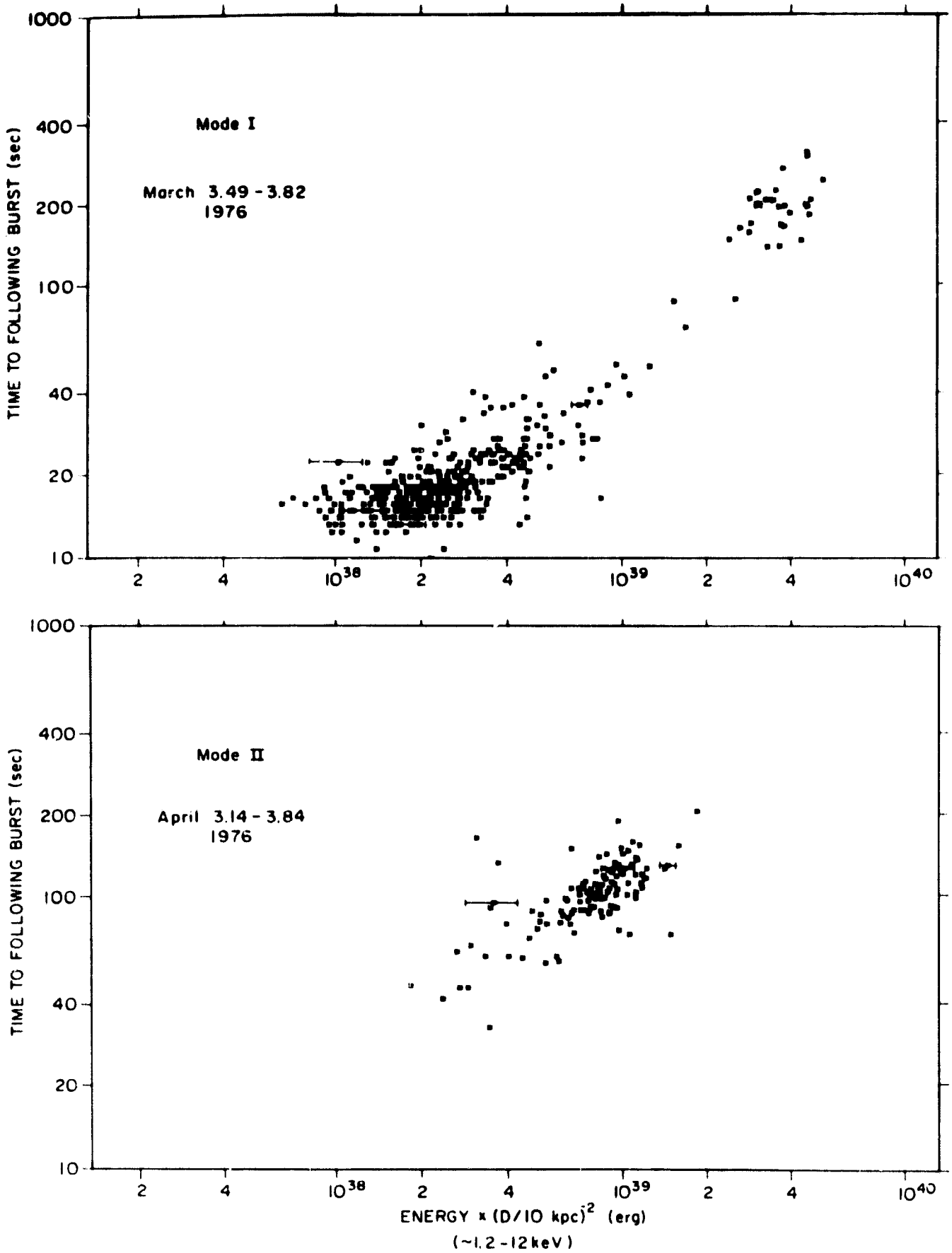
Mode I
March 3.49 - 3.82
1976
TIME TO FOLLOWING BURST (sec)
1000
400
200
100
40
20
10
2
4
10^38
2
4
10^39
2
4
10^40
Mode II
April 3.14 - 3.84
1976
TIME TO FOLLOWING BURST (sec)
ENERGY x (D/10 kpc)^2 (erg)
(~1.2 - 12 keV)

Figure 25

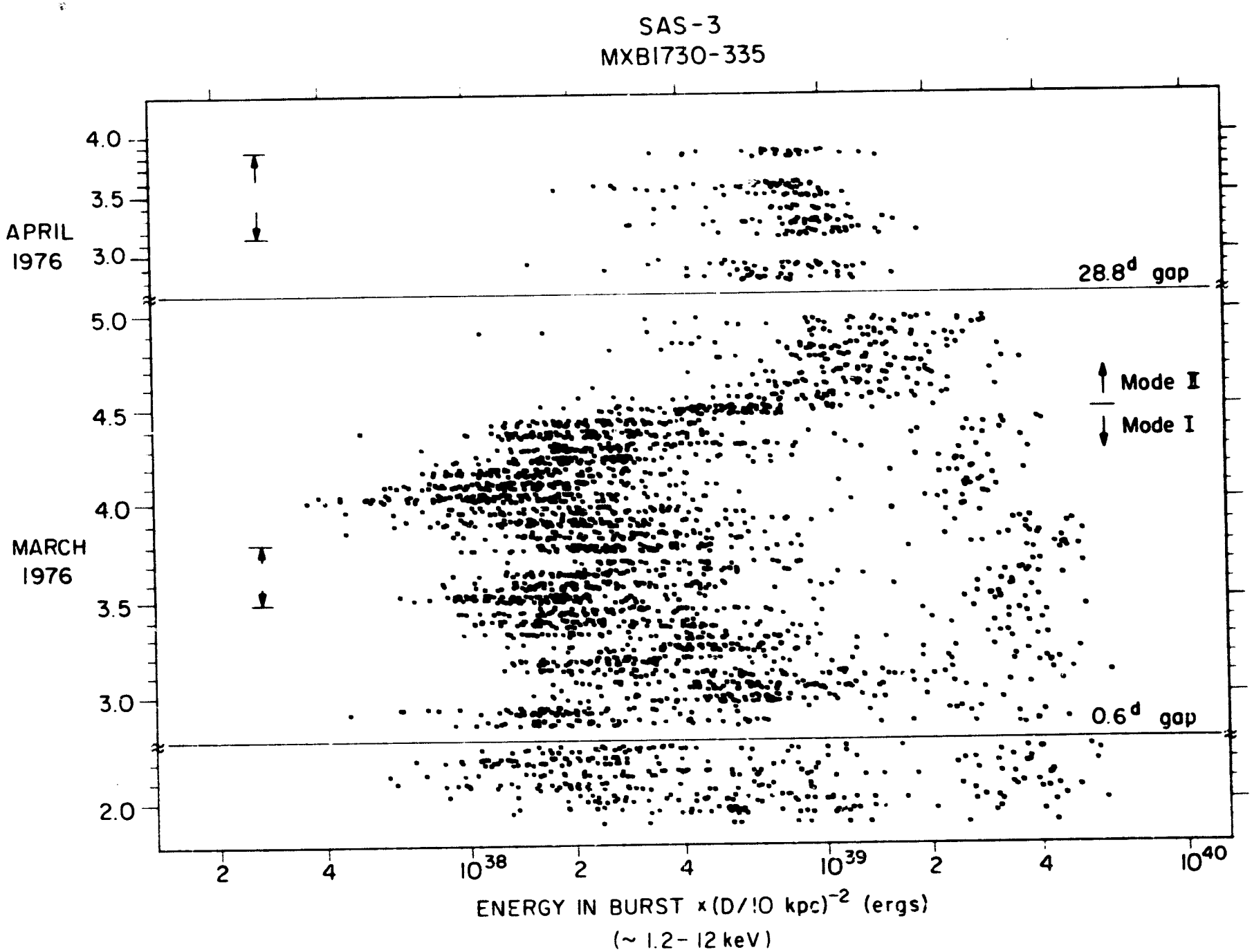
SAS-3
MXB1730-335
APRIL
1976
MARCH
1976
4.0
3.5
3.0
5.0
4.5
4.0
3.5
3.0
2.0
28.8d gap
0.6d gap
Mode II
Mode I
2
4
10^38
2
4
10^39
2
4
10^40
ENERGY IN BURST x(D/10 kpc)^-2 (ergs)
(~ 1.2 - 12 keV)

Figure 26

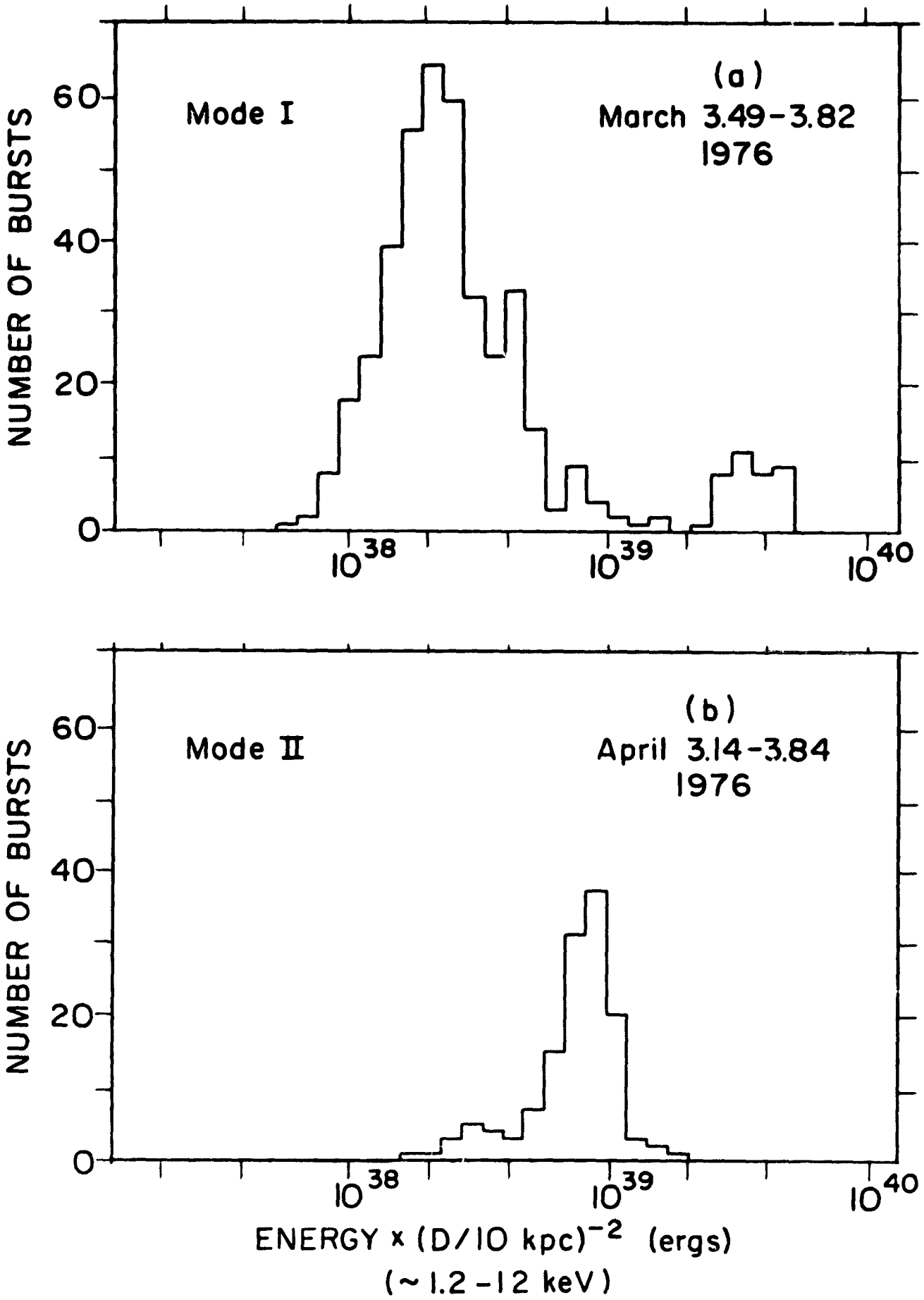
(a)
Mode I
March 3.49-3.82
1976
NUMBER OF BURSTS
60
40
20
0
10^{38}
10^{39}
10^{40}
(b)
Mode II
April 3.14-3.84
1976
NUMBER OF BURSTS
60
40
20
0
10^{38}
10^{39}
10^{40}
ENERGY x (D/10 kpc)$^{-2}$ (ergs)
(~ 1.2 - 12 keV)

Figure 27

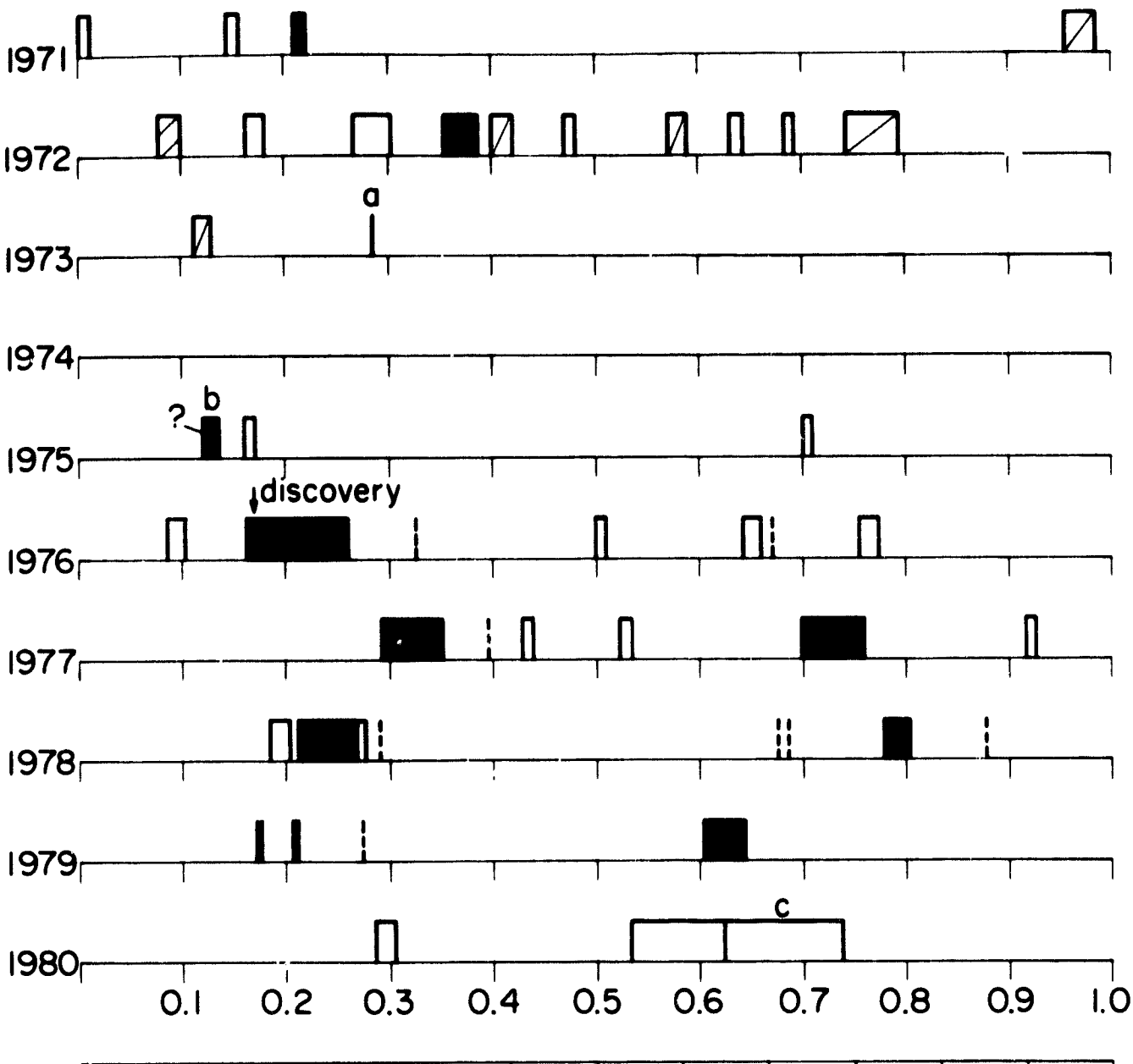
Observations of MXB1730-335
1971
1972
a
1973
1974
?
b
1975
discovery
1976
1977
1978
1979
c
1980
0.1
0.2
0.3
0.4
0.5
0.6
0.7
0.8
0.9
1.0
J
F
M
A
M
J
J
A
S
O
N
D

Figure 28

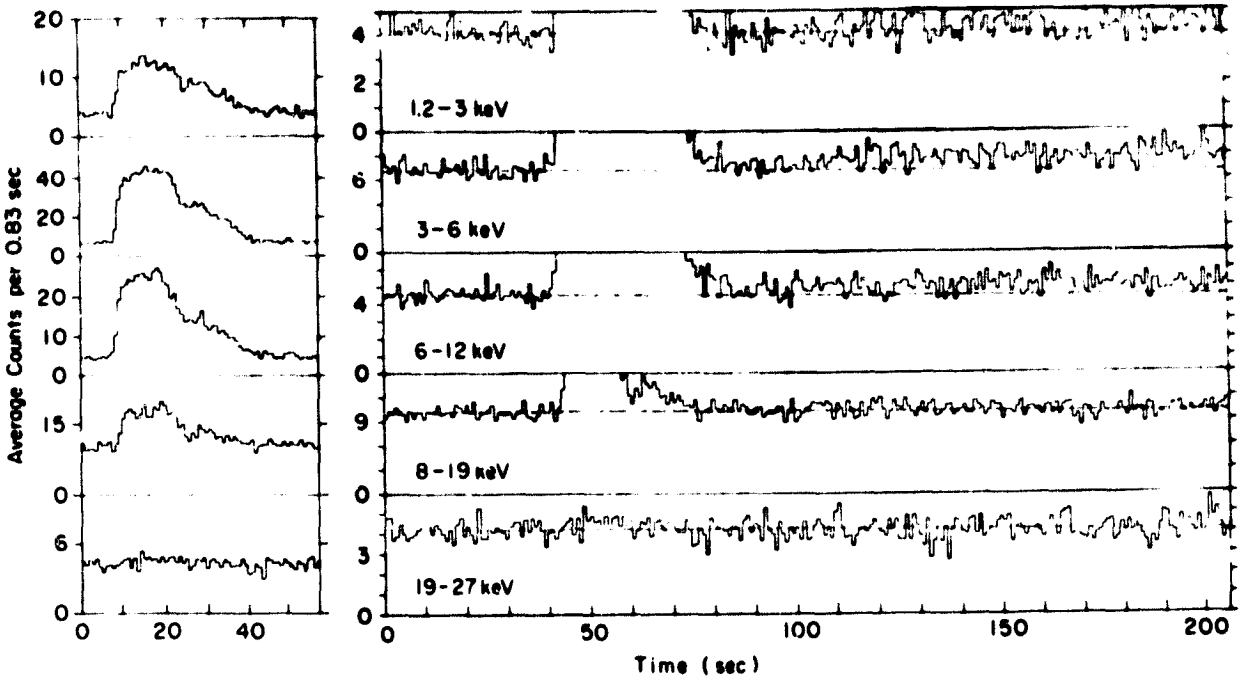
Average Counts per 0.83 sec
1.2-3 keV
3-6 keV
6-12 keV
8-19 keV
19-27 keV
Time (sec)

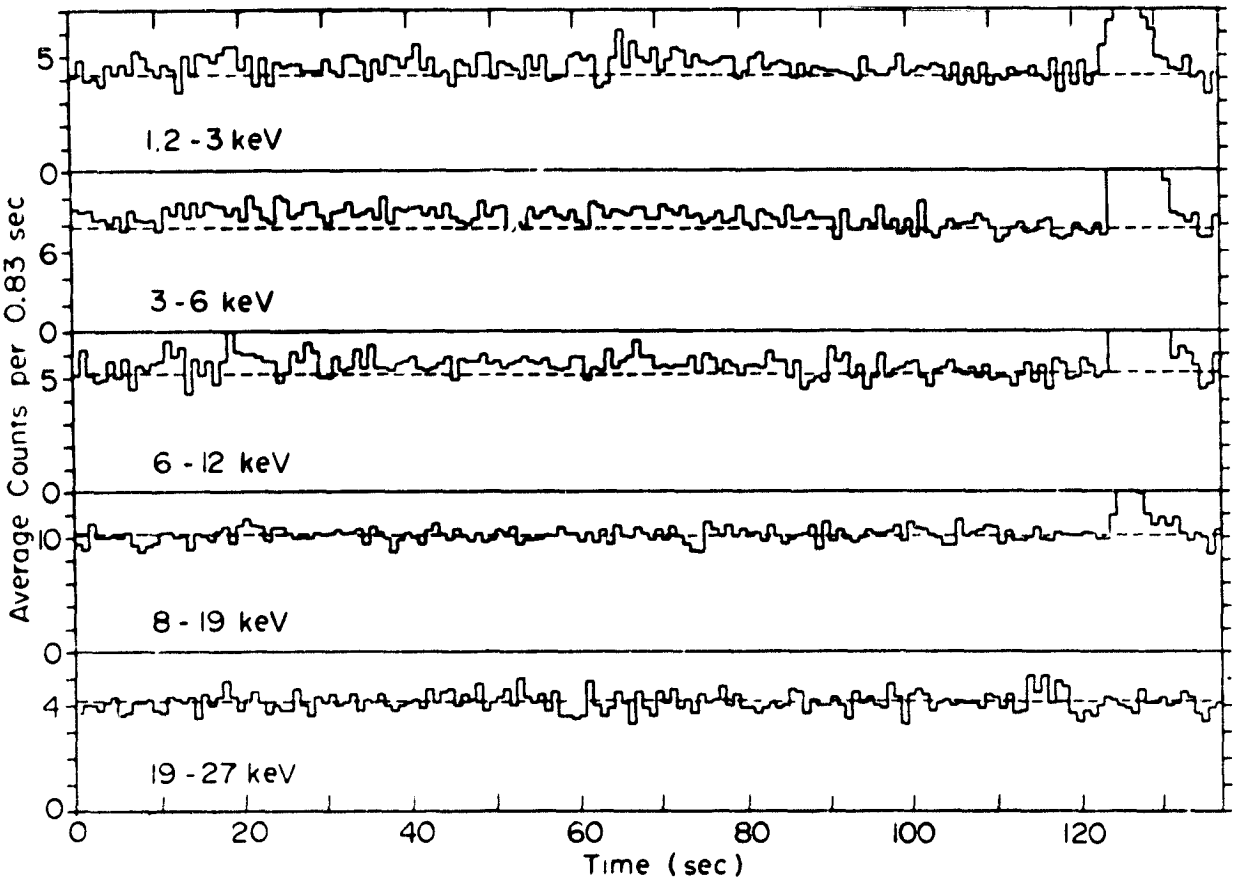
Average Counts per 0.83 sec
1.2 - 3 keV
3 - 6 keV
6 - 12 keV
8 - 19 keV
19 - 27 keV
Time (sec)

Figure 29

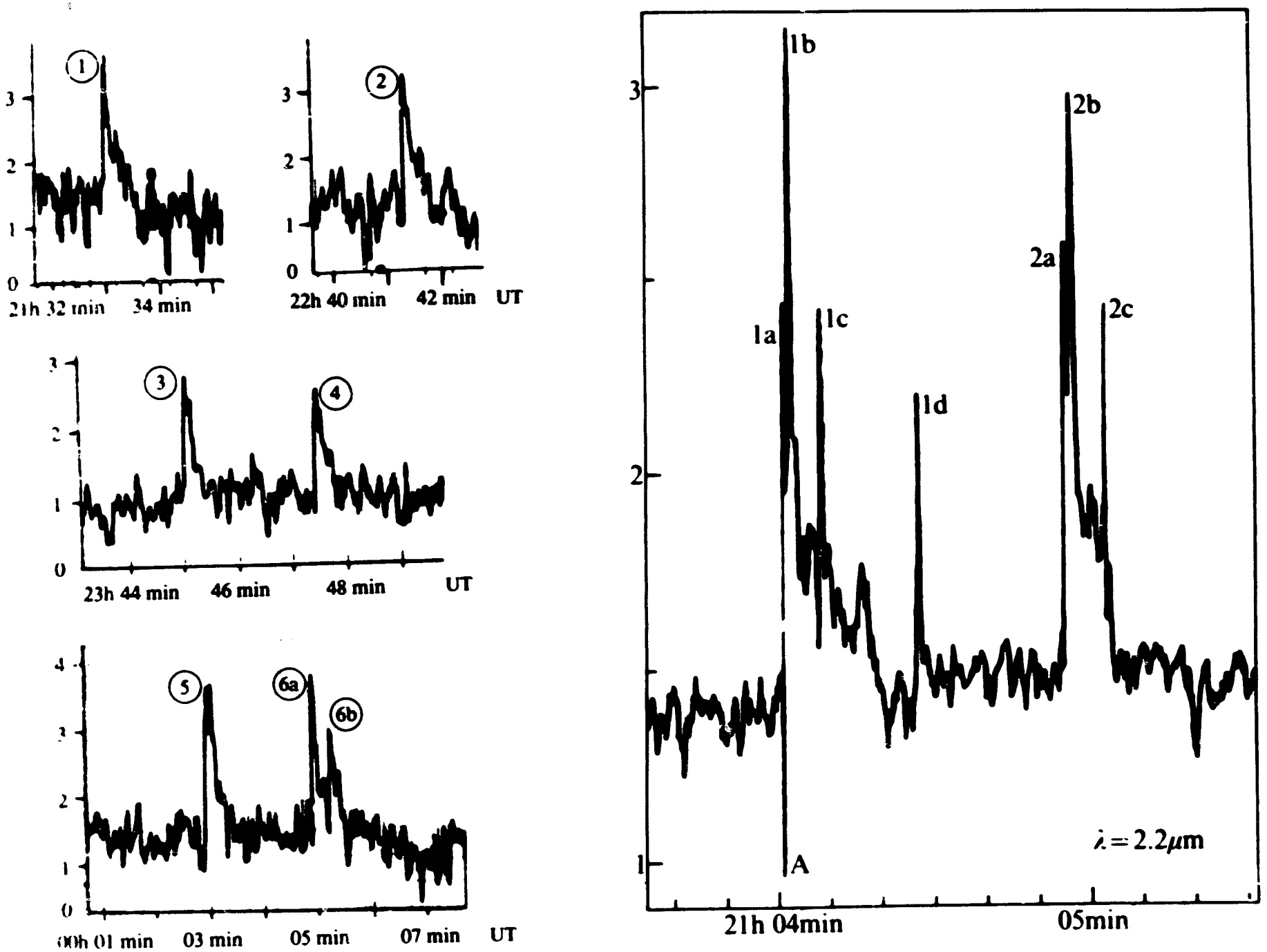
1
2
3
4
5
6a
6b
1a
1b
1c
1d
2a
2b
2c
A
λ = 2.2μm
0
1
2
3
21h 32 min
34 min
22h 40 min
42 min
23h 44 min
46 min
48 min
00h 01 min
03 min
05 min
07 min
21h 04min
05min
UT

Figure 30

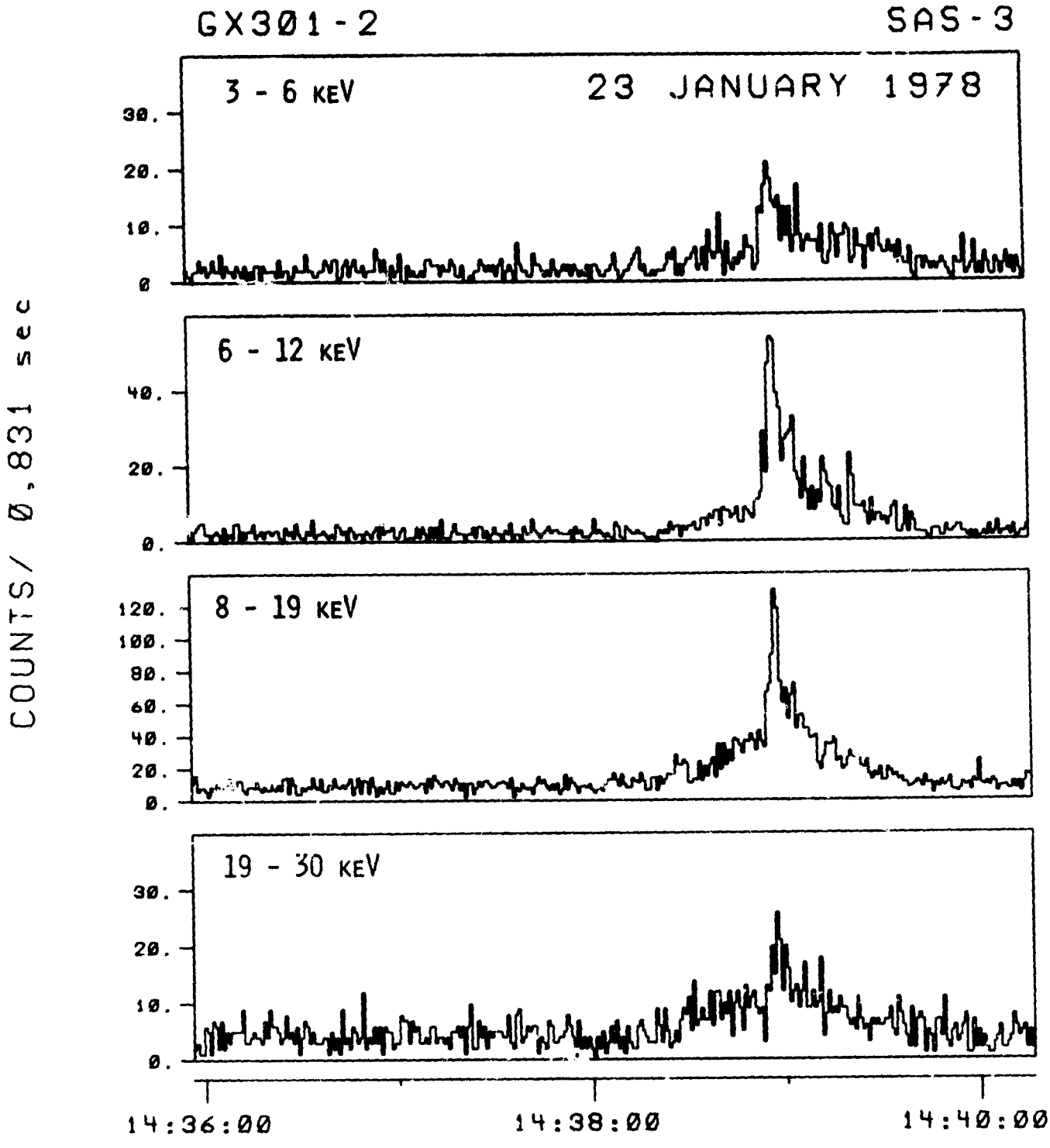
GX301-2
SAS-3
3 - 6 KEV
23 JANUARY 1978
30.
20.
10.
0
6 - 12 KEV
40.
20.
0.
8 - 19 KEV
120.
100.
80.
60.
40.
20.
0.
19 - 30 KEV
30.
20.
10.
0.
14:36:00
14:38:00
14:40:00
COUNTS/ 0.831 sec

Figure 31

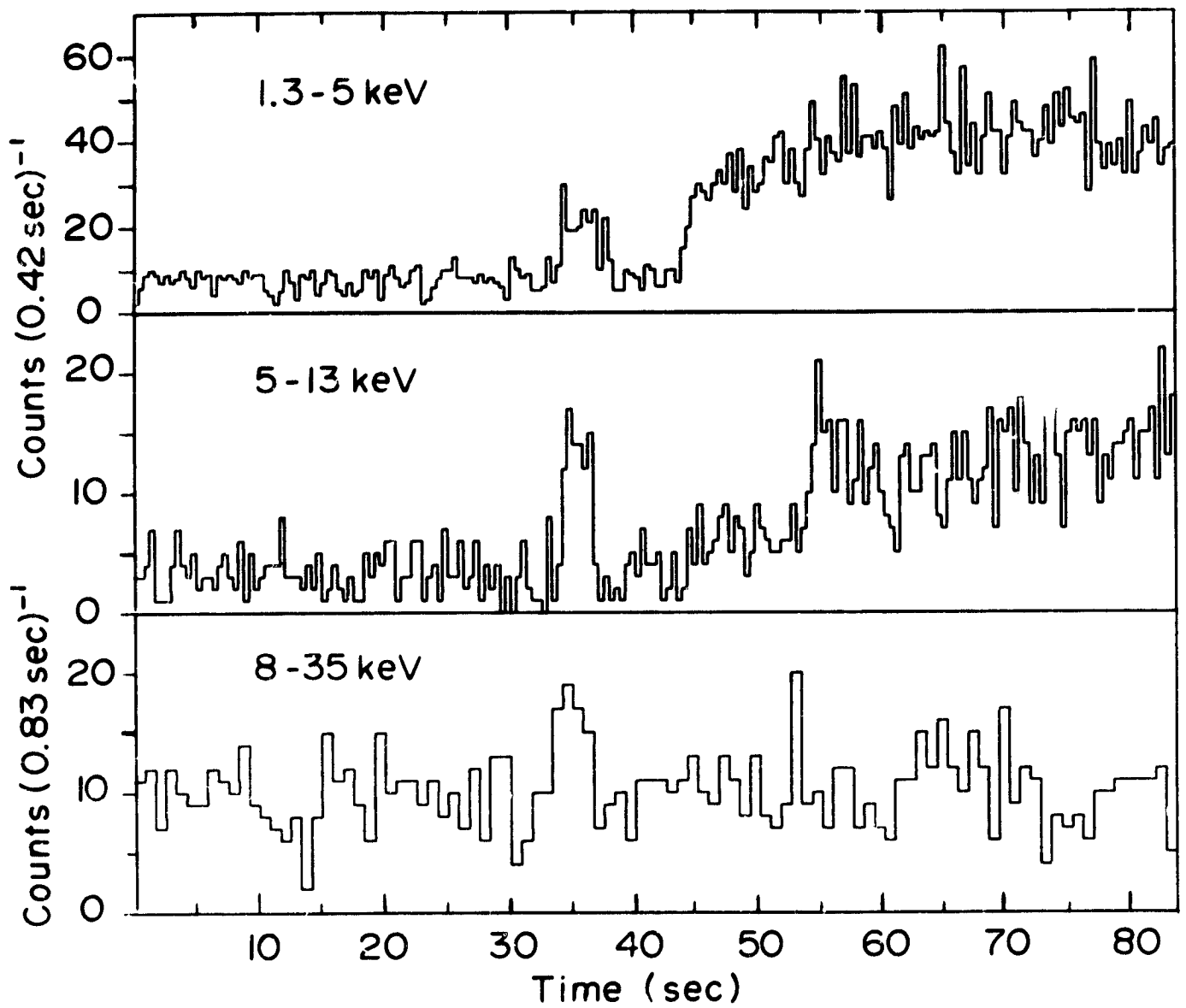
Precursor of the 1977 February 7
Fast Transient Event SAS-3
1.3-5 keV
5-13 keV
8-35 keV
Counts (0.42 sec)⁻¹
Counts (0.83 sec)⁻¹
Time (sec)

Figure 32

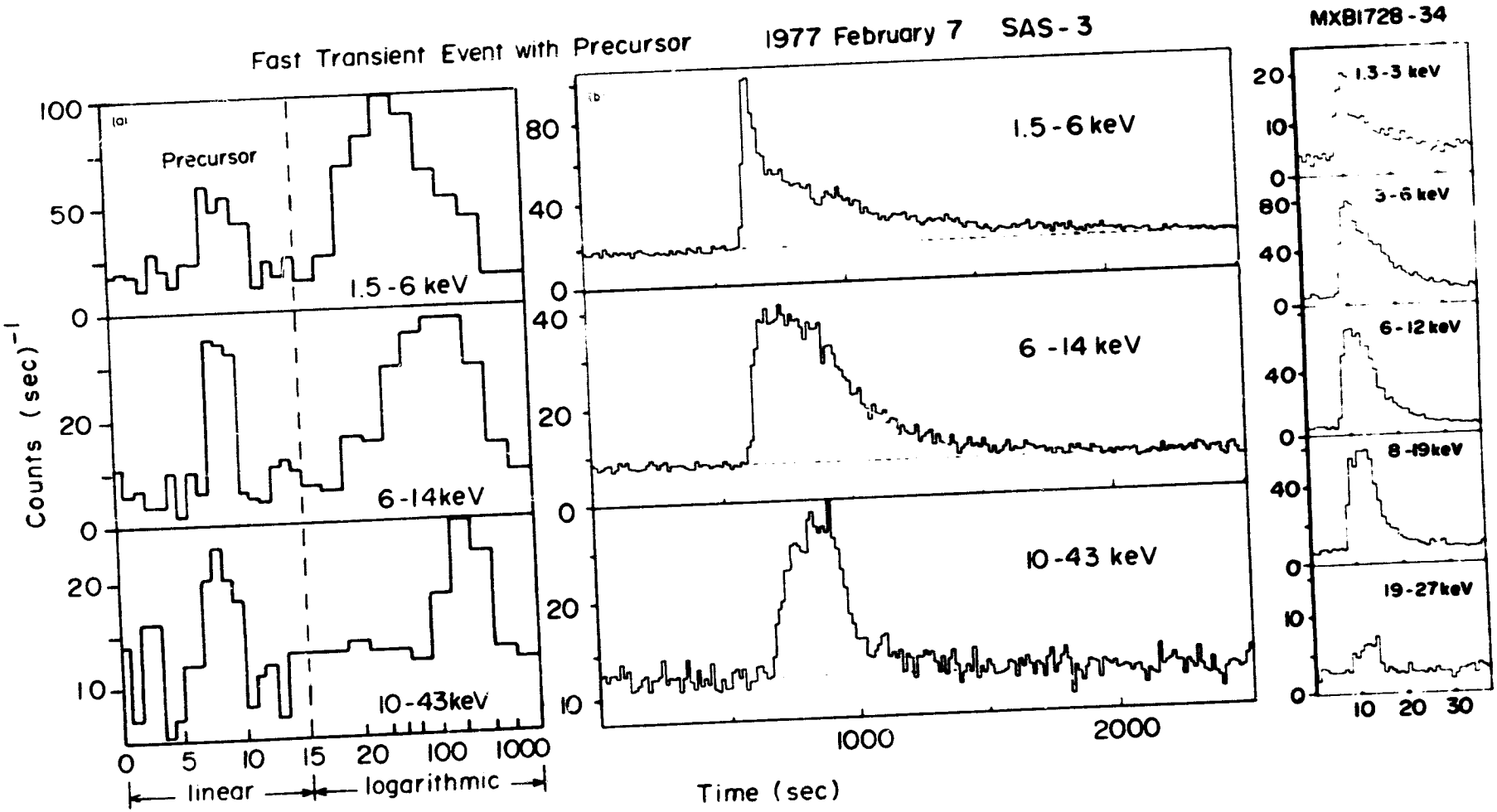

Figure 33a

Figure 33b

Figure 33c

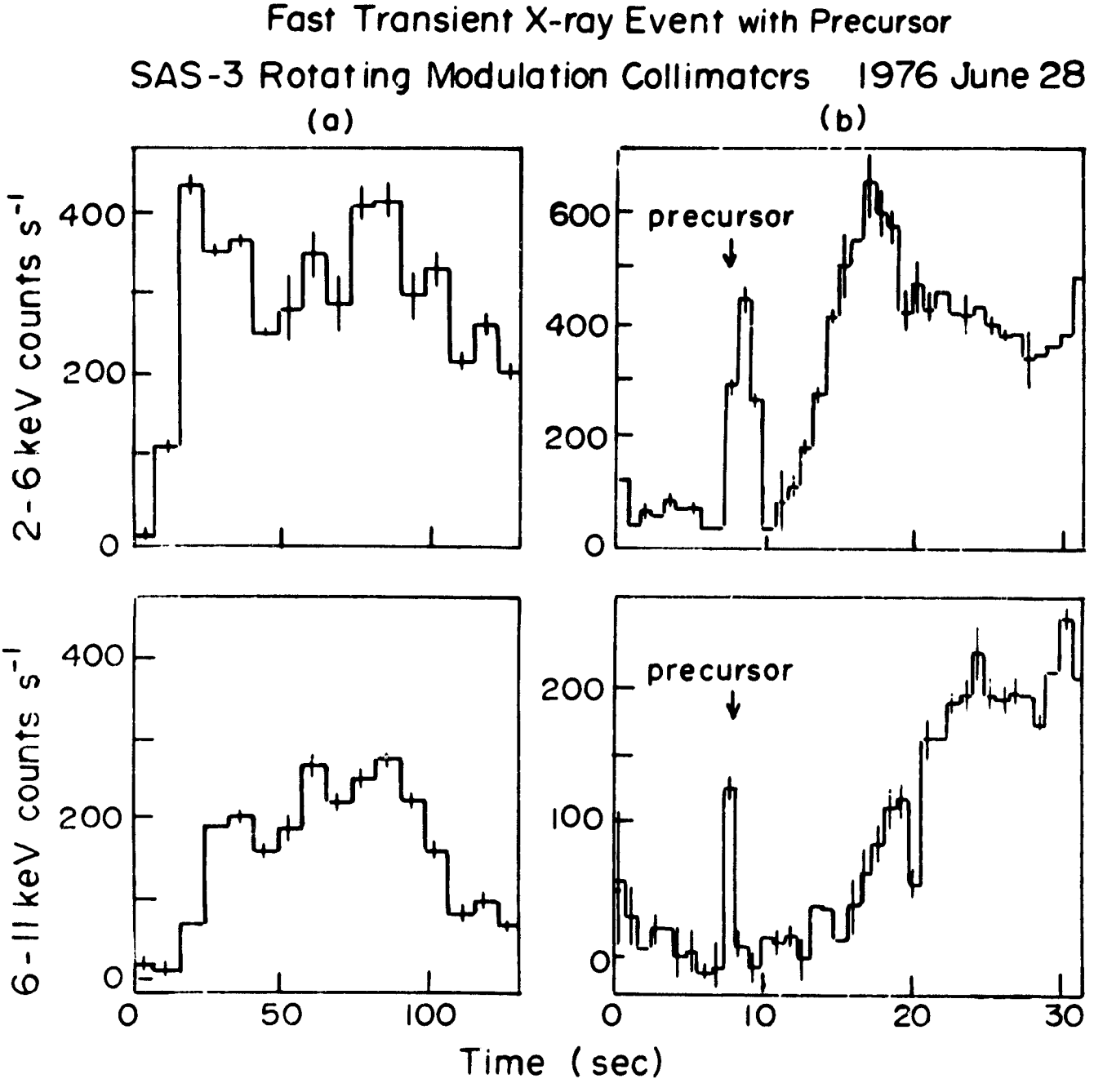
Fast Transient X-ray Event with Precursor
SAS-3 Rotating Modulation Collimators 1976 June 28
(a)
(b)
2-6 keV counts s⁻¹
6-11 keV counts s⁻¹
precursor
precursor
Time (sec)

Figure 34

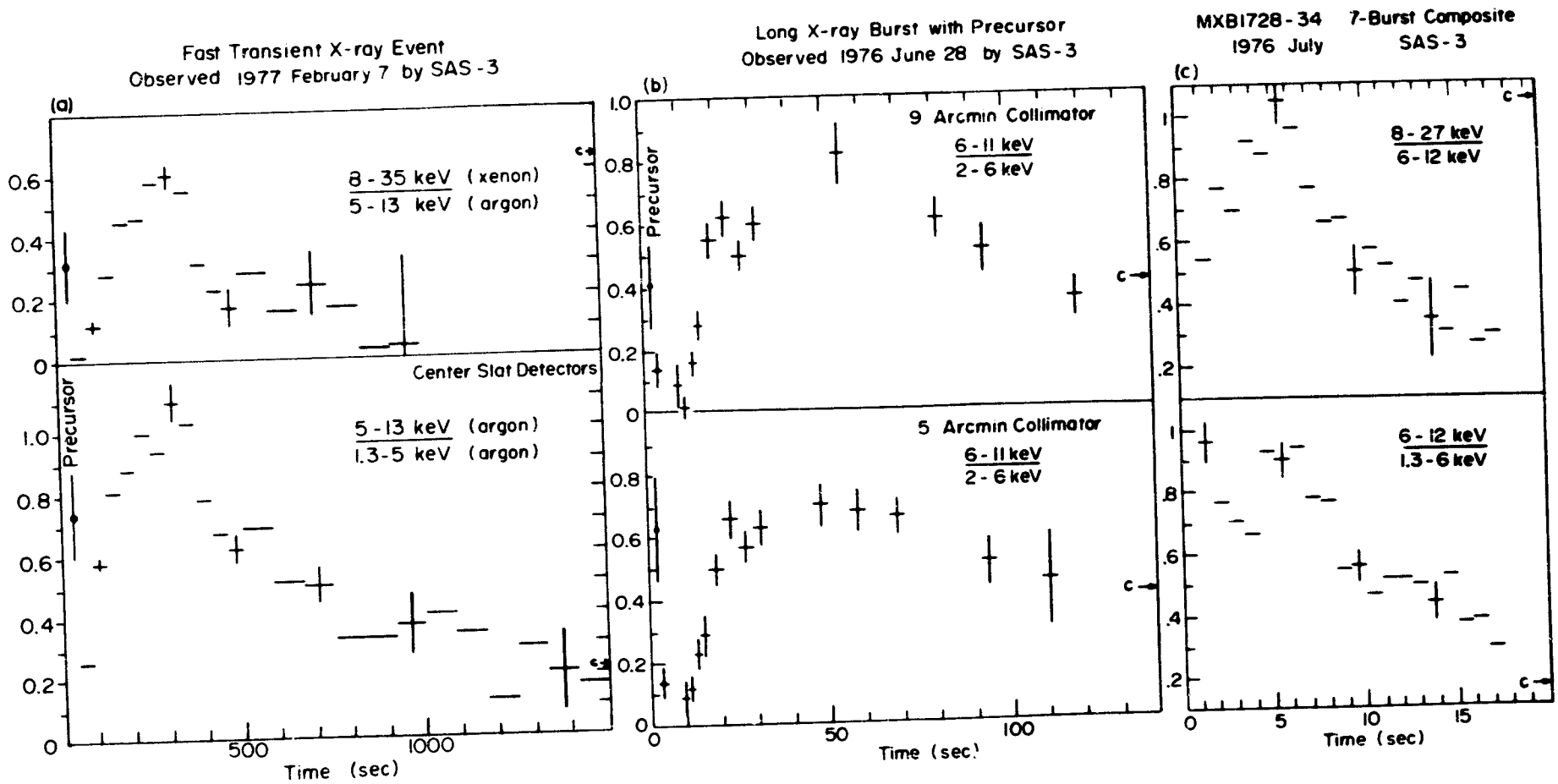
Fast Transient X-ray Event
Observed 1977 February 7 by SAS-3
(a)
8-35 keV (xenon)
5-13 keV (argon)
Center Slat Detectors
5-13 keV (argon)
1.3-5 keV (argon)
Precursor
Time (sec)
Long X-ray Burst with Precursor
Observed 1976 June 28 by SAS-3
(b)
9 Arcmin Collimator
6-11 keV
2-6 keV
5 Arcmin Collimator
6-11 keV
2-6 keV
Precursor
Time (sec)
MXB1728-34
1976 July
7-Burst Composite
SAS-3
(c)
8-27 keV
6-12 keV
6-12 keV
1.3-6 keV
Time (sec)

Figure 35

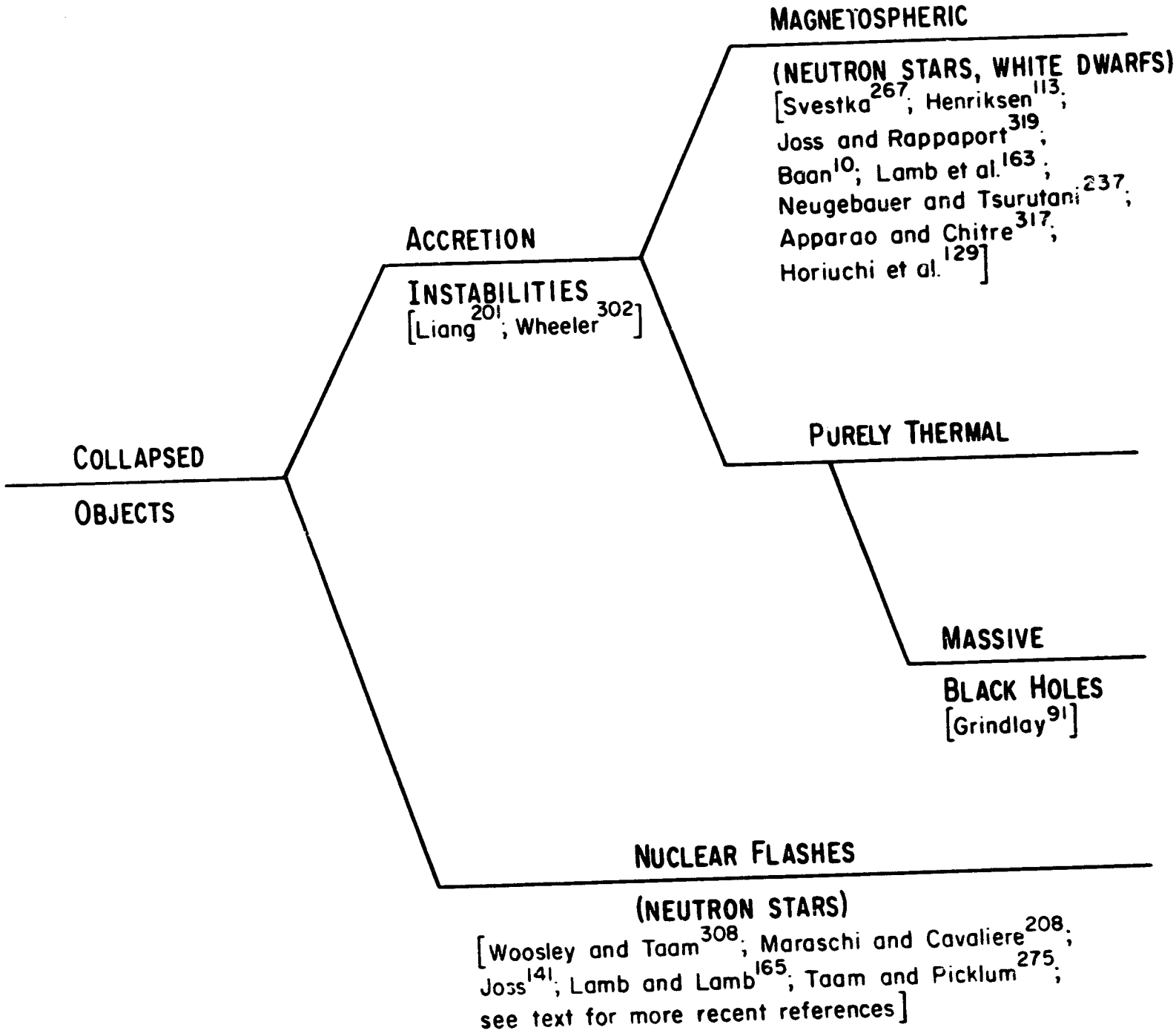
COLLAPSED OBJECTS
ACCRETION INSTABILITIES [Liang[201]; Wheeler[302]]
MAGNETOSPHERIC (NEUTRON STARS, WHITE DWARFS) [Svestka[267]; Henriksen[113]; Joss and Rappaport[319]; Baan[10]; Lamb et al.[163]; Neugebauer and Tsurutani[237]; Apparao and Chitre[317]; Horiuchi et al.[129]]
PURELY THERMAL
MASSIVE BLACK HOLES [Grindlay[91]]
NUCLEAR FLASHES (NEUTRON STARS) [Woosley and Taam[308]; Maraschi and Cavaliere[208]; Joss[141]; Lamb and Lamb[165]; Taam and Picklum[275]; see text for more recent references]

Figure 36

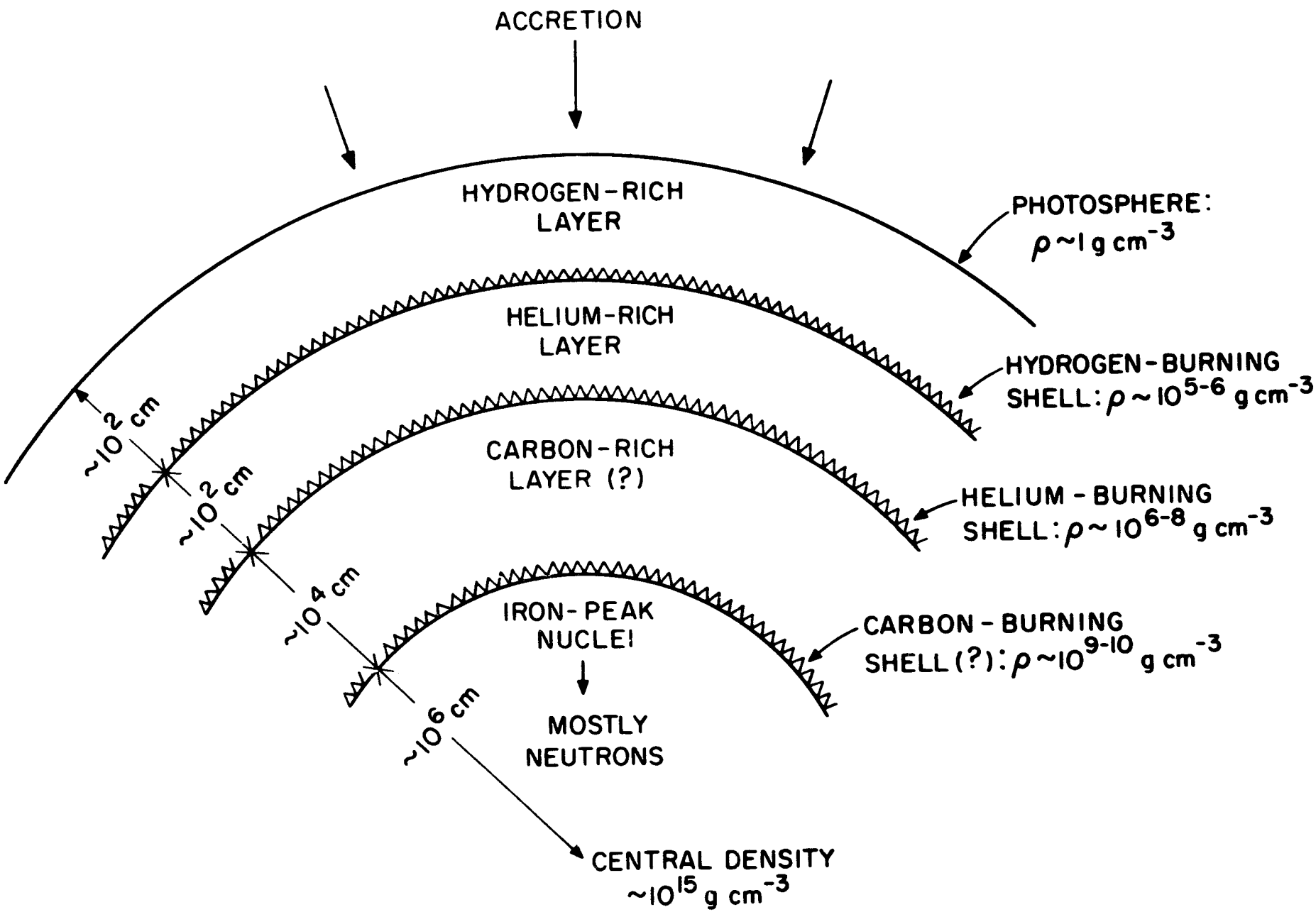
ACCRETION
HYDROGEN-RICH LAYER
PHOTOSPHERE: $\rho \sim 1$ g cm^{-3}
HELIUM-RICH LAYER
HYDROGEN-BURNING SHELL: $\rho \sim 10^{5-6}$ g cm^{-3}
$\sim 10^2$ cm
CARBON-RICH LAYER (?)
$\sim 10^2$ cm
HELIUM-BURNING SHELL: $\rho \sim 10^{6-8}$ g cm^{-3}
$\sim 10^4$ cm
IRON-PEAK NUCLEI
CARBON-BURNING SHELL (?): $\rho \sim 10^{9-10}$ g cm^{-3}
$\sim 10^6$ cm
MOSTLY NEUTRONS
CENTRAL DENSITY $\sim 10^{15}$ g cm^{-3}

Figure 37

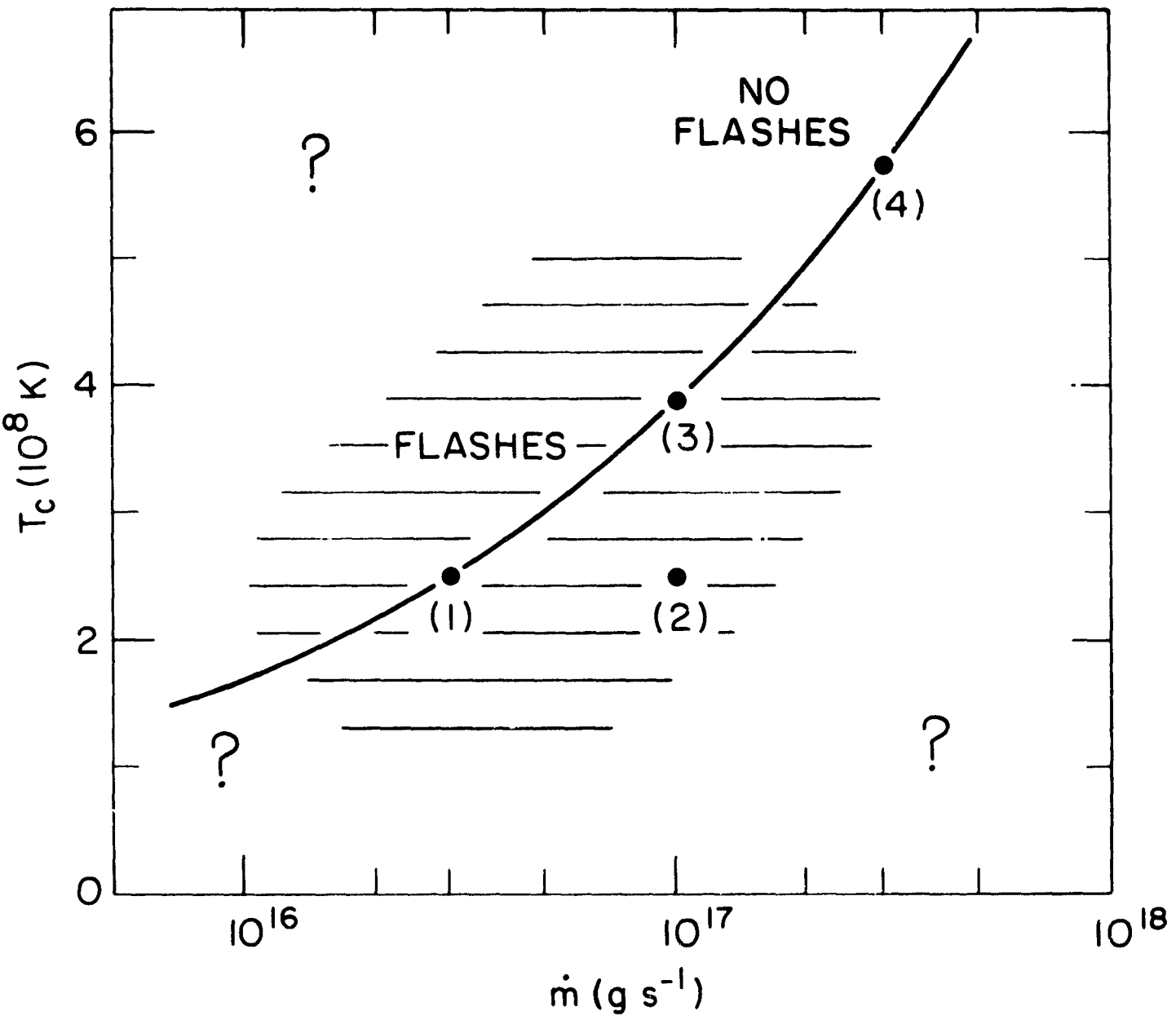

Figure 38

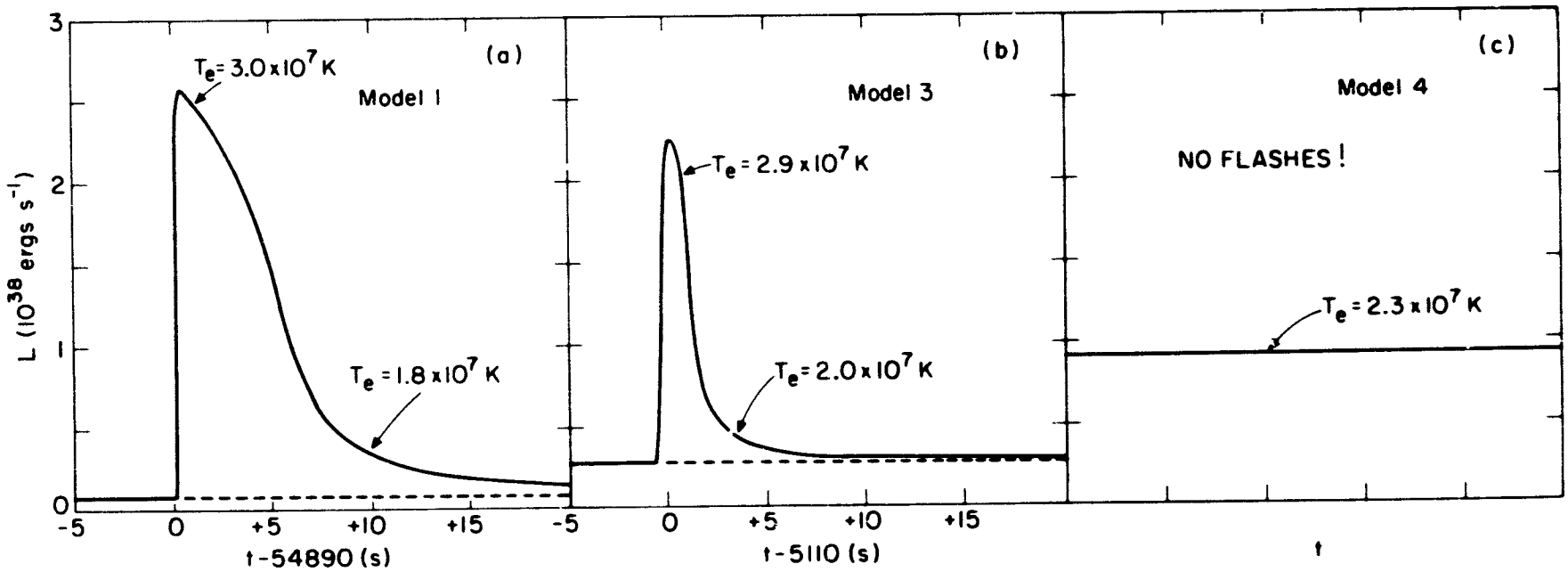
3
2
1
0
L (10^{38} ergs s^{-1})
(a)
Model 1
T_e = 3.0 x 10^7 K
T_e = 1.8 x 10^7 K
-5
0
+5
+10
+15
t-54890 (s)
(b)
Model 3
T_e = 2.9 x 10^7 K
T_e = 2.0 x 10^7 K
-5
0
+5
+10
+15
t-5110 (s)
(c)
Model 4
NO FLASHES !
T_e = 2.3 x 10^7 K
t

Figure 39

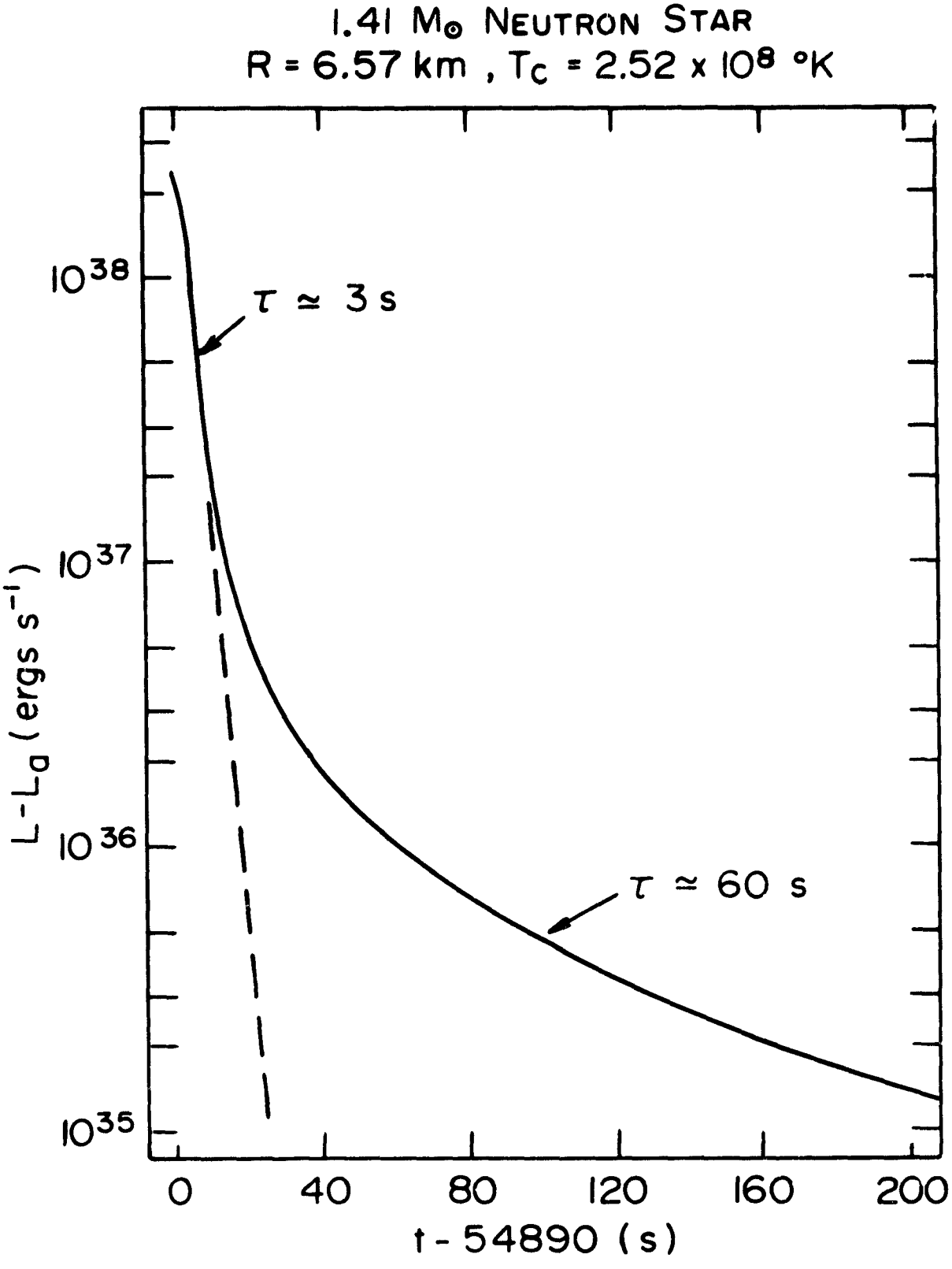
1.41 M⊙ NEUTRON STAR
R = 6.57 km , Tc = 2.52 x 10^8 °K
10^38
10^37
10^36
10^35
τ ≃ 3 s
τ ≃ 60 s
L-La (ergs s^-1)
0
40
80
120
160
200
t - 54890 (s)

Figure 40

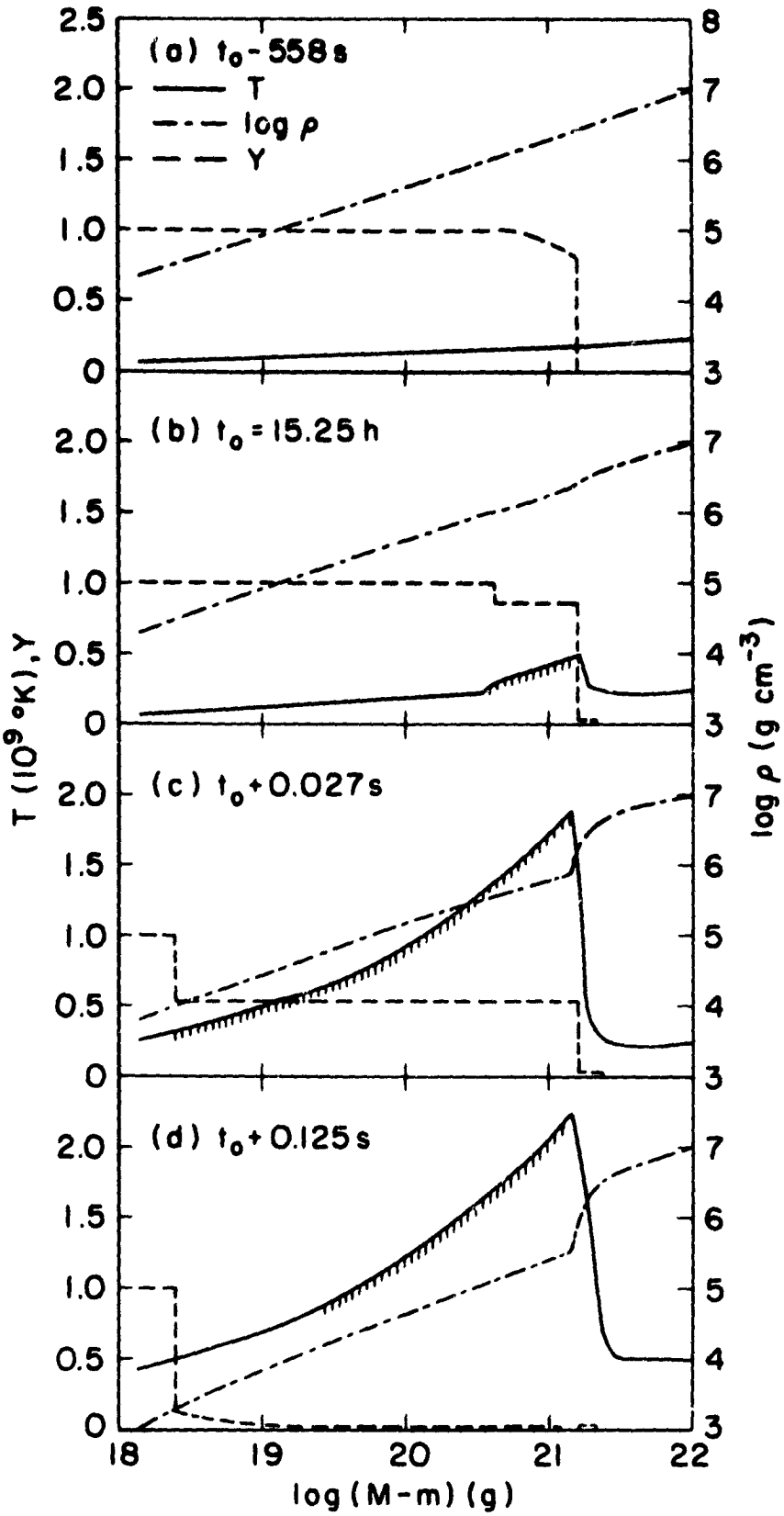
1.41 M⊙ NEUTRON STAR
R=6.57km, ṁ=3x10^16 g s^-1, T_c=2.52x10^8 °K
(a) t_o-558s
T
log ρ
Y
(b) t_o=15.25h
(c) t_o+0.027s
(d) t_o+0.125s
T (10^9 °K), Y
log ρ (g cm^-3)
log (M-m) (g)

Figure 41

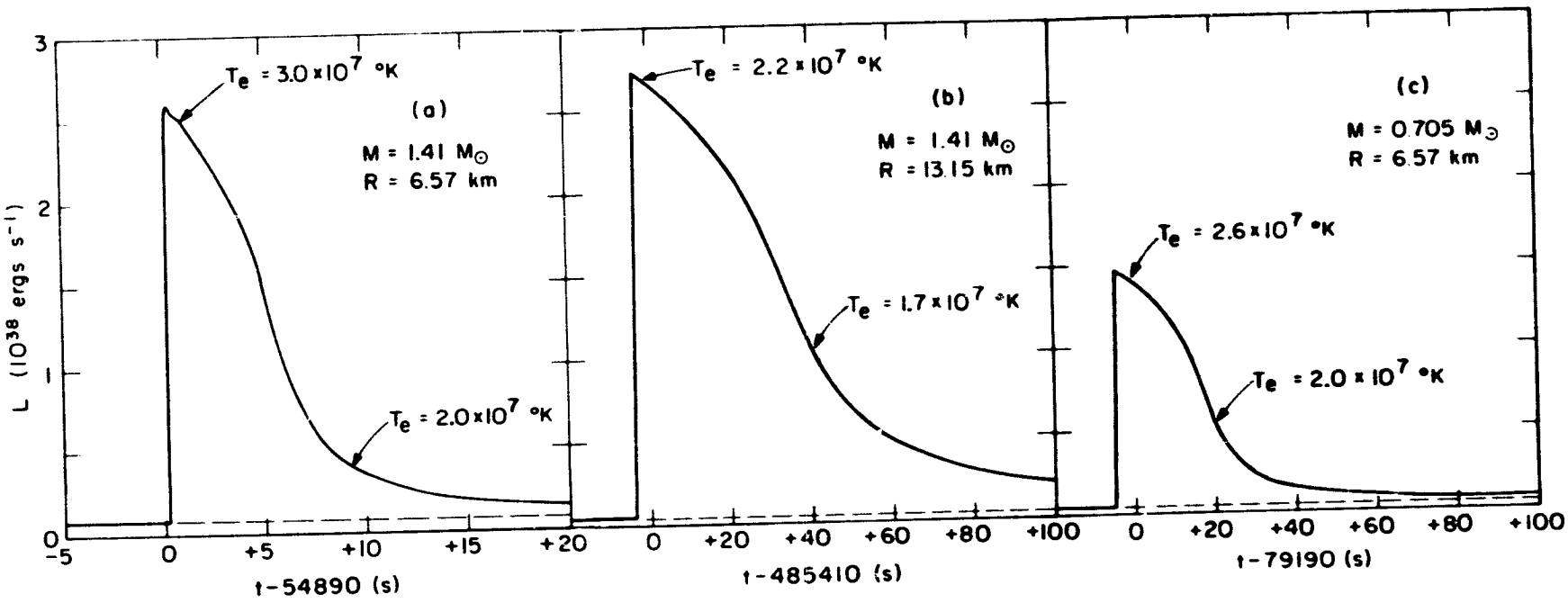
L (10^38 ergs s^-1)
3
2
1
0
(a)
M = 1.41 M⊙
R = 6.57 km
Te = 3.0 x 10^7 °K
Te = 2.0 x 10^7 °K
(b)
M = 1.41 M⊙
R = 13.15 km
Te = 2.2 x 10^7 °K
Te = 1.7 x 10^7 °K
(c)
M = 0.705 M⊙
R = 6.57 km
Te = 2.6 x 10^7 °K
Te = 2.0 x 10^7 °K
-5 0 +5 +10 +15 +20
t-54890 (s)
0 +20 +40 +60 +80 +100
t-485410 (s)
0 +20 +40 +60 +80 +100
t-79190 (s)

Figure 42

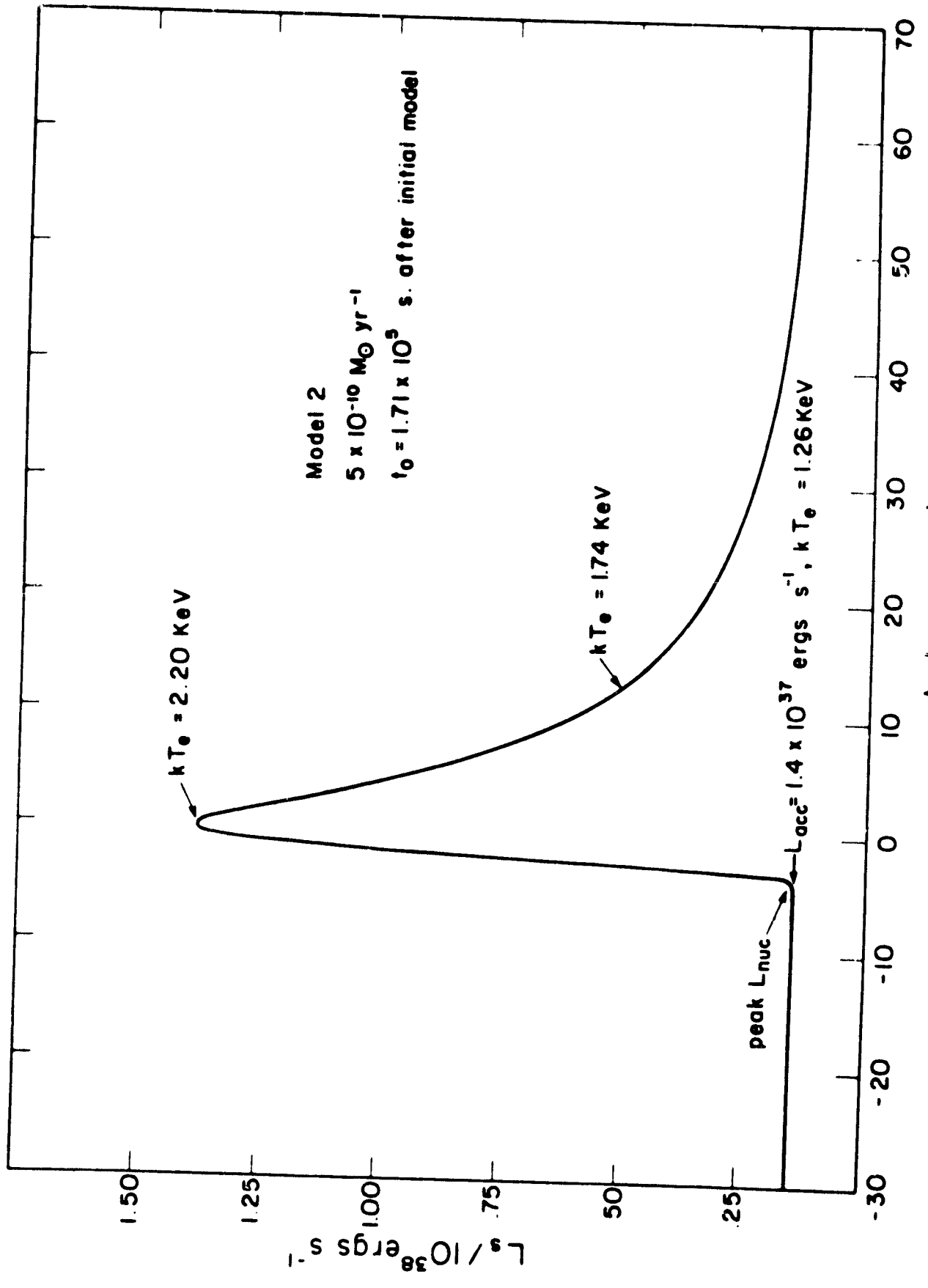
Model 2
5 x 10⁻¹⁰ M⊙ yr⁻¹
t₀ = 1.71 x 10⁵ s. after initial model
kT_e = 2.20 KeV
kT_e = 1.74 KeV
peak L_nuc
L_acc = 1.4 x 10³⁷ ergs s⁻¹, kT_e = 1.26KeV
t - t₀, seconds
L_s / 10³⁸ ergs s⁻¹
1.50
1.25
1.00
.75
.50
.25
-30
-20
-10
0
10
20
30
40
50
60
70

Figure 43